

A hydromechanical erosion model for surface-mined areas
by Kuang-Jung Tsai

A thesis submitted in partial fulfillment of the requirements for the degree of Doctor of Philosophy in Crop and Soil Science
Montana State University
© Copyright by Kuang-Jung Tsai (1983)

Abstract:
Observations of surface-mined areas at Colstrip, located in southeastern Montana, indicate that there is a potential for severe erosion on minesoils lacking vegetative cover. Quantitative data are unavailable on the erodibility of these minesoils.

The purpose of this study was to set up an effective mathemetical model, based on physical processes of rainfall and runoff to predict soil loss or sediment yield generated from these mined areas. The mathematical relationships of the model were used to describe the dynamics of the erosion subprocesses, such as soil detachment and transport by rainfall and runoff.

Soil erosion was simulated for several combinations of slope gradient, simulated rainfall intensity, runoff rate, and soil texture. Results were presented graphically. An interactive statistical analysis package was used to analyze data collected in the laboratory. A rainfall simulator with 827 tubing tips was coupled to a specially designed erosion plot (61 X 61 X 10 cm) with slope adjustable from one to sixty percent. Currently-available empirical equations like the Universal Soil Loss Equation cannot provide such descriptive simulation of this complex process. However, the proposed erosion model will also require modification of its mathematical relationships and introduction of some other components related to the simulated erosion process to adequately predict soil loss. This model lends itself to expansion into a more comprehensive model if the soil loss data are made available.

It is expected that this study will provide an effective erosion model that can be utilized to improve future erosion research for surface-mined areas and other disturbed lands, and to predict sediment yield more accurately for reclamation planning.

A HYDROMECHANICAL EROSION MODEL FOR SURFACE-MINED AREAS

by

KUANG-JUNG TSAI

A thesis submitted in partial fulfillment
of the requirements for the degree

of

Doctor of Philosophy

in

Crop and Soil Science

MONTANA STATE UNIVERSITY
Bozeman, Montana

June 1983

D378
T782
cop. 2

APPROVAL

of a thesis submitted by

Kuang-Jung Tsai

This thesis has been read by each member of the thesis committee and has been found to be satisfactory regarding content, English usage, format, citations, bibliographic style, and consistency, and is ready for admission to the College of Graduate Studies.

May 26, 1983
Date

William M. Schafer
Chairperson, Graduate Committee

Approved for the Major Department

May 26, 1983
Date

Dwane H. Miller
Head, Major Department

Approved for the College of Graduate Studies

6-6-83
Date

Michael P. Malone
Graduate Dean

STATEMENT OF PERMISSION TO COPY

In presenting this thesis in partial fulfillment of the requirements for a doctoral degree at Montana State University, I agree that the Library shall make it available to borrowers under rules of the Library. I further agree that copying of this thesis is allowable only for scholarly purposes, consistent with "fair use" as prescribed in the U.S. Copyright Law. Requests for extensive copying or reproduction of this thesis should be referred to University Microfilms International, 300 North Zeeb Road, Ann Arbor, Michigan 48106, to whom I have granted "the exclusive right to reproduce and distribute copies of the dissertation in and from microfilm and the right to reproduce and distribute by abstract in any format."

Signature Kuang-Jung Hsu

Date May 24, 1983

ACKNOWLEDGMENTS

The author wishes to express his appreciation to Dr. W. M. Schafer, major advisor, for his patience, guidance, suggestions and corrections during the course work and the completion of this manuscript.

A sincere thanks is also extended to Drs. A. H. Ferguson, G. A. Nielsen, F. F. Munshower and T. T. Williams for serving on the graduate committee and providing invaluable suggestions and guidance throughout the development of this thesis.

An acknowledgment is due to the Agricultural Engineering Department for the use of laboratory facilities. Appreciation to Montana State University for financial assistance that made this work possible is also extended.

A special thanks to his parents and his wife; for without their encouragement and assistance the completion of this thesis would not have been possible.

TABLE OF CONTENTS

	Page
APPROVAL	ii
STATEMENT OF PERMISSION TO USE	iii
VITA	iv
ACKNOWLEDGMENTS	v
TABLE OF CONTENTS	vi
LIST OF TABLES	viii
LIST OF FIGURES	xi
LIST OF SYMBOLS	xiii
ABSTRACT	xix
CHAPTER	
I. INTRODUCTION	1
II. LITERATURE REVIEW	3
Physical Process of Water Erosion	3
Erosion and Sedimentation Problems	5
Water Erosion Models Classification and Discussion	7
Mining Reclamation and Water Erosion Related Problems	9
III. METHODS AND PROCEDURES	15
Site Characterization	15
Selection of Sites for Sample Collection	15
Site Description	17
Data Base Collection and Analysis	21
Rainfall Simulation in Laboratory	22
Measurement of Runoff and Sediment	27
Particle Size Analysis	32

TABLE OF CONTENTS—Continued

IV. EROSION MODEL DEVELOPMENT 33

Basic Principle 33
Surface Runoff 40
Mathematical Simulation Process 50
Model Modification 59

V. RESULTS AND DISCUSSION 62

Rainfall Simulation 62
Particle Size Distribution 70
Sediment Yields Estimation 75

VI. EROSION MODEL APPLICATION AND DISCUSSION 102

VII. CONCLUSION AND RECOMMENDATIONS 106

LITERATURE CITED 108

LIST OF TABLES

Tables		Page
1.	Representative Rates of Erosion from Various Land Uses	7
2.	Types of Models	8
3.	Coal Reserves in the Northern Great Plains	10
4.	Comparative Rates of Erosion	12
5.	Runoff Soil Losses on Unmined Rangeland and on Vegetated Mine Spoil	12
6.	Laboratory Analysis of Boxwell-2 Soil	19
7.	Laboratory Analysis of Chinook-1 Soil	20
8.	Annual Precipitation at Colstrip, Montana for the Years 1928-1977	22
9.	Efficiency of Forms of Water Erosion	34
10.	Equations Relating KE and Intensity	36
11.	Limited Range of ϕ, ψ and MF for Different Soil Texture and Runoff Rate	61
12.	Raindrop Size Calculation	63
13.	Floatmeter Reading vs. Variation of Rainfall Intensity Over the Plot Area	65
14.	Rainfall Intensity Calibration Data	66
15.	Linear Regression Analysis of Intensity vs. Floatmeter Reading	68
16.	Analysis of Covariance for Test of Homogeneity of Regression Coefficients	68
17.	Test of Homogeneity of Adjusted Means With Equal Regression Coefficients	68
18.	KE vs. Drop Diameter and Velocity for Selected Rainfall Simulators	69

Tables

		Page
19.	Variation in Plot Dimensions vs. Percent Slope	71
20.	KE Variation Due to Slope Changes	71
21.	Average Sediment Yield for Each Soil Under 36 Treatment Combinations	76
22.	ANOV of Comparisons Among Soil Texture	79
23.	ANOV of Comparisons Among Soil Texture	79
24.	Duncan's Multiple Range Test	80
25.	Results of Duncan's Multiple Range Test	80
26.	ANOV of Factorial Experiment for Sandy Loam	80
27.	Multiple Slope Comparisons of Sandy Loam	81
28.	Multiple Intensity Comparisons of Sandy Loam	81
29.	Multiple Runoff Rate Comparisons of Sandy Loam	81
30.	ANOV of Factorial Experiment for Sandy Clay Loam	82
31.	Multiple Slope Comparisons of Sandy Clay Loam	82
32.	Multiple Intensity Comparisons of Sandy Clay Loam	82
33.	Multiple Runoff Rate Comparisons of Sandy Clay Loam	82
34.	ANOV of Factorial Experiment for M1 (SL/SCL) Soil	83
35.	Multiple Slope Comparisons of M1 Soil	83
36.	Multiple Intensity Comparisons of M1 Soil	83
37.	Multiple Runoff Rate Comparisons of M1 Soil	83
38.	ANOV of Factorial Experiment for M2 (SCL/SL) Soil	84
39.	Multiple Slope Comparisons of M2 Soil	84
40.	Multiple Intensity Comparisons of M2 Soil	84
41.	Multiple Runoff Rate Comparisons of M2 Soil	84
42.	ANOV of Factorial Experiment for M3 (SL mixed with SCL) Soil	85

Tables

		Page
43.	Multiple Slope Comparisons of M3 Soil	85
44.	Multiple Intensity Comparisons of M3 Soil	85
45.	Multiple Runoff Rate Comparisons of M3 Soil	85
46.	Runoff Over Sandy Loam Surface With R = 0 cm^3/sec	86
47.	Runoff Over Sandy Clay Loam Surface With R = 0 cm^3/sec	86
48.	Runoff Over Sandy Loam Surface With R = 21 cm^3/sec	87
49.	Runoff Over Sandy Clay Loam Surface With R = 21 cm^3/sec	87
50.	Runoff Over Sandy Loam Surface With R = 42 cm^3/sec	88
51.	Runoff Over Sandy Clay Loam Surface With R = 42 cm^3/sec	88
52.	Sediment Yield Difference Between Actual Measurement and Model Prediction	95
53.	Soil Losses Comparison Between USLE and Model	104

LIST OF FIGURES

Figures		Page
1.	Possible interaction between transport and detachment processes	4
2.	Annual costs of sediment pollution	6
3.	Map showing Colstrip study area location	16
4.	Location of Chinook-1 and Boxwell-2 sites near Colstrip, Montana	18
5.	Sketch of the Tahoe Basin rainfall simulator	24
6.	Picture of the selected rainfall simulator	25
7.	Rainfall intensity measurement	26
8.	Rainfall intensity calibration processes	27
9.	Erosion plot	28
10.	Simulated runoff pipe and erosion plot	30
11.	Soil textures and their combinations	31
12.	Differential soil movement caused by raindrop splash	35
13.	Curves showing relation between drop diameter and terminal velocity after 12 different height of fall	13
14.	Parameters for describing the geometry of splash shape	38
15.	Splash parameter change with time from impact	39
16.	Steps in drop crater formation	39
17.	Typical erosion and deposition occurrences	41
18.	Characteristics diagram of kinematic wave	47
19.	Water surface profile during buildup	47
20.	Water surface profile during decay	49
21.	Transport/detachment interaction models	51

Figures Page

22. Rill and interrill erosion on sloping surface 53

23. The cross-section of rill, force acting on submerged soil particles and rill flow conditions assumed for theoretical analysis 54

24. Flow detachment-sediment load interaction 55

25. Linear relationship between rainfall intensity and floatmeter reading 64

26. Particle size curves for sandy loam after erosion and before erosion 72

27. Particle size curves for sandy clay loam after erosion and before erosion 73

28. Particle size curves for mixed soils (SL mixed with SCL) after erosion and before erosion 74

29. MF distribution with respect to ψ and ϕ for sandy loam with $R = 0$ cm^3/sec 89

30. MF distribution with respect to ϕ and ψ for sandy clay loam with $R = 0$ cm^3/sec 90

31. MF distribution with respect to ϕ and ψ for sandy loam with $R = 21$ cm^3/sec 91

32. MF distribution with respect to ϕ and ψ for sandy clay loam with $R = 21$ cm^3/sec 92

33. MF distribution with respect to ϕ and ψ for sandy loam with $R = 42$ cm^3/sec 93

34. MF distribution with respect to ϕ and ψ for sandy clay loam with $R = 42$ cm^3/sec 94

35. Slope-dependent soil loss for different intensities (SL) 96

36. Slope-dependent soil loss for different runoff rates (SL) 97

37. Runoff-dependent soil loss for different intensities (SL) 98

38. Intensity-dependent soil loss for different runoff rates (SL) 99

39. Runoff-dependent soil loss for different slopes (SL) 100

40. Intensity-dependent soil loss for different slopes (SL) 101

LIST OF SYMBOLS

Symbol	Nomenclature	Chapter
A	area	IV
ANOV	analysis of variance	V
C	Chezy's constant	IV
	crop factor of the USLE	VI
C′	constant	IV
C″	constant	IV
CRD	Completely Randomize Design	V
D	the amount of soil being detached	IV
	hydraulic depth	IV
d	flow depth	IV
D_b	the amount of soil being detached by runoff at the toe of the slope	IV
D_c	the amount of soil being detached by runoff or detachment capacity by flow	IV
D_F	soil detachment of runoff	II
D_f	soil detachment of flow	IV
D_i	delivery rate of particles detached by interrill erosion to rill flow	IV
D_R	soil detachment by rainfall	II
	detachment rate of rill erosion	IV
D_s	splash detachment rate	IV
DF	degree of freedom	V
F	frictional force	IV

Symbol	Nomenclature	Chapter
	F-value of ANOV	V
f	friction factor or infiltration rate	IV
F_r	Froude number	IV
G	sediment load	IV
g	acceleration of gravity	IV
G_e	soil losses estimated by model	IV
G_m	soil losses measured in the laboratory	IV
H	splash height of raindrop impact	IV
	height of drop fall	V
h	height	IV
H_0	hypothesis of ANOV	V
I	rainfall intensity	IV,V,VI
i	rainfall intensity	IV
i_0	net inflow rate to surface runoff (rainfall excess)	IV
i_*	magnitude of constant rainfall excess	IV
J	Joule	IV
K	soil factor of the USLE	III,VI
k	constant	IV
KE	kinetic energy	III,IV,V
L	total slope length	IV,V
	characteristic length or length of overland flow	IV
M	mass	III
m	mass or kinematic wave constant	IV
M1	SL on top/SCL at bottom (layered soil)	III
M2	SCL on top/SL at bottom (layered soil)	III

Symbol	Nomenclature	Chapter
M3	SL mixed with SCL (mixed soil)	III
MF	Modification factor	IV
MRT	Multiple Range Test	V
MS	Mean of Square	V
n	surface roughness	IV
P	conservation factor of the USLE	VI
p	wetted perimeter	IV
PE	potential energy	IV
Q	total discharge	IV
q	discharge per unit width	IV
Q_s	sediment discharge	IV
Q_w	water discharge or flow rate	IV
q_o	the runoff discharge per unit width at the toe of the slope	IV
q_L	lateral discharge	IV
R	rainfall factor of the USLE	III,V,VI
	hydraulic radius	IV
	runoff factor	V,VI
r	radius	III
R_e	Reynold's number	IV
R_d	floatmeter reading	V
r^2	correlation coefficient	V
S	actual sediment transport	IV
	slope factor	III
S_b	slope factor at the toe of the slope	IV

Symbol	Nomenclature	Chapter
S_c	slope factor at any particular point	IV
S_*	the ratio of S_b and S_c	IV
SCL	sandy clay loam	III
SL	sandy loam	III
SS	Sum of Square	V
SV	Source of Variation	V
T_b	the amount of soil being transported by runoff at the toe of the slope	IV
T_c	the amount of soil being transported by runoff	IV
T_R	transport by rainfall	II
T_F	transport by runoff	II
T_f	transport of flow	IV
t	time	IV
t_c	time of concentration	IV
t_p	a characteristic overland flow time at peak	IV
t_r	time of duration during a storm	IV
U	mean velocity	IV
u	the product of S_* and X_0	IV
V	Velocity	III
v	velocity	IV
W	crater width of raindrop impact	IV
	weight of soil submerged	IV
X	flow direction at x-axis	IV
X_0	the fraction of slope length	IV
x	the direction of flow, or distance downslope	IV

Symbol	Nomenclature	Chapter
x_w	position of disturbance wave	IV
X_{wr}	position of disturbance wave for $t=t_r$	IV
Y	dependent variable	V
$\hat{Y}_x$	statistic parameter	V
y	depth of flow	IV
y_b	the elevation of deposited material	IV
y_L	flow depth at x=L	IV
y_{Lr}	flow depth at x=L, $t=t_r$	IV
τ	shear stress	IV
τ_f	soil shear strength	IV
η	eddy viscosity	IV
ν	kinematic viscosity	IV
γ	unit weight of sediment discharge	IV
ρ	density of fluid	IV
ρ_b	the mass density of deposited material	IV
α	sheet angle of raindrop impact	IV
	kinematic wave constant	IV
	significant level	V
	correction factor of soil loss	VI
β	splash angle of raindrop impact	IV
	correction factor of soil loss	VI
ϕ	modification constant	IV
ψ	modification constant	IV
θ	slope gradient of channel bed	IV
σ	standard deviation	V

Symbol	Nomenclature	Chapter
σ_1	standard deviation within each trial	V
σ_2	standard deviation among each trial	V
μ	dynamic viscosity	IV
	mean of rainfall intensity	V
$\bar{\mu}$	general mean of rainfall intensity	V

ABSTRACT

Observations of surface-mined areas at Colstrip, located in southeastern Montana, indicate that there is a potential for severe erosion on minesoils lacking vegetative cover. Quantitative data are unavailable on the erodibility of these minesoils.

The purpose of this study was to set up an effective mathemetical model, based on physical processes of rainfall and runoff to predict soil loss or sediment yield generated from these mined areas. The mathematical relationships of the model were used to describe the dynamics of the erosion subprocesses, such as soil detachment and transport by rainfall and runoff.

Soil erosion was simulated for several combinations of slope gradient, simulated rainfall intensity, runoff rate, and soil texture. Results were presented graphically. An interactive statistical analysis package was used to analyze data collected in the laboratory. A rainfall simulator with 827 tubing tips was coupled to a specially designed erosion plot (61 X 61 X 10 cm) with slope adjustable from one to sixty percent. Currently-available empirical equations like the Universal Soil Loss Equation cannot provide such descriptive simulation of this complex process. However, the proposed erosion model will also require modification of its mathematical relationships and introduction of some other components related to the simulated erosion process to adequately predict soil loss. This model lends itself to expansion into a more comprehensive model if the soil loss data are made available.

It is expected that this study will provide an effective erosion model that can be utilized to improve future erosion research for surface-mined areas and other disturbed lands, and to predict sediment yield more accurately for reclamation planning.

CHAPTER I

INTRODUCTION

Soil erosion is a major problem not only today but will be an even serious problem in the future. Research on soil erosion has been the focus of the work of the U.S. Soil Conservation Service (SCS) since erosion was recognized as a serious problem in the late 1920s (Bennett and Chapline, 1928). Substantially new approaches to soil erosion research have been developed since 1960. The most significant new development is the much more detailed re-examination of the geomorphological and hydrological processes of erosion. Consequently, the basic assumptions of the Universal Soil Loss Equation (USLE) are being questioned, especially in surface-mined areas. Recently, newly developed soil erosion and sediment load prediction models have become very beneficial as design tools in developing plans to control sediment loads and soil losses in land use planning. Several techniques are potentially useful for this purpose, but little research has been done on soil erosion prediction, processes and sediment transportation in surface-mined areas.

Erosion and sediment production from surface-mined areas are extensive, serious natural problems in watershed management, because surface mining operations like all other large-scale earth moving operations, have potential to generate large volumes of sediments. If the sediment generated is contained on the mining site, it will not cause a serious off-site problem. However, if it washes into adjacent streams, it becomes a pollution problem. The eroded materials are detrimental to reservoirs, highway maintenance, drainage systems, streams and cultivated farmland.

Hill (1971) estimated that 1.2×10^6 hectares of land have been disturbed by surface mining in the United States. Open-pit mining accounts for about 35% and strip mining for

56% of the disturbed land. Two-thirds (8.1×10^5 hectares) require some form of treatment to reclaim and prevent environmental pollution. Curtis (1971) indicated that land in Appalachia is being disturbed by strip mining at the rate of about 13,000 hectares a year. Recently, increasing public concern, combined with the greater reliance being placed on coal for energy as America strives for energy independence, makes it likely that an increased amount of land will be disturbed in the future. Hence, the severity of the erosion problem will be increasingly recognized by the public. Accurate estimates of sediment yields from surface-mined areas are essential for erosion control and reclamation planning. In the past, most soil erosion research has focused primarily on agriculture. Very few attempts have been made to mathematically simulate the process of erosion by water in surface-mined areas. Also, it is difficult to develop a comprehensive erosion model to be used for surface-mined areas, because of the many possible variations in climate, mining operations and watershed conditions involved. It is impossible to develop a comprehensive correlation covering all types and gradations among these variables. Nevertheless, it is necessary to develop an erosion model to estimate sediment loads and describe the process of erosion by water in surface-mined areas.

The purpose of this study is to set up a mathematical erosion model based on physical principles of hydraulics, sediment transport, and erosion mechanics. The modification of this model will be accomplished through laboratory study. The purpose of the model is to predict sediment loads and erosion in surface-mined areas.

CHAPTER II

LITERATURE REVIEW

Physical Process of Water Erosion

More than thirty years ago, Ellison defined soil erosion as "a process of detachment and transportation of soil material by erosive agents" (Ellison, 1947). For erosion by water, these agents are rainfall and run-off. He pointed out that each has both a detaching and transporting capacity, and that these must be studied separately. Similarly, the soil erodibility can be divided into its detachability and transportability components. This report also suggests an approach to erosion simulation that considers (a) soil detachment by rainfall (D_R), (b) transport by rainfall (T_R), (c) soil detachment by runoff (D_F), and (d) transport by runoff (T_F) as separate but interrelated phases of the process of soil erosion by water (Fig. 1). The dynamics of each phase then may be described by fundamental hydraulics, hydrology and other physical relationships plus parameters describing the soil properties that influence erosion. Based on the definition, the mechanics of erosion are composed of four subprocesses: D_R, D_F, T_R, T_F. Although not all subprocesses occur on all source areas, each has its part in the total erosion process. Meanwhile, Meyer et al. (1975) indicated that erosion processes can be divided into interrill erosion and rill erosion according to the source of the eroded sediment. In general, runoff on erodible soil surface concentrates in many small, definable flow concentrations called rills. Erosion occurring in these small channels is defined as rill erosion, while erosion occurring on the areas between the rills is defined as interrill erosion (Meyer et al., 1975). Based on this definition, the erosion process begins when soil particles or aggregates are detached from the soil mass.

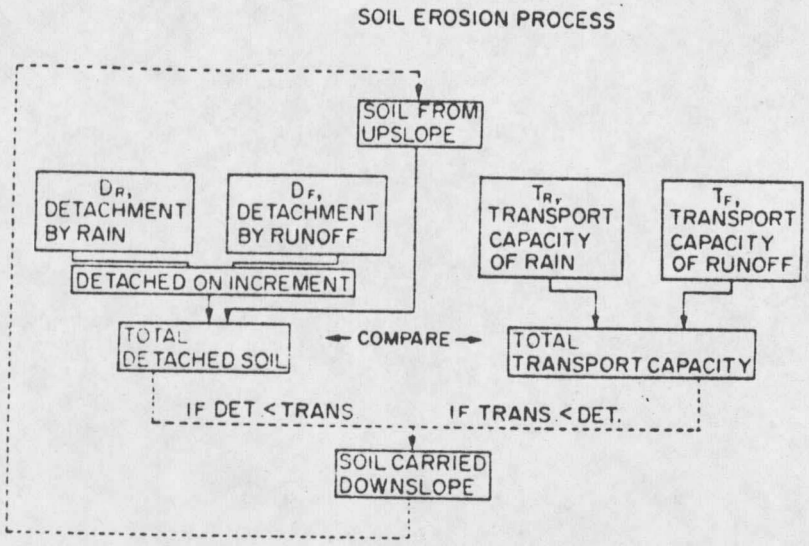


Figure 1. Possible interaction between transport and detachment processes (from Meyer and Wischmeier, 1969).

Basically, raindrop impact is the dominant factor in the detachment of soil particles on interrill areas. Raindrop impact is a major producer of sediment and can easily detach more sediment than overland flow on short slopes. Individual raindrops strike the soil surface, creating very intense hydrodynamic forces at the point of impact. Overland flow detaches and/or transports soil particles when its erosive forces exceed the resistance of soil to erosion. Detachment by raindrops occurs over a broad area, transportation by flow is often concentrated in small definable channels, such as rills. As a result, raindrop impact and very thin overland flow combine to transport detached soil particles to the concentrated flow channels. In general, detachment on interrill areas by flow will be small enough to be neglected since flow's shear stress is small because of the shallow water depth and small flow rates which occur on interrill areas. Interrill soil particles will be detached, however, by raindrop and transported by runoff.

Erosion and Sedimentation Problems

Erosion and sediment load is the most critical problem in watershed management. Erosion problems are localized and related to construction, forest harvest, mining, overgrazing, and other human activity. Erosion and resultant sediment loads from both natural and man-made sources are widely regarded as the greatest source of water pollution in the United States. Sediment is displaced soil—the smaller particles of displaced soil can be transported longer distances and remain suspended in water for longer periods of time. This suspended sediment causes turbidity that degrades the usefulness of water for many purposes and increases the costs of water quality treatment. The following is a list of some detrimental effects caused by erosion (EPA, 1976).

(1) Occupies water storage in reservoirs

(2) Fills, lakes and ponds

(3) Clogs stream channels

(4) Settles on productive land

(5) Destroys aquatic habitat

(6) Creates turbidity that detracts from recreational use of water and reduces photosynthetic activity

(7) Degrades water for consumptive uses

(8) Increases water treatment costs

(9) Damages water distribution systems

(10) Acts as a carrier of other pollutant (plant nutrients, insecticides, herbicides, heavy metals)

(11) Acts as a carrier of bacteria and viruses.

The annual damage from sediment in streams was estimated to be $262 million in 1966 (Stall, 1966). The breakdown of this cost is shown in Figure 2.

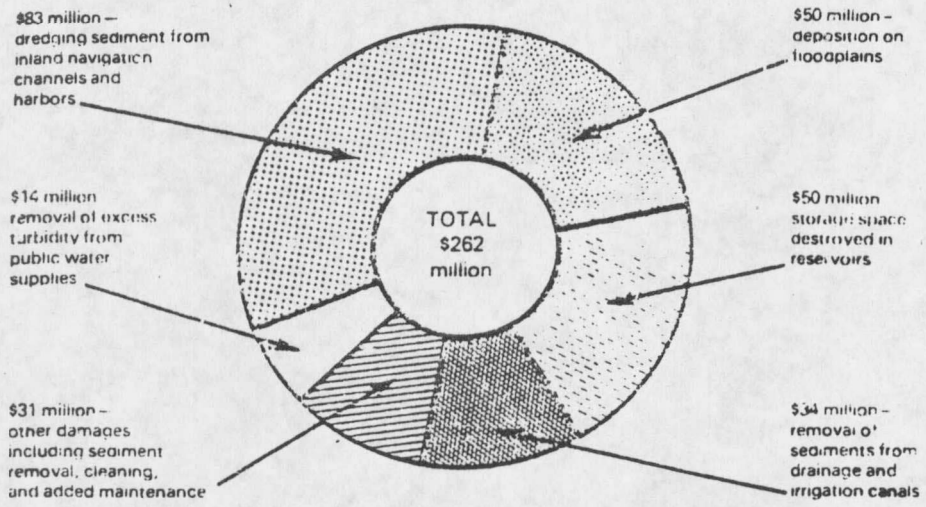


Figure 2. Annual costs of sediment pollution.

Approximately 3.6×10^9 tons of sediment are produced by erosion in the United States annually. About 1.8×10^9 tons of this amount reaches stream systems. About 1.18×10^9 tons are trapped in reservoirs, and some 0.72×10^9 tons reach tidewater. It is estimated that 50% of the sediment comes from agricultural land, 30% from geologic erosion, 10% from range and forest land and 10% from construction, roads, and mining (Highfill and Kimberlin, 1977). Construction and surface mining, though not as widespread, can produce large quantities of sediment to nearby waterways, causing severe adverse effect. Table 1 lists representative rates of erosion from various types of land use (EPA, 1976). It can be seen that on the basis of a uniform area of disturbance, active surface mining operations and construction operations have the highest rates of erosion.

Table 1. Representative Rates of Erosion from Various Land Uses.

Land use	Metric tons per km² per year	Tons per mi² per year	Relative to forest = 1
Forest	8.5	24	1
Grassland	85.0	240	10
Abandoned surface mines	850.0	2,400	100
Cropland	1,700.0	4,800	200
Harvested forest	4,250.0	12,000	500
Active surface mines	17,000.0	48,000	2,000
Construction	17,000.0	48,000	2,000

Source: *Methods for Identifying and Evaluating the Nature and Extent of Nonpoint Sources of Pollutants*, EPA 4030/9-73-014. Washington, D.C., U.S. Environmental Protective Agency, Oct. 1973.

Water Erosion Models Classification and Discussion

Soil erosion as a problem, and soil erosion models, have been concerned with agricultural areas. Hence, many different types of models have been developed for estimating soil losses (see Table 2) (Morgan, 1979). Most of the models used in soil erosion studies are of the parametric gray-box type (where some detail of how the system works is known). They are based on defining the most important factors, measuring them, and using statistical methods, relating them to measurement of soil erosion. Black-box models (where only main inputs and outputs are studied) most commonly rely on multiple regression methods, usually with logarithms of sediment yield and other variables to produce a multiplicative regression form of predicting equation similar to that of the Universal Soil Loss Equation (USLE). This equation is the basic erosion model that has been the most widely applied and tested site by site (USDA, 1978; SCSA, 1976). Although the improvement of the USLE over the past few years has been significant, very few attempts have been made to apply USLE to soil erosion prediction on surface-mined areas. Meanwhile, due to a lack of knowledge of modern erosion control technology in surface-mined areas and a lack of information from the surface-mined areas, accelerated soil losses from surface-mined areas continue to be a national problem.

Table 2. Types of Models.

Type	Description
Physical	Scaled-down hardware models usually built in the laboratory; need to assume dynamic similitude between model and real world.
Analogue	Use of mechanical or electrical systems analogous to system under investigation, e.g., flow of electricity used to simulate flow of water.
Digital	Based on use of digital computers to process vast quantities of data.
(a) Deterministic	Based on mathematical equations to describe the processes involved in the model, taking account of the laws of conservation of mass and energy.
(b) Stochastic	Based on generating synthetic sequences of data from the statistical characteristics of existing sample data; useful for generating input sequences to deterministic and parametric models where data are only available for short period of observation.
(c) Parametric	Based on identifying statistically significant relationships between assumed important variables where a reasonable data base exists. Three types of analysis are recognized: *black-box*: where only main inputs and outputs are studied; *gray-box*: where some detail of how the system works is known; *white-box*: where all details of how the system operates are known.

After Morgan (1979).

The available models for predicting soil erosion by raindrop impact and overland flow transportation are mainly based on statistical analysis of observed data from experimental field watershed plots. In recent years, it has been realized that this approach is less than satisfactory meeting another important objective of models, that is increasing our understanding of how the erosion system functions and responds to changes in the controlling factors. Hence, the model with physical meaning seems to be more useful, effective and meaningful than the regression model. In addition, since the USLE was designed for use on field size areas, even though it was also tested on construction sites (Clyde et al., 1976), it can result in errors on surface-mined areas. These errors may be due to mining operations, top-soiling, overburden selection and other actions associated with post-mine reclamation.

For land use planning, modification of USLE for predicting soil erosion on surface-mined areas is necessary. Greatest emphasis is being placed today on developing deterministic models or white-box parametric models (where all details of how the system operates are known). As a result, a switch is occurring, from using statistical analysis to employing mathematical simulations which frequently require the solution of partial differential equations. Stochastic models are needed to generate a sample sequence of events drawn from a known underlying distribution. As a forecasting tool they can be used for generating sediment yield directly (Woolhiser and Todorovic, 1971). In principle, stochastic rainfall inputs may also be linked to many physical bases or black-box parametric models to generate the time distribution of sediment yield and extrapolate from actual measurement periods to average years. Established hydrology, stochastic sediment models have tended to predict yields for drainage basins rather than hillslope plots (Kirkby and Morgan, 1980). Their range of application is therefore complementary to that for physically-based models, which have much more potential for the experimental plots study. Hence, before selecting an approach to modelling, the scale of study must be considered. The detail requirements for modelling erosion over a large drainage basin are different from those required by a short length of hillslope or at the point of an individual raindrop impact. So the success of erosion predicting models depends on how closely and accurately the estimate correlates with rates of erosion measured in the field, particularly with regard to the physical process of raindrop and runoff (overland flow).

Mining Reclamation and Water Erosion Related Problems

Coal is one of the major energy sources in the United States whose extraction rate can be increased in the event of a worldwide energy shortage. The United States possesses about 31% of the world's known coal reserves. One-third of these deposits can be extracted by surface mining (Hayes, 1979). Total coal reserves are estimated at 4,365 billion tons

(Averitt, 1975). Of this total, 482 billion tons lie less than 300 m below the surface and exceed 0.7 m in thickness. Thirty-two percent of this total, underlying 4 million ha, is considered minable by surface mining operations (Ward and Haan, 1980). Almost 50% of the total U.S. coal reserves is deposited in the Northern Great Plains (Table 3) (Averitt, 1975). Most coal deposited in this area are either lignitic or subbituminous, both of which contain less energy than bituminous coal, however, much of the coal is low in sulfur. It also occurs in thick seams relatively close to the surface. Owing to these features and low extraction cost, the demand for this coal has precipitated increased mining operations. Hence, extensive areas have been disturbed by surface mining activities (Schaller and Sutton, 1978). Several reports indicate that surface mining operations, haul road construction and timber operations increase sediment production by 100 to 2,000 times that from a forest area (Ward and Haan, 1980; EPA, 1976; Curtis, 1971). In the East, erosion rates on active mines may average 10 times that on cropland and 200 times that on grassland (Anderson and Briggs, 1979).

Table 3. Coal Reserves in the Northern Great Plains.*

State	Total estimate	Recoverable by mining
	----------tons × 10^6----------	
Colorado	434,211	870
Montana	421,639	42,563
North Dakota	530,602	16,003
South Dakota	3,185	428
Wyoming	935,943	23,674

*Source: Averitt, 1975.

Surface mining potentially could create water erosion problems. The major sources of these problems in surface mining are (1) areas being cleared, grubbed, and scalped, (2) haul and access roads, (3) spoil piles, (4) areas of active mining, and (5) areas being reclaimed. Theoretically, the problems related to water erosion and sedimentation can be described (EPA, 1976).

Areas are being cleared, grubbed and scalped: Factors contributing to water erosion in this area are (a) failure to install perimeter control measures prior to the start of cleaning and grubbing, (b) the destruction of natural soil structure, removal of natural vegetation and exposure of disturbed soil on steep slopes for an excessive length of time, (c) over-clearing—clearing too far above the high wall or below the outcrop line, (d) improper placement and/or protection of salvaged and stockpiled topsoiling material, (e) creation during clearing and grubbing operations of a soil surface that impedes infiltration and/or concentrates surface runoff. Hence, where erosion continues to expose new materials which are easily weathered, this process may go on indefinitely, causing serious erosion problems.

Haul and access roads: Roadways are one of the major sources of sediment from surface mining operations. They generally remain a source of sediment throughout the life of the mine. Roadways serve to intercept, concentrate and divert surface runoff. Long distance roadways significantly disrupt and intercept natural drainage and hydraulic systems. This results in severe soil losses from roadway surfaces, ditches, and cut slopes. Factors contributing to soil losses from haul and access roads are: (a) poor location of the roadway, resulting in more adverse conditions, (b) improper construction of roadbed, (c) improper layout and construction of drainage structures, (d) poor maintenance practices, (e) inadequate stabilization of cut and fill slopes, and (f) failure to protect safety berms. Table 4 provides an interesting comparison between the rates of erosion for different areas (EPA, 1976).

Spoil piles: At surface-mined areas, the unreclaimed and new reclaimed spoil piles are easily weathered and subjected to water erosion since loose, disturbed materials are less stable than the original consolidated strata. Also water infiltration and movement through spoils usually decrease as bulk density increases. Typical bulk density in undisturbed overburden ranges from 1.4 to 1.7 grams per cubic centimeter, whereas the bulk density of spoils usually vary from 1.1 to 1.4 grams per cubic centimeter (Power et al., 1978). Spoil

Table 4. Comparative Rates of Erosion.

Area	Yields (tons/mi²)	Factor
Unmined watershed	28	1
Mined watershed	1,930	69
Spoil bank	27,000	938
Haul road	57,600	2,065

Sources from EPA, 1976.

piles are usually smoothed with a bulldozer and overburden is commonly removed and piled with a dragline, both operations cause packing near the center axis of the piles and lesser packing on the outslopes, where materials are pushed or slide downslope. This uneven bulk density distribution within spoils may result in uneven settling and erosivity. Sandy spoils are sometimes severely compacted by heavy machinery, but due to the low water holding capacity of such spoils and to dry climatic situations, heavy equipment seldom causes severe compaction. The bulk density of spoil varies widely as a result of compaction. Also steep slope gradient of spoil piles increase the likelihood of runoff and erosion (Table 5). Slope length on many smoothed spoils may reach several hundred meters. This contributes to concentrated surface runoff and increases erosion.

Table 5. Run-off Soil Losses* on Unmined Rangeland and on Vegetated Mine Spoil (From Power et al., 1978).

Material	Slope (%)	Treatment	Runoff (in)	Soil loss (t/a)
Rangeland	9.0	none	0.59	0.09
Spoils	4.6	none	1.50	2.2
	10.0	none	1.69	5.3
	17.0	none	2.21	5.4
	10.4	topsoil (10")	1.81	31.7
	10.4	topsoil + straw	0.71	0.8

*4" of water in 4 hours added with artificial rainfall simulator.

Areas of active mining: Most intensive erosion problems occur during active mining. Soil disturbance occurs almost daily, and protective cover cannot be maintained. Four principles have been proposed by Anderson and Briggs (1979) for planning erosion control

during active mining. The first is to keep clean water clean. Runoff water from undisturbed areas should be diverted away from the active mining area so that it does not come in contact with disturbed materials. The second principle is to disturb as small an area as possible in order to minimize material handling and reduce sedimentation loads from mining areas. The third principle is to provide temporary cover on areas, such as stockpiles and road cuts, that must be disturbed for extended periods before final reclamation. The fourth principle is to provide sediment removal structures, such as sediment traps or basins and rock or vegetative filters, which can keep sedimentation discharge in the disturbed area. Otherwise, loss of soil from the active mining area due to rainfall and runoff can become a serious problem. Active mining areas can also change surface topography, disturb natural drainage systems, and change microclimates within watersheds at mining areas. Disturbed stockpiles yield water soluble products which are transported by surface runoff and may result in water pollution or be leached to degrade groundwater quality.

Areas being reclaimed: In the past reclamation referred to any process necessary to return the land to a useful purpose or to meet the requirements of state laws. Under the new federal law, reclamation is the process of returning surface mined land to a condition and/or use equal to or higher than that prior to mining (Persse et al., 1977). Public Law 95-87, the Surface Mining Control and Reclamation Act of 1977 (Sweeney, 1977), established nationwide standards for surface mining activities requires that all runoff water from areas disturbed by mining pass through a sediment pond before leaving the permit area. Although reclamation is a means of achieving overall environmental benefit, certain reclamation activities can be a major source of damaging sediment if they are not performed properly. From the standpoint of potential sediment damage, the most crucial stage in the reclamation of spoil areas is from the start of grading operations to the stabilization of the minesoil with vegetation or other engineering measures, because the entire grading area and portions of spoil piles along the perimeter become a critical source of erosion. These

conditions are very significant where area mining is performed. Especially the construction of excessively long steep slopes and the failure to stabilize grading areas can influence soil loss and offsite damage. Measures taken to revegetate the graded spoil, control runoff, reestablish soil conditions and groundwater hydrology, and stabilize land use capability will also have a major influence on soil loss. Most of these practices are thus an essential part of successful reclamation. The seriousness of on-site damage caused by erosion usually is greater on a reclaimed soil than on natural soil because of the absence of a well-developed topsoil and the presence of incompletely leached subsoils, which may become toxic upon exposure. So the effectiveness of erosion and sediment control practices on reclaimed areas depend on their compatibility with the surrounding topography and drainage system and with the projected land use capability of the reclaimed area.

CHAPTER III

METHODS AND PROCEDURES

Site Characterization

The site selected for this study was the Western Energy Company Rosebud Mine (Fig. 3). It was chosen as a study site due to its recent sedimentation problems and its relatively continuous and largely varied mining history since the Northern Pacific Railroad began mining coal to supply fuel for its steam locomotives in 1923. Also, Western Energy Company has mined 788 million tons of low-sulfur sub-bituminous coal and disturbed approximately 3200 acres of land in Colstrip since 1968 (Coenenberg, 1982).

Selection of Sites for Sample Collection

In selecting samples for this study, Dr. Frank Munshower, head of the Reclamation Research Unit at Montana State University and the environmental coordinator in Western Energy Coal Company were contacted to find out which mining areas might be the best suited for this study. Three criteria were met to select soil samples: (1) sites should be undisturbed, (2) soil samples should typically represent the common soil characteristics of this research area, (3) the soil sample should be selected from a benchmark soil for which laboratory data are available. Locations of soil sampling sites are shown on Figure 4. The sampling sites included Chinook-I located a mile northwest of Colstrip and Boxwell-2 located 2 miles northeast. The Chinook-I samples were taken from the A-horizon, and the Boxwell-II sample was from the B-horizon. Soil characteristics data were available for both soils (Schafer et al., 1979). These are shown on Tables 6 and 7.

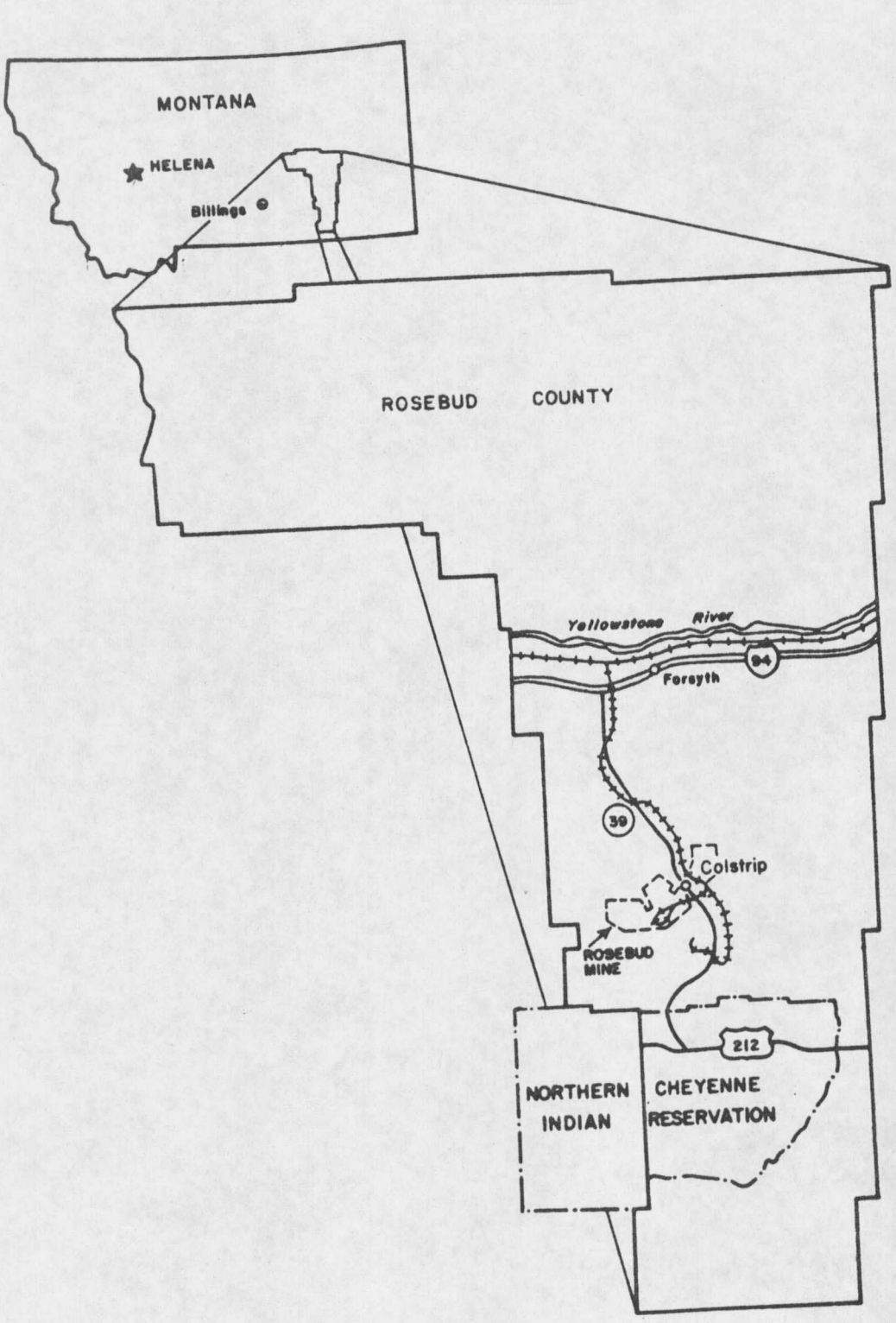


Figure 3. Map showing Colstrip study area location.

Site Description

The Western Energy Rosebud mine Company is located in southeastern Montana near the town of Colstrip which lies in the northern portion of the Powder River Basin in the Northern Great Plains physiographic province. It is about 30 miles south of Forsyth, Montana (see Fig. 4).

The Colstrip area is located within the eastern Montana unglaciated sedimentary plains. The predominant underlying bedrock is Fort Union Formation which is divided into the Tullock, Lebo, and Tongue River Members in southeastern Montana. The basal Tullock member of the Fort Union contains an abundance of sandstone and thin coal deposits. The Lebo member consists of shale and mudstones deposited in a fluvial environment. The Tongue River member of the Fort Union Formation is composed of some of the most extensive reserves of coal in the world. Claystones in the Tongue River member contain a mixture of illite and kaolinite with lesser amounts of smectite (Schafer et al., 1979). Therefore, the Fort Union Formation is composed of light colored sandstone, sandy shale, carbonaceous shale, and sub-bituminous coal.

The soils in the Colstrip area are weakly developed and usually coarse-loamy or fine-loamy in texture. Most of them are in a soil transition zone of Aridsols, Alfisols and Mollisols. Aridisols increase in abundance in the southern Powder River Basin where the climate is drier. Mollisols are common in the moister Great Plains of North and South Dakota to the east. Alfisols occur in the neighboring Big Horn Mountains and Black Hills regions. Entisols are locally common due to steep slope and recent fluvial activity. Major soil subgroups in the Colstrip area are Ustic Torriorthents, Borollic Camborthids, and Aridic Haploborolls (Schafer et al., 1979).

The vegetation in the Colstrip region is dominated by mixed-grass prairie and Ponderosa pine savannah vegetation type. Typically the area is a mosaic of mixed prairie grassland and pine woodland with localized areas of riparian vegetation. The major grasses in this

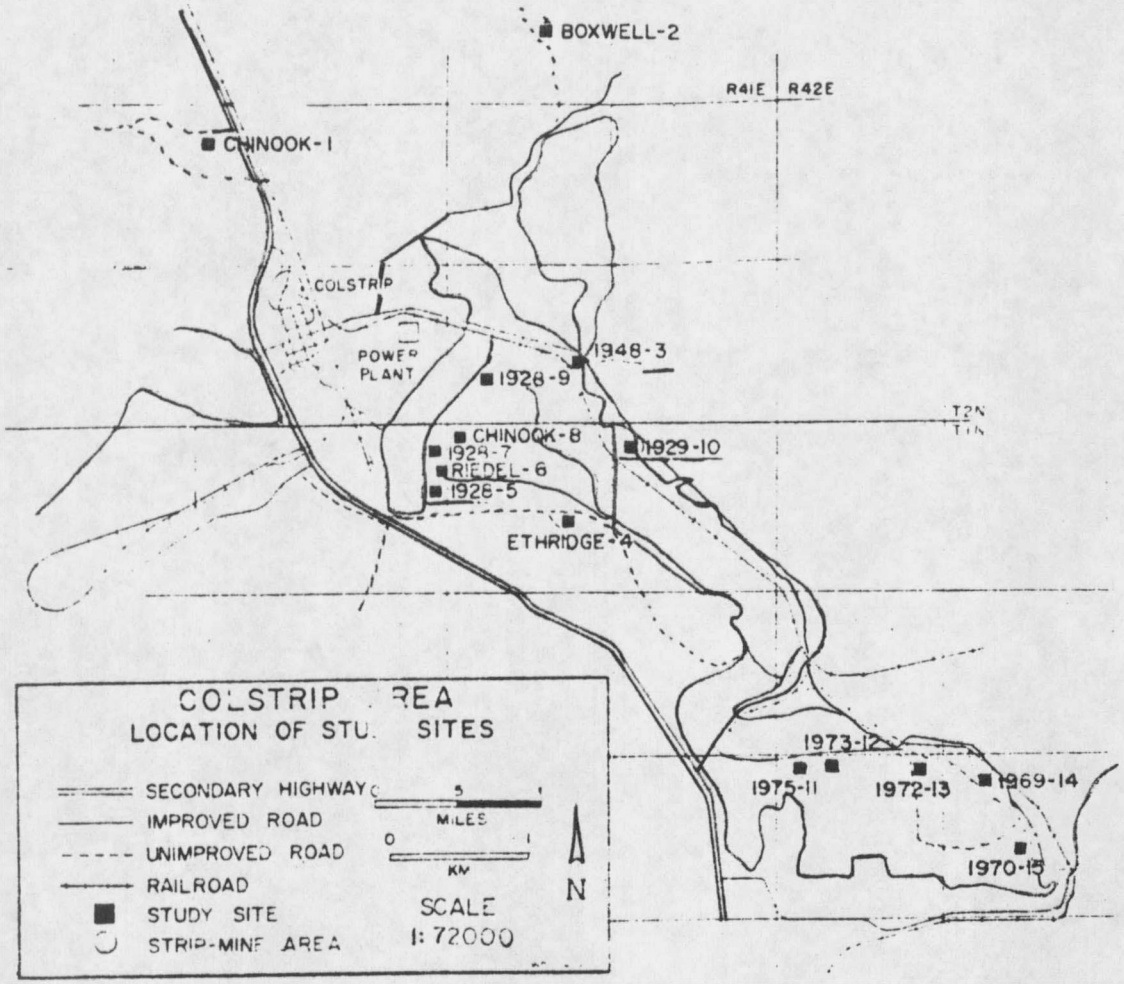


Figure 4. Location of Chinook-1 and Boxwell-2 sites near Colstrip, Montana. The site names represent the soil series (from Schafer et al., 1979).

Table 6. Laboratory Analysis of Boxwell-2 Soil (from Schafer et al., 1979).

SOIL CLASSIFICATION-BOROLLIC CAMBORTHID
FINE-LOAMY, MIXED
SERIES - - - - - - -YAMAC (Boxwell-2)

U. S. DEPARTMENT OF AGRICULTURE
SOIL CONSERVATION SERVICE, NTSC
NATIONAL SOIL SURVEY LABORATORY
LINCOLN, NEBRASKA

SOIL NO - - - - - - S76MT-087-2 COUNTY - - - ROSEBUD

GENERAL METHODS- - -1A, 1B1B, 2A1, 2B SAMPLE NOS. 76P0538-76P0549

DEPTH	HORIZON	PARTICLE SIZE ANALYSIS, LT 2MM, 3A1, 3A1A, 3A1B															RATIO
					FINE	SAND					SILT			FAML	INTR	FINE	NON-	8D1
		SAND	SILT	CLAY	CLAY	VCOS	CORS	MEDS	FNES	VFNS	COSI	FNSI	VFSI	TEXT	II	CLAY	CO3-	15-
		2-	.05-	LT	LT	2-	1-	.5-	.25-	.10-	.05	.02	.005-	SAND	.2-	TO	CLAY	BAR
		.05	.002	.002	.0002	1	.5	.25	.10	.05	.02	.002	.002	2-.1	.02	CLAY		TO
CM		PCT LT 2MM														PCT	PCT	CLAY
000-001	A11	48.7	36.4	14.9		.2	2.5	2.5	22.4	21.1	24.3	12.1		27.6			15	.86
001-002	A12	48.9	39.1	12.1		.4	.5	1.6	23.1	23.3	25.5	13.6		25.6			12	.68
002-005	A13	49.0	37.9	13.1		.2	.4	1.3	22.2	24.9	25.4	12.5		24.1			13	.44
005-010	A14	49.1	37.6	13.3		.1	.4	1.4	23.3	23.9	24.4	13.2		25.2			13	.43
010-022	A15	46.9	33.8	19.3		.1	.2	1.1	22.3	23.2	23.5	10.3		23.7			19	.38
022-038	B21	48.7	31.0	20.3		TR	.2	1.1	23.8	23.6	21.1	9.9		25.1			20	.41
038-050	B22	49.3	30.9	19.8		.1	.1	.9	22.5	25.7	20.9	10.0		23.6			20	.40
050-060	B23	47.1	33.2	19.7		.1	.1	.8	19.4	26.7	22.9	10.3		20.4			20	.41
060-075	B3CA	38.1	35.3	26.6		TR	.1	.6	12.8	24.6	24.3	11.0		13.5			20	.35
075-100	C1CA	42.3	34.9	22.8		TR	.1	.3	11.5	30.4	22.0	12.9		11.9			17	.36
100-145	C2	46.3	34.7	19.0		.0	.1	.3	13.3	32.6	21.9	12.8		13.7			19	.38
000-005	(A)																	

DEPTH	(PARTICLE SIZE ANALYSIS, MM, 3B, 3B1, 3B2)					(BULK DENSITY					(WATER CONTENT			CARBONATE		(PH	
	VOL.	WEIGHT															
	GT	GT															
	2	75			.074					1/10	1/3-	15-	WRD	2	.002	1/1	1/2
	MM	MM	75-20	20-5	5-2	LT	20-2	1/3-	OVEN	COLE	BAR	BAR	BAR	CM/				
CM	PCT	PCT	PCT	PCT	PCT	LT 75	LT20	BAR	DRY		PCT	PCT	PCT	CM	PCT	PCT	H2O	CACL
000-001	TR	0	0	TR	TR		TR	1.1 B					12.8				7.0	6.3
001-002	TR	0	0	TR	TR		TR	1.1 B					8.1				6.5	5.9
002-005	TR	0	0	TR	TR		TR	1.1 B					5.8				6.3	5.6
005-010	TR	0	0	TR	TR		TR	1.2 B					5.7				6.2	5.6
010-022	TR	0	0	0	TR		TR	1.43	1.48	.003		14.7	7.4	.10			6.4	5.9
022-038	TR	0	0	TR	TR		TR	1.59	1.67	.012		16.8	8.4	.13			6.6	6.1
038-050	0	0	0	0	0		0						7.9		TR		6.9	6.3
050-060	0	0	0	0	0		0						8.1		3		8.0	7.5
060-075	0	0	0	0	0		0	1.62	1.77	.028		14.2	9.3	.08	18	7	8.4	7.9
075-100	0	0	0	0	0		0						8.2		21	6	8.6	8.1
100-145	0	0	0	0	0		0	1.48	1.61	.028		19.4	7.2	.18	15		8.7	8.1
000-005								1.10	1.23	.040		21.3						

DEPTH	(ORGANIC MATTER)			IRON	PHOS	(EXTRACTABLE BASES 5B4A-)					ACTY	AL	(CAT EXCH)		RATIO	RATIO	CA	(BASE SAT)	
	6A1A	6B1A		6C2B		6NZE	6O2D	6P2B	6Q2B		6H1A	6G1E	5A3A	5A6A	8D1	8D3	5F1	5C3	5C1
	ORGN	NITG		EXT		CA	MG	NA	K	SUM	BACL	KCL	EXTB	NHAC	NHAC	CA	SAT	EXTB	NHAC
	CARB			FE						EXTB	TEA	EXT	ACTY		TO	TO	NHAC	ACTY	
CM	PCT	PCT	C/N	PCT	TOTL PCT	MEQ				/ 100	G				CLAY	MG	PCT	PCT	PCT
000-001	3.47	.376	9			13.7	4.4	TR	1.4	19.5	5.0		24.5	18.2	1.22	3.1	75	80	107
001-002	2.32	.207	11			8.2	2.9	.0	1.0	12.1	4.3		16.4	13.5	1.12	2.8	61	74	90
002-005	1.30	.118	11			5.8	2.2	.0	.7	8.7	3.4		12.1	10.5	.80	2.6	55	72	83
005-010	1.14	.106	11			6.7	2.1	.0	.7	9.5	3.2		12.7	11.0	.83	3.2	61	75	86
010-022	.88	.089	10			8.2	3.2	.0	.8	12.2	2.9		15.1	14.0	.73	2.6	59	81	87
022-038	.66	.071	9			8.1	4.4	.0	.5	13.0	2.6		15.6	15.4	.76	1.8	53	83	84
038-050	.56	.063	9			8.1	5.3	.0	.0	13.4	1.9		15.3	14.7	.74	1.5	55	88	91
050-060	.58	.070	8				8.5	.0	.4					13.9	.71				
060-075	.40	.046	9				8.9	.0	.4					11.0	.41				
075-100	.25	.029	9				13.8	.0	.3					10.1	.44				
100-145	.22	.022	10				17.1	.1	.3					10.6	.56				
000-005																			

DEPTH	(SATURATED PASTE)			NA	NA	SALT	GYP	(SATURATION EXTRACT BAI-										ATTERBERG	
	8E1	8C1B	8A	5D2	5E	8D5	6F1A	8A1A	6N1B	6D1B	6P1B	6W1B	6J1A	6J1A	6K1C	6L1C	6M1C	4F1	4F2
	REST	PH	H2O	ESP	SAR	TOTL		EC	CA	MG	NA	P	CO3	HCO3	CL	SO4	NO3	LQID	PLST
	OHM-					SOLU		MMHOS/										LMIT	INDX
CM	CM		PCT	PCT		PPM	PCT	CM	(- - - - - - - - - - MEQ / LITER - - - - - - - - - -)									PCT	
000-001		6.4	75.0			1000		1.71	11.5	7.3	.1	2.7	.0	16.8	.5	.8	.0		
001-002								.10C											
002-005								.10C											
005-010								.10C											
010-022								.10C											
022-038								.10C										28	9 D
038-050								.10C											
050-060								.20C											
060-075								.20C											
075-100	3900	8.4						.20C											
100-145	3700	8.3	39.2	1	1	100		.36	.6	2.1	1.0	.1	.0	2.5	.1	.5	.1	28	9 D
000-005																			

(A) CLOD OF A11, A12, AND A13 FOR BULK DENSITY AND MOISTURE RETENTION.
(B) ESTIMATE.
(C) 1:2 SOIL WATER RATIO.
(D) BY SOIL MECHANICS LABORATORY, USDA, LINCOLN, NE.

Table 7. Laboratory Analysis of Chinook-1 Soil (from Schafer et al., 1979).

SOIL CLASSIFICATION-ARIDIC HAPLORGSOLL
COARSE-LOAMY, MIXED
SERIES - - - - - - -CHINOOK

U. S. DEPARTMENT OF AGRICULTURE
SOIL CONSERVATION SERVICE, MTC.
NATIONAL SOIL SURVEY LABORATORY
LINCOLN, NEBRASKA

SOIL NO - - - - - - S76MT-087-1 COUNTY - - - ROSEBUD

GENERAL METHODS- - -1A, 1B1B, 2A1, 2B SAMPLE NOS. 76P0534-76P0537

DEPTH	HORIZON	PARTICLE SIZE ANALYSIS, LT 2MM, 3A1, 3A1A, 3A1B															RATIO
					FINE	SAND					SILT			FRAG	INTR	FINE	NON-	8D1
		SAND 2- .05	SILT .05- .002	CLAY LT .002	CLAY LT .0002	VCOS 2- 1	COS 1- .5	MEDS .5- .25	FNES .25- .10	VFNS .10- .05	COSI .05- .02	FNSI .02- .005	VFSI .005- .002	TEXT SAND 2-.1	.2- .02	CLAY TO CLAY	CO3- CLAY	15- BAR TO CLAY
CM		PCT LT 2MM														PCT	PCT	
000-010	A1	66.8	23.1	10.1		.3	.5	3.4	43.6	19.0	14.2	8.9		47.8			10	.62
010-050	B2	67.4	20.7	11.9		.3	.8	3.9	45.8	16.6	8.7	12.0		50.8			12	.45
050-100	B3CA	68.8	18.6	12.6		.8	.7	3.5	45.5	18.3	11.7	6.9		50.5			13	.43
100-200	2A1B	55.9	26.2	17.9		.1	.6	3.5	37.2	14.5	14.0	12.2		41.4			18	.51

DEPTH	(PARTICLE SIZE ANALYSIS, MM, 3B, 3B1, 3B2)					BULK DENSITY				WATER CONTENT			CARBONATE		(- -PH - -)	
	VOL. (- - - - - WEIGHT - - - - - -)					4A1D	4A1H	4D1	4B1C	4B1C	4B2	4C1	6E1B	3A1A	8C1A	8C1E
	GT 2	ST 75	75-20	20-5	5-2	LT .074	20-2	1/3-BAR	OVEN DRY	COLE	1/10 BAR	1/3-BAR	15-BAR	WRD CM/	LT 2	LT .002	1/1 H2O	1/2 CACL
CM	PCT	PCT	(- - - PCT LT 75 - - -)			LT20	G/CC	G/CC			PCT	PCT	PCT	CM	PCT	PCT		
000-010	TR	0	0	TR	1	1	1.3 A						6.3		TR		7.7	7.4
010-050	1	0	0	1	1	2	1.41	1.41	.000		10.9	5.4	.08		4	TR	8.2	7.7
050-100	2	0	0	1	2	2	1.4 A					5.4			12	TR	8.5	8.0
100-200	TR	0	0	TR	TR	TR	1.31	1.40	.023		17.0	9.1	.11		8	TR	9.0	8.3

DEPTH	(ORGANIC MATTER)			IRON	PHOS	(- -EXTRACTABLE BASES 5B4A- -)					ACTY	AL	(CAT EXCH)		RATIO		CA	(BASE SAT)	
	6A1A ORGN CARB	6B1A NITG	C/N	6C2B EXT FE	TOTL	6N2E CA	6O2D MG	6P2B NA	6Q2B K	SUM EXTB	6H1A BACL TEA	6G1E KCL EXT	5A3A EXTB ACTY	5A6A NHAC	8D1 NHAC TO	8D3 CA TO	5F1 SAT NHAC	5C3 EXTB ACTY	5C1 NHAC
CM	PCT	PCT		PCT	PCT	(- - - - - - - - - - -MEQ / 100 G- - - - - - - - - - -)									CLAY	MG	PCT	PCT	PCT
000-010	1.93	.159	12			TR	TR	.5			.0			9.8	.97				
010-050	.85	.081	10			4.0	.0	.4						7.9	.66				
050-100	.58	.050	12			5.3	TR	.4						4.5	.36				
100-200	1.06	.039	27			24.7	.1	.4						6.0	.34				

DEPTH	(SATURATED PASTE)			NA	NA	SALT	GYP	(- - - - - - - - - SATURATION EXTRACT 8A1- - - - - - - - -)									ATTERBERG	
	8F1 RESI OHM-	8C1B PH	8A H2O	5D2 ESP	5E SAR	8D5 TOTL SOLU	6F1A	8A1A FC	6N1B CA	6O1B MG	6P1B NA	6Q1B K	6I1A CO3	6J1A HCO3	6K1C CL	6L1C SO4	6M1C NO3	4F1 LQID LMIT	4F2 PLST INDX
CM	CM		PCT	PCT		PPM	PCT	MMHOS/CM	(- - - - - - - - - - MEQ / LITER - - - - - - - - - -)								PCT	
000-010		7.2	42.7			410		1.24	8.6	5.5	.1	.8	.0	12.2	.3	.9	.4		
010-050								.208											
050-100	7800	8.2	28.7			80		.40	1.6	2.0	.1	.5	.0	3.5	.1	.4	.0		
100-200	5000	8.8	34.3		1	150		.63	.3	4.5	1.7	.5	.0	4.7	.1	1.1	.2	26	7 C

(A) ESTIMATE
(B) 1:2 SOIL WATER RATIO.
(C) BY SOIL MECHANICS LABORATORY, USDA, LINCOLN, NE.

area are cool-season but some warm-season grasses are also present, especially in localized areas (Coenenberg, 1982). Mixed prairie sites produce from 1000-1800 kg/ha/yr, with mean production near 1500 kg/ha/yr (Munshower and Depuit, 1976).

The primary land use in the Colstrip area is livestock grazing on the grassland region. A limited amount of native rangeland has been converted to agricultural land uses including hay pasturage and cereal grain production. An increasing amount of land around the townsite is being used for urban development including single and multi-family dwellings, schools, commercial developments, parks, and roads. Power generating plants and associated settling ponds, cooling ponds, pipelines, and service roads occupy several hundred acres (Schafer et al., 1979).

The climate of Colstrip is semi-arid and continental with the mean monthly temperatures ranging from -5°C (23°F) to 24°C (73°F). The extreme temperature range fluctuated from -40°C to 44°C. The warmest month is July with mean daily temperature of 22°C. Average annual precipitation is 40.1 cm (15.8 inches) (NOAA, nd), about 30 cm of this occurs as rain during the period April to September. Approximately one-half of the annual precipitation falls in the months April through July. Fifteen cm of precipitation comes early in the growing season. Summer precipitation occurs as showers and high intensity thunderstorms. During the period 1928-1977, only 21.8 cm (8.6 inches) precipitation which occurred in 1934, the driest year, whereas 62.7 cm (24.7 inches) was recorded in 1944 the wettest year (Table 8).

Data Base Collection and Analysis (Experimental Study)

Soil erosion data collected from simulated rainfall plots consisted of four erosion-influencing variables at various levels: (1) slope steepness—1, 20, 40 and 60%; (2) rainfall intensity—1.5, 2.0 and 2.5 in/hr; (3) runoff rate—0, 21 and 42 cm^3/sec; and (4) soil texture—sandy loam, sandy clay loam and three mixed types of these two soils. These four

Table 8. Annual Precipitation at Colstrip, Montana for the Years 1928-1977.

Year	ppt (in)	Year	ppt (in)	Year	ppt (in)
		1941	17.7	1962	15.3
		1942	18.3	1963	17.8
		1943	17.7	1964	18.5
		1944	24.7	1965	14.3
		1945	13.8	1966	13.0
		1946	20.9	1967	17.2
		1947	11.3	1968	19.8
		1948	16.4	1969	17.6
1928	12.1	1949	11.9	1970	15.6
1929	12.0	1950	14.6	1971	19.2
1930	12.0	1951	14.8	1972	16.6
1931	11.3	1952	10.1	1973	16.9
1932	20.4	1953	19.3	1974	18.4
1933	18.2	1954	11.3	1975	—
1934	8.6	1955	17.5	1976	12.7
1935	16.7	1956	13.6	1977	16.1
1936	10.7	1957	18.4		
1937	12.0	1958	17.0		
1938	12.3	1959	10.5	Average 15.4 inches	
1939	14.3	1960	10.4	(39.1 cm)	
1940	19.7	1961	14.7		

*Source from NOOA, nd, and Schafer et al., 1979.

factors are related, respectively, to Universal Soil Loss Equation (USDA, 1978; SCSA, 1976; Meyer and Monke, 1965): the slope steepness factor (S); the rainfall factor (R) and the soil factor (K). These variables and levels of each were studied as a factorial set of treatments (Li, 1966). These variables were studied through the laboratory research which is described below.

Rainfall Simulator

Rainfall simulators have been used for many years by researchers to accelerate and extend their studies of erosion. Simulators make it possible to produce predetermined storms or rainfall intensity at any time and location, and make the replication of research

easier and facilitate the study of erosion processes. But it is difficult to accurately simulate raindrop size distribution and the impact velocity of natural rainfall, since the rainfall energy or momentum and terminal velocities of natural rainfall drops are too complicated to control. More complete reviews of rainfall simulators can be found in other publications (Meyer, 1958, 1965; Smith and Wischmeier, 1962; Mutchler and Hermsmeier, 1965; Dangler and El-Swaify, 1976; Barnett and Dooley, 1972; Grieson et al., 1977; USDA, 1981; Floyd, 1981).

The rainfall simulator used for this study (Figs. 5 & 6) was developed from University of California, Davis (Munn, 1971). This rainfall simulator is similar in concept to the polyethylene type drop formed by tubing tips presented by Chow and Harbaugh (1965). The rainfall unit is supported by a lightweight frame that provides a drop fall of 2.33-2.67 meters and that can be adjusted to fit slopes of up to 60%. A float system was added to supply reservoirs so that head pressure could be held constant and adjusted to desired levels. Water was supplied by a 20-liter carboy that sits above an airtight rainfall chamber with 827 drop forming polyethylene tubing tips. A carboy reservoir similar to that developed by Meeuwig (1971) is used to supply water to the rainfall chamber. Water is passed from the carboy through a 1.3 cm (½ inch) tube to a 1.3 cm (½ inch) gate valve and is then siphoned through a Manostat floatmeter into a five outlet manifold where it is distributed to the rainfall chamber. The plexiglass rainfall chamber is 76.2 X 76.2 X 2.5 cm (30 X 30 X 1 inch) and the drop formers cover a 71 X 71 cm (28 X 28 inch) area. The drop forming area gives 5.1 cm (2 inches) of overlap on each side of the plot to overcome possible errors in centering the chamber. The polyethylene drop formers are 2.2 cm (7/8 inch) long sections cut from 0.058-cm-inside-diameter (ID) and 0.097-cm-outside-diameter (OD) catheter tubing. Each tube extends 0.48 cm (3/16 inch) into the rainfall chamber to allow larger particles from the water supply to settle below, rather than plug the tubes; and to slow the rate of dripping while the valve is shut by reducing the head over the tubes. The

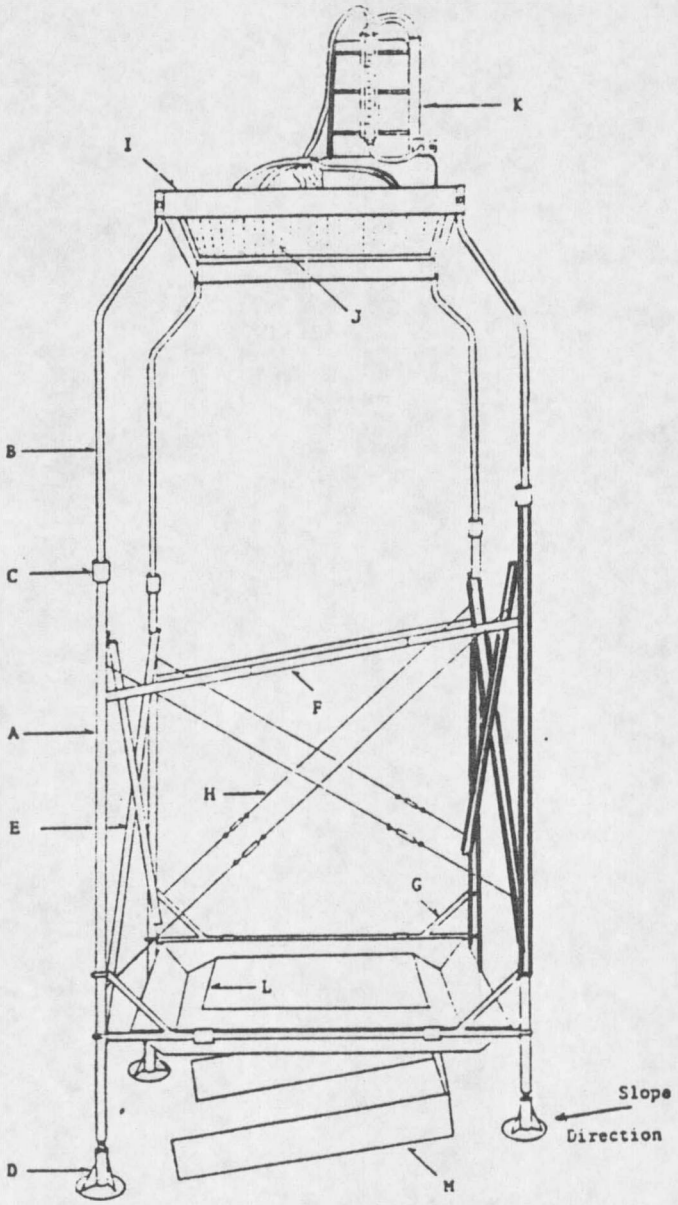


Figure 5. Sketch of the Tahoe Basin rainfall simulator. Legend: A, main support legs; B, adjustable legs; C, adjustment collars; D, adjustable pads; E, cross braces; F, adjustable side braces; G, side braces; H, adjustable chains; I, rainfall chamber frame; J, rainfall chamber; K, water supply reservoir; L, gutter trough; M, plot perimeter shield.

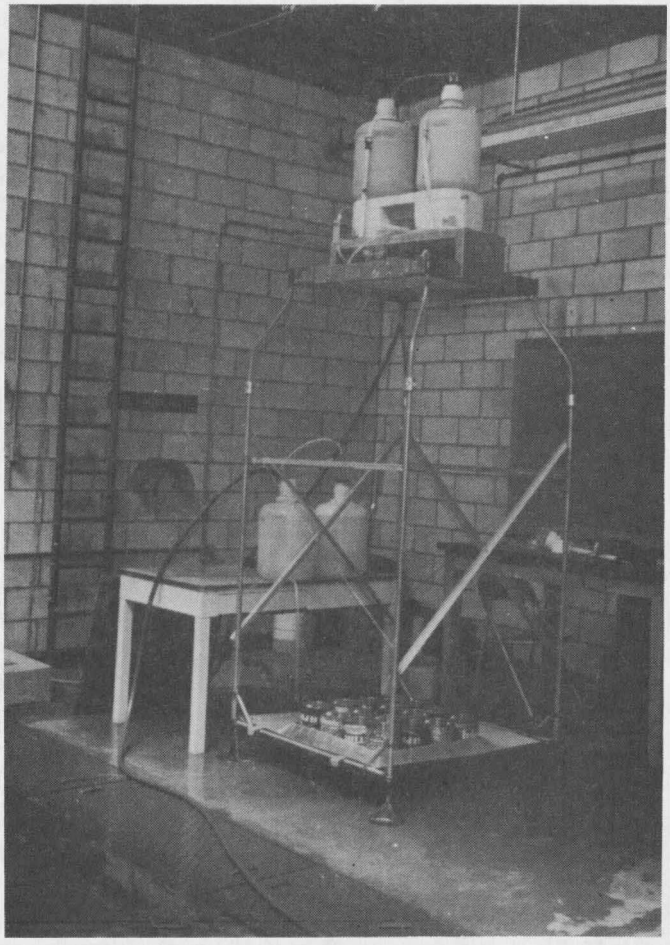


Figure 6. Picture of the selected rainfall simulator.

five inlets on the top of chamber were mainly used to distribute the flow of water evenly into the rainfall chamber. The low flow rate through each inlet, which has widely spaced U-type connections, is necessary to exclude air from tubes supplying water from the reservoirs. A floatmeter and valve is used to regulate the flow rate to the rainfall chamber and consequently the rainfall intensity.

Regression analysis, analysis of covariance and a test of homogeneity were used to develop the equation which describes the relationship between floatmeter reading and rainfall intensity. The kinetic energy (KE) of raindrop delivered to the soil surface was calculated through the kinetic energy equation ($KE = 1/2\ MV^2$). The falling velocity

involved in this equation is determined from Laws (1940, 1941). The intensity of rainfall in relation to the floatmeter reading was determined by measuring the amount of artificial rainfall collected by 16 aluminum containers each having a radius of 7.75 cm (3.05 inches) (Figs. 7 & 8).

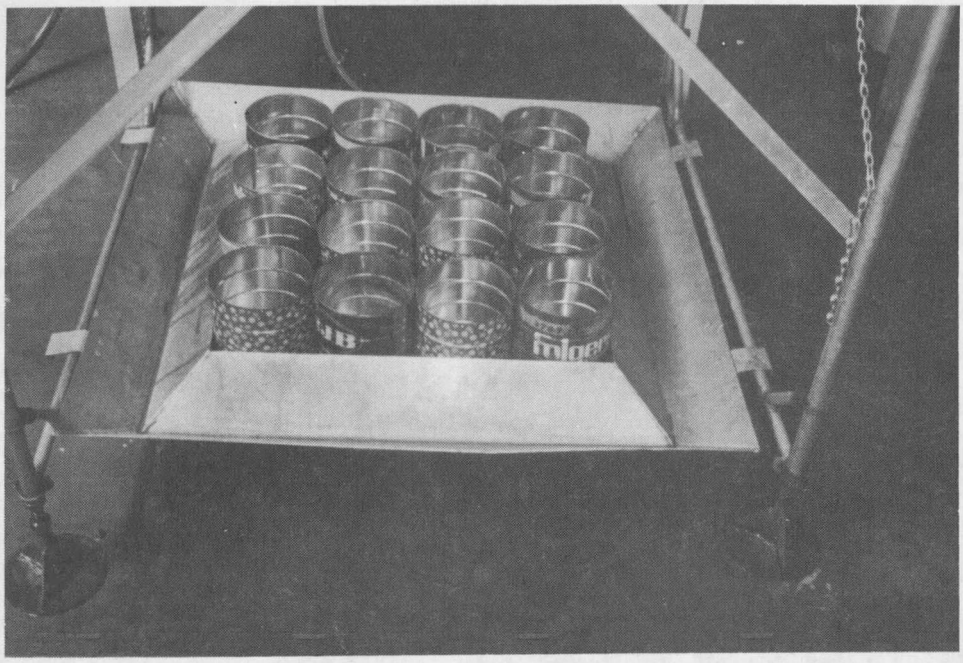
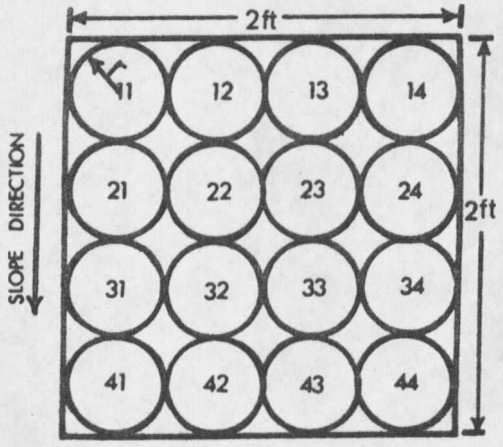


Figure 7. Rainfall intensity measurement.

Measurement of Runoff and Sediment

The erodibility study was conducted in the laboratory so that rainfall simulator conditions and other environmental problems such as wind, temperature, relative humidity could be controlled. The 61 X 61 cm (2 X 2 ft) plot size with adjusted slope of 0% $\sim$ 60% (Fig. 9) was selected as the largest area that one person could effectively handle. Two 61-cm (2-foot) P.V.C. pipes with thirteen holes, 3/32 mm ID, were used to simulate two different flow rates. They were installed at the topmost edge of the plot. A carboy reservoir, which was of the same design as that used to supply water to the rainfall chamber,



pot area $= \pi r^2 = 3.1416\,(3.05'')^2 = 29\ \text{in}^2$

sample area $= 16(\pi r^2) = 468\ \text{in}^2$

$$\%\ \text{of total sample area} = \frac{16\pi r^2}{b^2} \times 100\% = \frac{468}{576} \times 100\% = 81\%$$

$$\text{rainfall intensity} = \frac{\text{volume (in}^3\text{/pot)}}{(\text{area of pot})(\text{time})}$$

$$\text{Example: rainfall intensity} = \frac{400/16.38}{(29.00)(10/60)} = \frac{24.42}{4.875}$$

$$\cong 5\ \text{in/hr} \cong 127\ \text{mm/hr}$$

Figure 8. Rainfall intensity calibration processes.

was connected to the P.V.C. pipe used to simulate runoff. The water pressure in the pipe was controlled by a vertical plastic tube installed at the top right side. The pressure in the pipe determined whether the flow rate was evenly distributed to the runoff plot. Hence, if we maintain positive pressure in the plastic tube then we should have a constant flow rate uniformly distributed to the erosion plot. Water level changes will also occur with decrease or increase of slope, but a constant water level and hence a constant flow rate, is necessary during the test. Therefore, another water level reservoir was also required to keep a con-

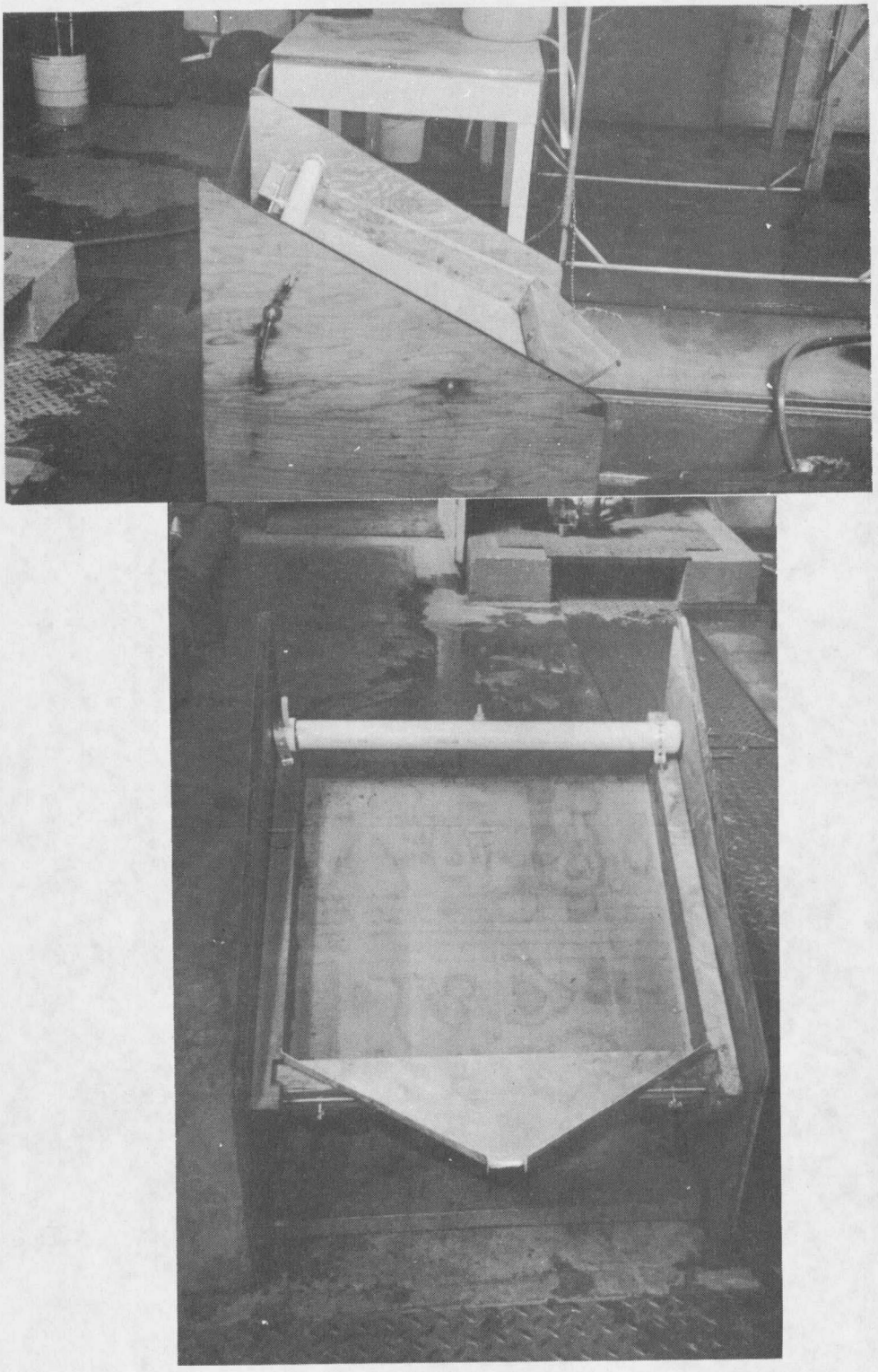


Figure 9. Erosion plot.

stant head in the carboy in order to maintain constant positive pressure in the pipe. This is illustrated in Figure 10.

The erosion box (61 X 61 X 10 cm) shown in Figure 9 also served as the soil container for the erosion plot. The box has a pattern milled into the bottom only to allow water that infiltrates the soil to drain from the box. A nonwoven filter fabric used for two layers of overlapping window screen at the bottom of the box prevented passing of most particles. Runoff and sediment transported across the lower edge of the plot were collected by a 61 cm (2 ft) wide aluminum trough connected with the erosion plot that can be adjusted 2.54 cm (1 inch) vertically. The lip of the collection trough is bent downward 90 degrees (Figs. 9 & 10). Hence, runoff and sediment were concentrated into a trough moulded to the edge of the box and was collected in a 1 liter graduated cylinder. The erosion plot was placed beneath the rainfall simulator, and each erosion test was replicated three times. One percent was selected as the minimum slope that would provide adequate control of soil loss. Twenty percent was selected as the maximum allowable slope by reclamation techniques. Both 40% and 60% were selected to study soil erosion on steep slopes. The zero flow rate was selected for the study of soil detached by raindrop alone. Twenty-one and 42 cm^3/sec flow rate were selected to study overland flow erosion (rill, interrill and sheet erosion) and splash erosion. Three rainfall intensities; 38.1, 50.8 and 63.5 mm/hr (1.5, 2.0 and 2.5 in/hr) were superimposed upon each overland flow rate. Two soil textures and three mixtures of these two textures served as representative soil conditions in surface mining areas. Details are illustrated in Figure 11. These soil texture combinations were tested for 30 minutes in a wet state at each combination of three flow rates, three rainfall intensities and four slope steepnesses. The wet state was identified as the condition of a soil sample 4 hours after a 30-minute rainfall simulator run. The dry state was the condition of an air dried soil sample when it was compacted into the erosion plot. The 30-minute rainfall duration for the test was chosen because overland flow gener-

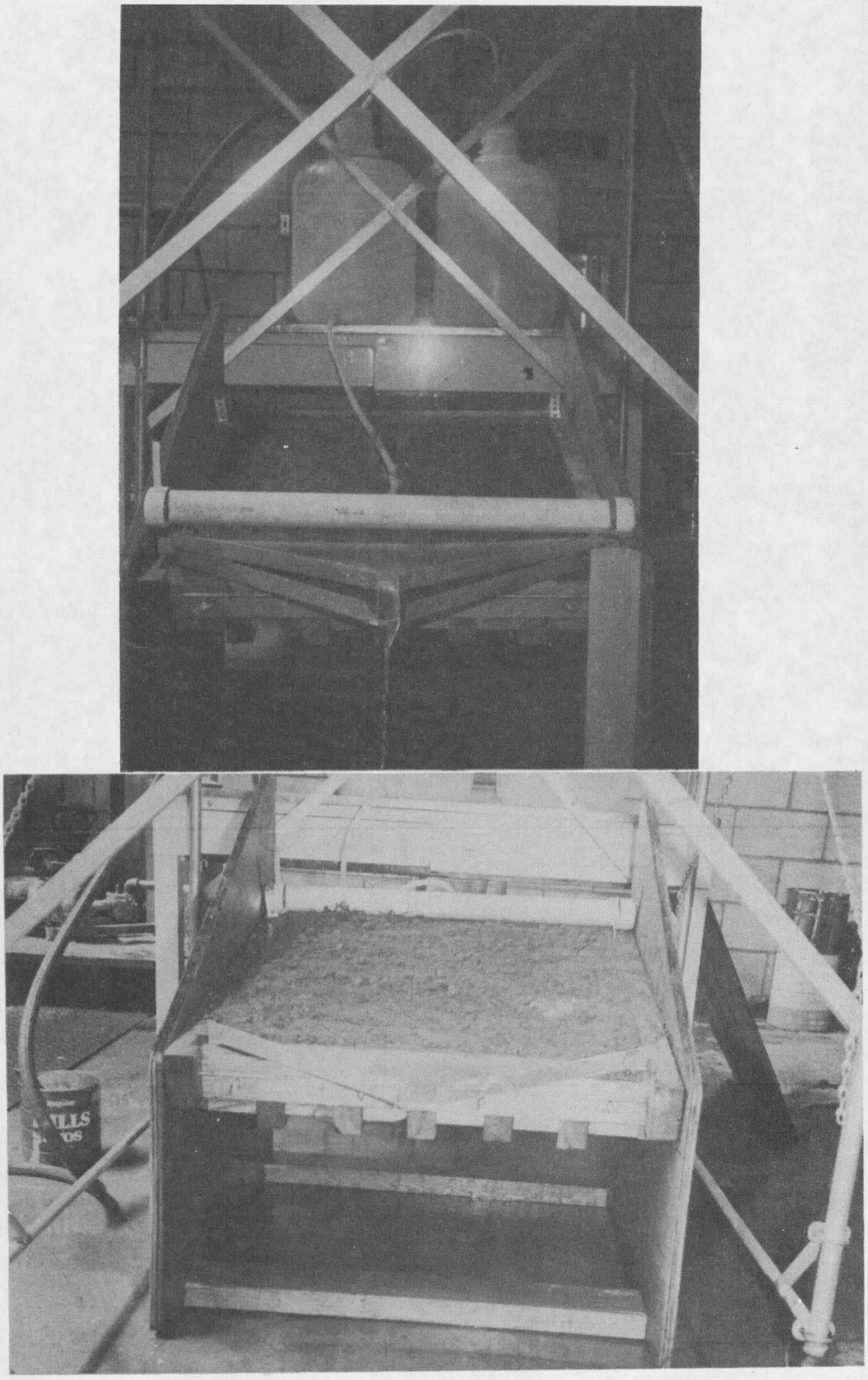


Figure 10. Simulated runoff pipe and erosion plot.

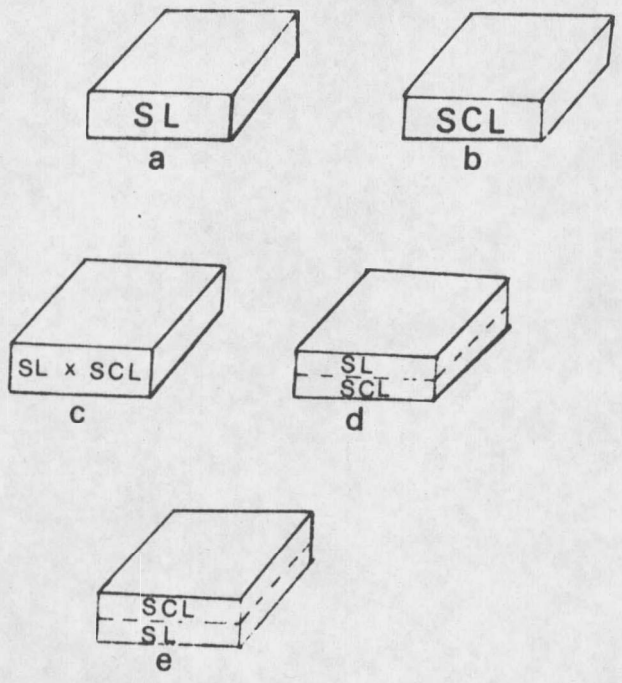


Figure 11. Soil textures and their combinations. (a) Sandy loam, (b) sandy clay loam, (c) M3: SL mixed with SCL, (d) M1: SL on top/SCL at bottom, (e) M2: SCL on top/SL at bottom.

ally occurred uniformly on these 3-inch soil profiles after approximately 28 minutes. Rainfall simulator runs of 4 hours were operated on each soil sample at each slope condition. These runs indicated that 30-minute duration runs were much more representative of the erosion in the wet state than in the dry state. Hence, rill, interrill and splash erosion resulting from 30-minutes durations on soil samples in the wet condition are the basic measures in this study. For all tests the soil loss was determined from the 24-hour oven-dry weight of sediment. The temperature of the oven-dry process was controlled at 105°C.

Particle Size Analysis

Sediment particle size analysis is important for several reasons. Sands are transported differently than fines (silts and clays) and present a special computational need. Sand sizes, generally greater than 0.062 mm travel primarily as bed load in a channel (ASAE, 1977). Likewise, sand in sandy soils is more easily deposited near eroded sites in upland portions of a watershed. If the sediment source is predominantly silt and clay, a simple relation may be used to represent transport of gross erosion. A combination of sands and fines in the watershed soils required a more complicated transport modeling procedure. Usually surface soils have different texture than subsoils. This is particularly significant when chemicals travel attached to clay particles, whereas only small amounts of chemicals are attached to sand. It is, therefore, very helpful in understanding erosion dynamics and chemical transport to measure particle size distribution of the sediment, and the soil before and after erosion.

A sieve analysis was conducted on each sample. Size fractions included 4.75, 2.00, 0.85, 0.425, 0.22, 0.15, and 0.075 mm sieve (#4, #10, #20, #40, #80, #100, and #200 sieve). Hydrometer analysis of sediment particles passing the #10 (2.00 mm) sieve determined the finer particle size distribution. A corrected sieve analysis was used in this study. Hydrometer analysis is an extension of the sieve analysis into fine-grained materials that are too small to be accurately measured by sieve analysis. The computations of hydrometer analysis in this study include corrections for temperature, hydrometer reading and viscosity of the liquid. The sieve analysis, corrected sieve analysis and hydrometer analysis were combined to give the complete sediment particle size distribution.

CHAPTER IV

EROSION MODEL DEVELOPMENT

Basic Principle

Based on the mechanics of erosion by water, soil erosion is a two-phase process consisting of the detachment of individual particles from the soil mass and their transport by erosive agents such as surface run-off.

The severity of erosion depends both on the quantity of material supplied by detachment and the capacity of the eroding agents to transport it. Where the agents have the capacity to transport more material than is supplied by detachment, the erosion is described as detachment-limited. Where more material is supplied than can be transported, the erosion is transport-limited (Morgan, 1979). Regardless, whether a system is detachment-limited or transport-limited, the energy of the erosive agents is the most important factor affecting the erosion process.

The energy available for erosion takes two forms: potential and kinetic. Both of them are exchangeable. Potential energy (PE) is the product of mass (m), height difference (h) and acceleration due to gravity (g).

$$PE = mgh \tag{1}$$

It results from the difference in height of one body with respect to another. When the potential energy is converted into kinetic energy (KE), the energy of motion, erosion increases. It is also related to the mass (m) and velocity (v) of the eroding agents in the expression:

$$KE = \frac{1}{2} mv^2 \tag{2}$$

From equations (1) and (2), the erosive force is related to the mass (m) and velocity (v) of the eroding agents. Also, it is time dependent. If most of the energy of erosion could be dissipated, the erosion would subsequently be reduced. Several reports indicated (Rubey, 1952; Pearce, 1976) that most of this energy is dissipated in friction with the surface over which the agent moves so that only 3 to 4 percent of the energy of running water and 0.2 percent of that of falling raindrops is used in erosion. Hence, increasing surface friction (surface roughness) will reduce erosion. The efficiencies of water erosion can be obtained by means of calculation of kinetic energy (Table 9).

Table* 9. Efficiency of Forms of Water Erosion.

Form	Mass**	Typical velocity (ms^{-1})	KE†	Energy for erosion††
Raindrops	R	9	40.5 R	0.081 R
Sheet flow	0.5 R	0.01	2.5×10^{-5} R	7.5×10^{-7} R
Rill flow	0.5 R	10	25 R	0.75 R

*Source from Morgan, 1979.
**Assumes rainfall of mass R of which 50% contributes to runoff.
†KE based on $1/2\ MV^2$.
††Assume 0.2% of the KE of raindrop and 3% of the KE of runoff is expended in erosion (from Rubey, 1952; Pearce, 1976).

From Table 9, we can realize that the concentration of running water in rills affords the most powerful erosive agent but raindrops are also potentially erosive agents which cannot be neglected. So there are two critical erosive agents, raindrop and runoff, which should be considered in erosion research:

(1) Raindrops–Most of raindrop energy is used in detachment, so that the amount available for transport is relatively small. Field studies by Morgan (1979) show that the transport across a one cm width of an 11° slope amounted to 400 g of sediment by overland flow, and only 20 g by raindrop (Morgan, 1979). The action of a raindrop on soil particles is most easily understood by considering the momentum of a single raindrop falling on a sloping surface. The downslope component of this momentum is transferred in

full to the soil surface but only a small proportion of the component normal to the surface is transferred, the rest being reflected (Fig. 12).

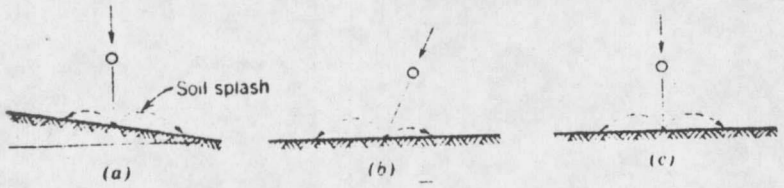


Figure 12. Differential soil movement caused by raindrop splash. (a) Sloping land, (b) Inclined rainfall, (c) Vertical rainfall (from Kohuke and Bertrand, 1959).

Hence, raindrops falling on level, bare soil in the absence of wind tend to spatter equally in all directions. Therefore, soil movement out of the area is matched by soil movement into the area from other splashes. Thus, there may be a lot of soil movement by raindrop impact, but no net soil loss from a particular unit of soil surface (Fig. 12). On sloping land the splash moves farther downhill than uphill not only because the soil particles travel further, but also because the angle of impact causes the splash reaction to be in a downhill direction (Fig. 12). Components of wind velocity up or down the slope have an important effect on soil movement by splash (Fig. 12). It has been suggested that the percent of downslope splash from the point of raindrop impact is equal to 50 percent plus the percent slope of the land (Ekern, 1951; Hudson, 1981).

The transferred momentum of raindrop to the soil particles has three effects each of which is involved in the erosion process. First, it provides a consolidating force, compacting the soil and puddling the surface layer of soil. Second, it breaks aggregates and clods into small aggregates and individual particles. Third, it imparts a velocity to some of the soil particles, launching them into the air. On landing, they transfer their own downslope momentum to other particles and the jumping process is repeated. Thus, raindrops cause consolidation, dispersion and detachment of soil. They also reduce the soil infiltration rate and permeability, causing more water to run off the soil surface. Raindrops impact not

only on soil particles but also on thin water surfaces. Although the impact of raindrops on shallow overland flow may not splash soil, it does cause turbulence, providing a greater sediment carrying capacity. Palmer (1964, 1965) has measured the impact of raindrops beneath a water film, and found first an increasing impact until the water layer thickness was about 85 percent of the drop diameter, and then a decline as a function of time.

In general, soil detachability is related to the kinetic energy of the raindrop, raindrop size distribution, soil texture, rainfall intensity, slope and time. The KE of a raindrop is commonly correlated with intensity. The results of these studies have been presented as mathematical equations compared in Table 10. It has also been suggested that splash detachment rate (D_s) can be expressed in terms of rainfall intensity (I) (Foster and Meyer, 1975).

$$D_s \alpha I^2 \tag{3}$$

Recently, a simple relationship to predict soil detachment due to a single raindrop impact has been presented in the International System of Units (UI) (Al-Durrah and Bradford, 1981, 1982):

$$D = a + b\,(KE/\tau_f) \tag{4}$$

Table 10. Equations Relating KE and Intensity.

Equation	Energy units	Intensity units
1. E = 916 + 331 log I	ft-tons/acre-in	in/hr
2. E = 210 + 89 log I	ton-m/ha-cm	cm/hr
3. E = 11.9 + 8.7 log I	J/m^2-mm	mm/hr
4. E = 30 - 125/I	J/m^2-mm	mm/hr
5. E = 9.81 + 11.25 log I	J/m^2-mm	mm/hr

Sources: 1) Wischmeier et al., 1958; 2 and 3) Wischmeier & Smith, 1978; 4) Hudson, 1965; 5) Zanchi and Torri, 1981.

D is the amount of soil detached (mg/drop), KE is the raindrop kinetic energy (J is a unit of KE; J = Joule), τ_f is the soil shear strength (kPa) and a,b are constants. On the other hand, some research has shown that the rate of raindrop detachment seems to be a time-

dependent function (Kirkby and Morgan, 1980). In some cases, the detachability increases rapidly at the beginning, reaches a peak and decays through time to a steady state. Moreover, the detachment rate has been found to increase with an increase in particle size but the transportability increases as soil particle size decreases. That is, clay particles are more difficult to detach than sand, but clay is more easily transported. Meanwhile, Laws (1941) studied the relationship between drop diameter and terminal velocity over a range of drop sizes from 0.2 to 6.0 mm. Natural rain contains drop diameter from less than 0.25 mm to 7 mm (Laws and Parsons, 1943). He found that smaller drops reach "still air" terminal velocity in a shorter distance but that all normal drops reach still air terminal velocity after falling 10 m or less. Larger drops have larger KE than small drops due to larger mass and faster rate of fall. Laws (1941) also presented his data in a graphic form (Fig. 13).

A high-speed photographic study of raindrop impact by Mutchler (1967) shows that splash shape geometry could be described by the parameters shown on the vertical cross-section of splash in Figures 14 and 15. The sheet angle α and the sheet radius r which describe the profile of the cylindrical shell of flowing water, has not been particularly useful. The angle β which describes the direction which droplets travel away from the splash sheet, has been useful in computing energy dissipation under the impacting water drop. The parameters H and W describe the splash sheet height and the crater width of the splash shape respectively. The successive steps that take place in drop-crater formation are illustrated in Figure 16. Two-thirds of the energy of the raindrop is expended forming an impact crater and moving soil particles, the remainder to forming spray (Mihara, 1952). Hence, the interactions of raindrop size, velocity and shape, the duration of the storm, the wind speed and the shape and steepness of the slope, control the erosive power of rainfall.

During a storm, rain may fall on surface water in the form of puddles or overland flow. Palmer (1964) studied the influence of a thin water layer on water drop impact forces. He found that drop impact is more effective when a thin film of water covers the

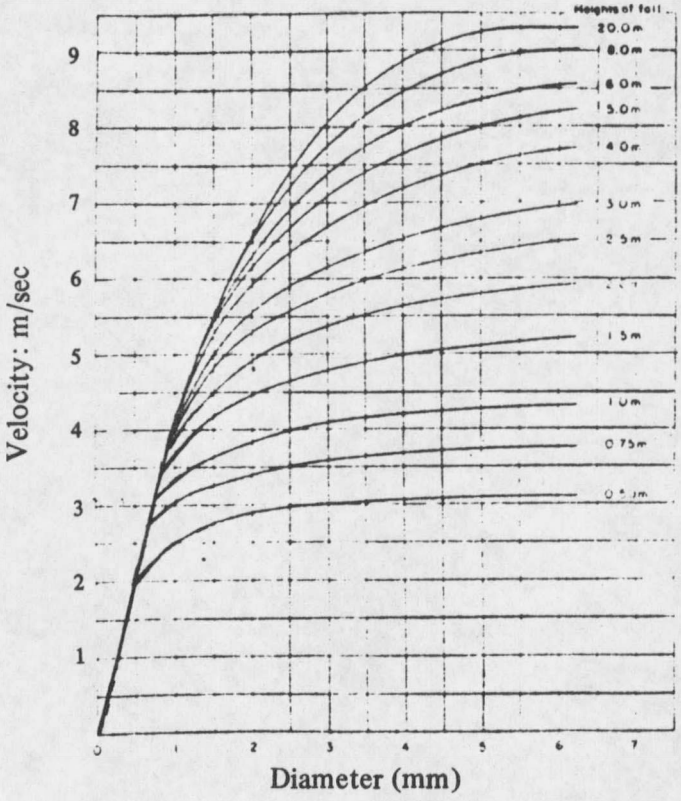


Figure 13. Curves showing relation between drop diameter and terminal velocity after 12 different height of fall (from Laws, 1941).

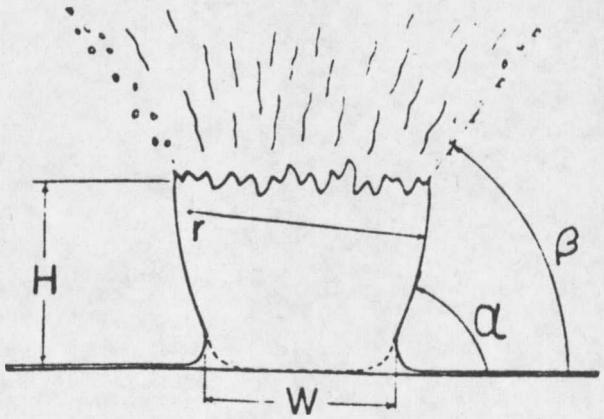


Figure 14. Parameters for describing the geometry of splash shape (from Mutchler, 1967).

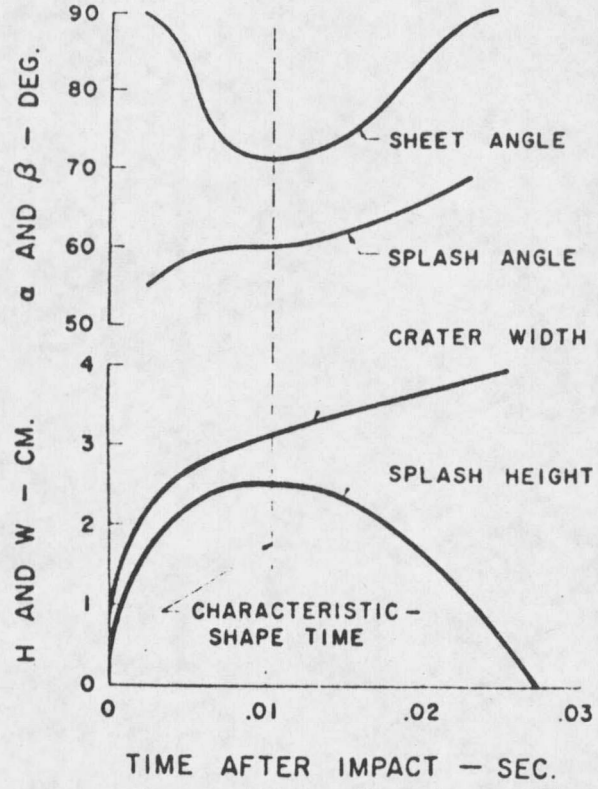


Figure 15. Splash parameter change with time from impact. The characteristic shape time was selected at the time for maximum splash height (from Mutchler, 1967).

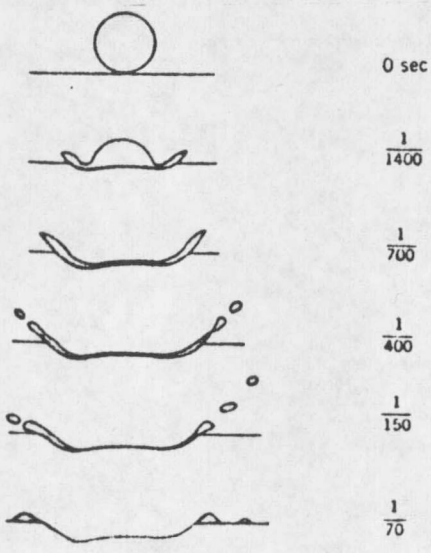


Figure 16. Steps in drop crater formation (after Mihara, 1952).

soil surface and maximum dispersion of soil particles occurs when critical water depth is about the same as three raindrop diameters. The reason for this is the turbulence which impacting raindrops impart to the water. However, when a critical water depth is reached the raindrop energy is dissipated in the water, not affecting the soil surface. Also, raindrop splash imparts turbulence to laminar flow thus increasing the transporting potential of the flowing water by lifting detached soil particles into the flow. Splash erosion decreases where the flow depth exceeds about three drop diameters which is the critical depth of flowing water to protect the soil from raindrop impact.

Surface Runoff (Overland Flow)

Overland flow is defined as the flow of water over the land surface toward a stream channel and is the initial phase of surface runoff. It is sometimes referred to as sheet flow because the water is envisioned as moving in a sheet downslope over a plane surface to the nearest concentration point. But sheet flow is usually considered to be a special description of overland flow. Almost all surface runoff starts as overland flow in the upper reaches of a watershed and travels at least a short distance in this manner before it joins a rill or gully (Fig. 17). In modelling overland flow, the variables are more difficult to define precisely and the use of a simple hydraulic procedure for predicting overland flow and its characterizations is also difficult because overland flow is both unsteady and spatially varied since it is supplied by rainfall and depleted by infiltration. Moreover, the flow may be either laminar or turbulent or a combination of these two conditions which can be called transitional flow. Flow depth may be varied with respect to time and location. That is, the flow depth may be either above or below critical, or the depth may change from subcritical to supercritical. Under certain conditions the flow may become unstable and may give rise to the formation of roll waves, or rain waves as they are often called. Iwagaki (1955) was the

first to use the kinematic-wave method incorporating a continuous lateral inflow to analyze in detail the hydrograph of overland flow.

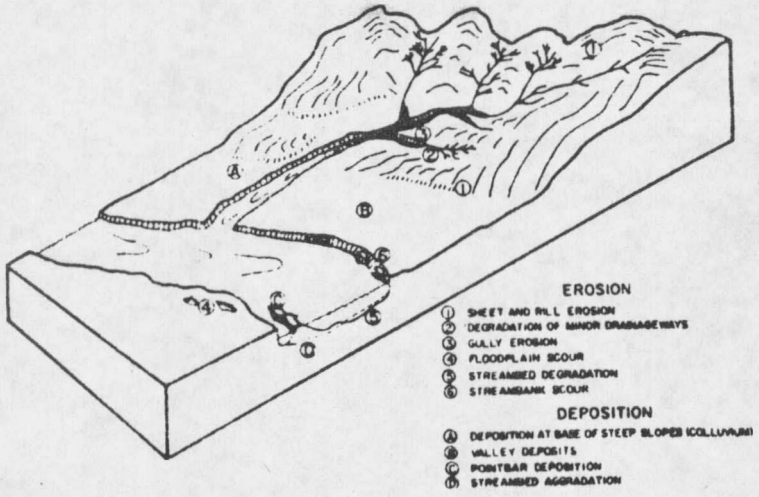


Figure 17. Typical erosion and deposition occurrences (Vanoni, 1977).

The hydraulic characteristics of overland flow depend on many factors or parameters these include the intensity and the duration of precipitation (or melting snow and ice), soil texture and structure reflected by its influence on infiltration rate and permeability; the antecedent soil moisture content; the density and type of vegetation; and topographic characteristics including the number and size of surface depressions and mounds, the shape, steepness and length of slope. The geomorphic characteristics are dependent on the hydraulic characteristics, but no simple description of the hydraulics of overland flow is possible because hydraulic parameters vary rapidly with respect to time and space.

Hence, detailed observations of overland flow under actual field conditions seems to be necessary. Application of field observations to draw generalizations about hydraulic flow parameters are also significant. On the other hand, the verification and modification of the hydraulic characteristics of overland flow by means of laboratory experiments is also required to provide generalizations for the effects of each variable despite the difficulties of direct transfer to the field case. As more and more general observations of overland

flow are available, the mathematical modelling of overland flow becomes critical. Analytical and theoretical solutions to the hydraulics of overland flow are still partially incomplete, primarily due to the paucity of physical observation of overland flow. Hence, the real-phenomenon research become important. It is not only to provide correct input information to the modelling attempts, but also to provide modification of model and verification of the theoretical prediction.

From Newton's viscosity equation, the shear stress for detachment and transport can be expressed:

$$\tau = \mu \frac{\partial v}{\partial y} \tag{5}$$

where τ is shear stress, μ is dynamic viscosity, v is particle velocity and y is depth position. For convenience in the fields of hydraulics and physics, the dynamic viscosity can be expressed in the equation form:

$$\mu = \rho \gamma \tag{6}$$

where γ is kinematic viscosity and ρ is density of fluid. But unfortunately, the equation (5) can only be useful for laminar flow, because turbulent flow is controlled by eddy currents (vortex). So equation (5) must be modified by the following expression:

$$\tau = (\mu + \eta) \frac{\partial v}{\partial y} \tag{7}$$

where η is the eddy viscosity. When raindrops impact a wet soil surface or a thin sheet flow on the soil surface, muddy flow can be seen on the surface. Mud flow does not have Newton flow characteristics (laminar flow) due to the impact of the raindrop. Hence, the general form of mud flow shear stress (CSCHE, 1975):

$$\tau = \mu \left(\frac{\partial v}{\partial y}\right)^{n} \tag{8}$$

Thus, the larger the impactive force of raindrop the greater the turbulence due to large shear stress caused by the velocity of particles in the flow. The greater the turbulence, the

greater is the erosive power generated by the flow. Reported velocity of overland flow from laboratory and field plot studies has shown a range from 1.5 $\sim$ 4.0 cm per second (Young and Wierama, 1973) to 30 cm per second (Ellison, 1947). Velocity of 16 cm per second are required to erode soil particles of 0.3 mm diameter (Hjulstrom, 1935) and velocity as low as 2 cm per second will carry 0.002 mm particles in suspension (Morgan, 1979). Recently, based on the energy standpoint, Schwab et al. (1981) pointed out that overland flow velocities are about 0.3 $\sim$ 0.6 m per second when raindrops have velocities of about 6 $\sim$ 9 m per second. Hence, the transporting capacity of flowing water is function of velocity.

In general, the hydraulic characteristics of flow are described by its Reynolds number (R_e) and its Froude number (F_r) (Chow, 1959) defined as follows:

$$R_e = \frac{vL}{\nu} = \frac{vR}{\nu} \tag{9}$$

$$F_r = \frac{v}{\sqrt{gL}} = \frac{v}{\sqrt{gD}} \tag{10}$$

where v = the mean velocity of the flow

g = acceleration of gravity

L = characteristic length

R = hydraulic radius

D = hydraulic depth

ν = kinematic viscosity

The Reynolds number is an index of the turbulence of the flow. Laboratory studies (D'Souza and Morgan, 1976) have been shown that soil loss varied with the Reynolds number. At numbers less than 500 laminar flow prevails and at value above 2000 flow is fully turbulent. Values between 500 and 2000 are indicative of transitional or disturbed flow (Chow, 1959). Studies by Emmett (1970) show that raindrop impact will impart tur-

bulence to otherwise laminar flow. In general, a Froude number of more than 1.0 denotes supercritical or rapid flow which is more erosive than subcritical or tranquil flow in which the Froude number is less than 1.0. Field studies of overland flow in Bedfordshire reveal that Reynolds numbers are between 1 and 50 and Froude numbers between 0.01 and 0.1 (Morgan, 1979). The regime of this flow in the field can be defined as subcritical-laminar flow which is not commonly encountered in applied open channel hydraulics, but occurs frequently where there is very thin flow depth (sheet flow). Another supercritical-laminar regime, may occur in laboratory studies of overland flow, which is rarely generated in open channel hydraulics.

The important factor in the overland flow studies is flow velocity. The flow velocity is dependent on the hydraulic radius (R) of the channel, flow depth (d), the roughness of the surface (n) and the slope including gradient, shape and length. This relationship can be expressed by the Manning equation (Chow, 1959).

$$V = \frac{1}{n} R^{2/3} S^{1/2} \tag{11}$$

The Manning equation assumes that the flow is fully turbulent, uniform, and moving over a rough surface. Where the flow does not satisfy this condition, the exponents in the equation change in value and Savat (1977) recognized the following variation with Reynolds number.

$$V \alpha R^{1.7} S^{0.95} \quad \text{for} \quad R_e = 250 \tag{12}$$

$$V \alpha R^{0.95} S^{0.7} \quad \text{for} \quad R_e = 500 \tag{13}$$

$$V \alpha R^{0.5} S^{0.4} \quad \text{for} \quad R_e = 1000 \tag{14}$$

Using the Manning's equation and continuity equation, Meyer (1965) showed that

$$V \alpha S^{1/3} Q_w^{1/3} \tag{15}$$

where Q_w is the water discharge or flow rate. In 1969, Meyer and Wischmeier (1969) assumed that the detachment (D_f) and transporting (T_f) capacities of flow vary respectively with the square and fifth power of velocity. They found the relationship between these parameters can be expressed by the following equation

$$D_f \alpha S^{2/3} Q_w^{2/3} \tag{16}$$

$$T_f \alpha S^{5/3} Q^{5/3} \tag{17}$$

More recently, Carson and Kirkby (1972) derived the equation from consideration of the hydraulics of sediment transport:

$$Q_s = 0.0158\, Q_w^{1.75} k^{-1.11} (\sin\theta \cos\theta)^{1.625} \tag{18}$$

where Q_s is the sediment discharge per unit width and k is the particle size of the surface material with 84% of the grains being finer. It can be seen from the above that the amount of soil loss resulting from erosion by runoff (overland flow) varies with the flow velocity, state and regime of flow, fluid viscosity, surface roughness, soil particles and slope.

Another important characteristic of flow is the flow profile which is defined as the surface curve of the flow. The flow profile of overland flow can be used for describing water surface variations with respect to time and space. The general solution to these overland flow problems is thus contained in the continuity and momentum equation with lateral inflow (q_L) assumed equal to zero (Eaglesen, 1970)

$$\frac{\partial y}{\partial t} + \frac{\partial q}{\partial x} = i - f = i_o \tag{19}$$

and

$$q = \alpha y^m \tag{20}$$

where y = depth of flow

t = time

q = discharge per unit width

x = the direction of flow

i = rainfall intensity

f = infiltration rate

i_o = net inflow rate to surface runoff (rainfall excess)

This quasi-steady approach was developed by Lighthill and Whitham (1955) and is known as the kinematic wave approximation, since any wavelike behavior must enter through the continuity equation. Also, the dynamic uniformity of the approach precludes solutions which exhibit changes in water surface profile due to dynamic variation. Meanwhile, boundary and initial conditions are imposed only for solution of the continuity equation; therefore, changes in water-surface profile will be caused only by changes in local flow rate and will be transmitted in the direction in which a kinematic wave propagates, that is the downstream direction. Hence, the characteristic of a kinematic wave can be illustrated by Figure 18. These characteristic curves trace out the space-time path of any flow disturbance. Also, we can find the limiting characteristic curve AB in Figure 18 which explains the water flow in the x-direction from upslope and begin at x=0, where there is no inflow from upsteam. In other words, as the rain begins to fall at $t=t_o=0$, which t is time and t_o is initial time, the local depth will increase everywhere at the rate of equation (21) and travel downstream

$$\frac{dy}{dt} = i_o \tag{21}$$

along the limiting characteristic curve AB, where local depth continues to grow until the limiting characteristic point in question is reached. It will remain constant after reaching the point in question. From the kinematic wave equation solved by the method of Eaglesen (1970), we can find the relationships between variables affecting overland flow, such as y_L, q_L, t_c, t_r and t_p, and construct the entire water surface profile at any time $t_r > t_c$ (Fig. 19) (Case I)

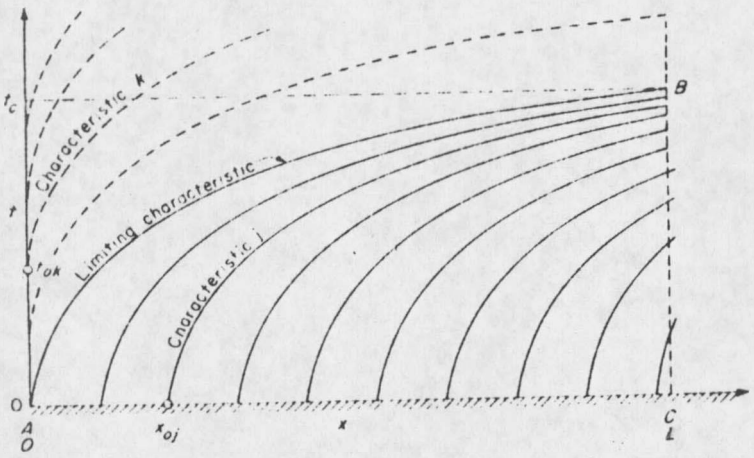


Figure 18. Characteristics diagram for kinematic wave.

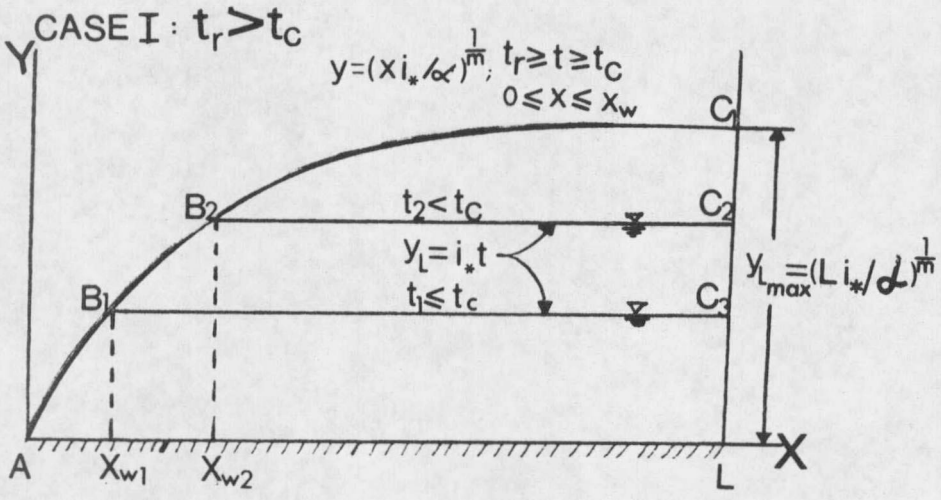


Figure 19. Water surface profile during buildup.

$$q_L = \alpha y_L^m \tag{20a}$$

$$y_L = \begin{cases} i_* t; 0 \leq t \leq t_c \leq t_r, x > x_w & (22) \\ (\frac{L i_*}{\alpha})^{1/m}; t_r \leq t \leq t_c, x = L & (23) \end{cases}$$

$$L = \alpha y_L^{m-1}[y_L i_*^{-1} + m(t - t_r)], t > t_r \geq t_c \tag{24}$$

$$x_w = \alpha m \int_0^t y^{m-1} dt \tag{25}$$

Suppose at Case II $t_r < t_c$, the entire water surface profiles can be sketched in Figure 20 and illustrated by the following equations

$$q_L = \alpha y_L^m \tag{20a}$$

$$y_L = \begin{cases} i_* t, & 0 < t \leq t_r < t_c \\ i_* t_r, & t_c > t_r < t \leq t_p \end{cases} \tag{26, 27}$$

$$L = \alpha y_L^{m-1} [y_L i_*^{-1} + m(t - t_r)] \tag{28}$$

$$t_c = \frac{L i_*^{1-m}}{\alpha}^{1/m} \tag{29}$$

$$t_p = t_r + \frac{L}{\alpha m y_{Lr}^{m-1}} - \frac{t_r}{m} \tag{30}$$

where t = time (t)

t_p = a characteristic overland-flow time at peak (t)

t_r = time of duration during a storm (t)

t_c = time of concentration (t)

i_* = magnitude of constant rainfall excess (Lt^{-1})

y = flow depth (L)

y_L = flow depth at x = L(L)

y_{Lr} = flow depth at x = L, t = t_r(L)

q_L = lateral inflow ($L^2 t^{-1}$)

x_w = position of disturbance wave (L)

X = flow direction at x-axis (L)

X_{wr} = position of disturbance wave for t = t_r (L)

L = length of overland flow (L)

α = kinematic-wave parameter ($L^{2-m}t^{-1}$)

m = kinematic-wave constant (dimensionless)

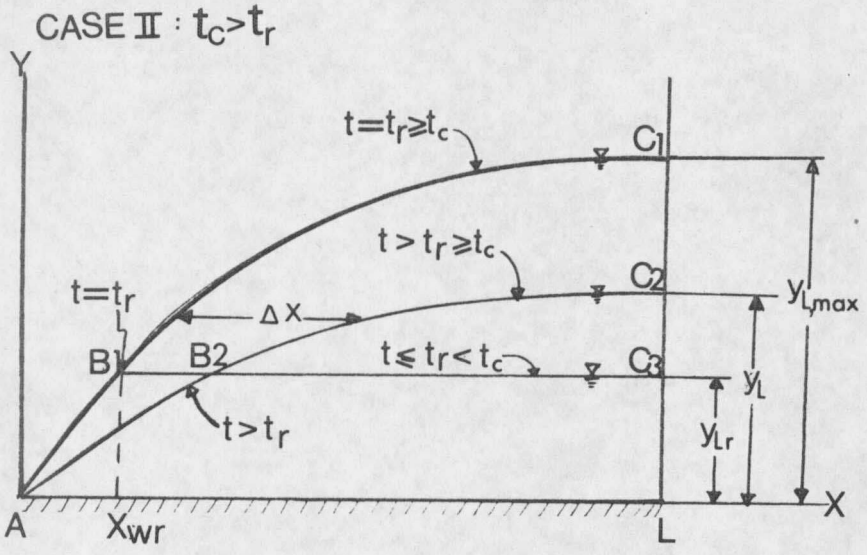


Figure 20. Water surface profile during decay.

From Figures 19 and 20, curves AB_2C_2, AB_1C_3 represent water surface profiles at successive time less than t_c during the storm. Curve AC_1 is the limiting, steady-state profile which is reached, for long storms, at time t_c. At this time, the outflow reaches its maximum values, which must equal the inflow point B_1 on Figure 20 on the profile AB_1C_1 at time $t=t_r$. Curves AB_1C_1 and $AB_1B_2C_1$ are the limiting profile for long storms and the curve AB_2C_2 on Figure 20 is a subsequent profile for a time following cessation of rainfall. On Figure 20, when point B_1 moves to B_2 by constant depth at a later time, the end depth $y_{Lr}=i_* t_r$ is the maximum depth reached during the build-up phase and remains constant until these two points are coincided. This occurs at time $t=t_p$. For the time $t > t_p$, the decay (recession) phase occur, this can be illustrated from equations 26 and 27. If we

assume $t > t_p$, $t \to \infty$, $m > 1$, then let $y_L \to 0$, we can see $L \to 0$ as the depth y approach to zero. Thus, the erosive power of overland flow varied enormously during the decay and build-up processes. This is because of variations of flow depth, velocity, raindrop impactive force, regime and state of flow in the processes of decay and buildup involved.

Based on the previous discussion of raindrop impact and runoff transporting capacity and the definition of the water erosion process by Ellison (1947), the mechanics of soil erosion by water is composed by detachment and transporting capacities of runoff and raindrop. In general, most raindrop energy is used in detaching soil particles and increasing transporting capacity of runoff, while the energy of runoff is used for transporting the detached soil particles. The physical functions of these two erosive agents can be either separated respectively, or interactions related to each other. Both of them are dependent on time and space which can be described by Figure 21 (Kirkby and Morgan, 1980).

Mathematical Simulation Process

Mathematical simulations useful for evaluating soil erosion systems originated more than forty years ago. Zingg (1940) published an empirical equation expressing soil loss as a function of slope length and steepness. Other researchers used this equation as a basis to develop many erosion mathematical models and equations applicable to some specific climatic regions and topographical areas. Wischmeier (1960, 1962) developed a useful technique for bringing effects of local rainfall distribution and topographical parameters into practice evaluations. He overcame regional boundaries and developed an Universal Soil Loss Equation (USLE) (Wischmeier and Smith, 1960, 1965) which has been widely applied to actual field conditions. More recently, some mathematical simulation models have been proposed to simulate physical process of water erosion and to describe soil movement along the slope at any time (Meyer & Wischmeier, 1969).

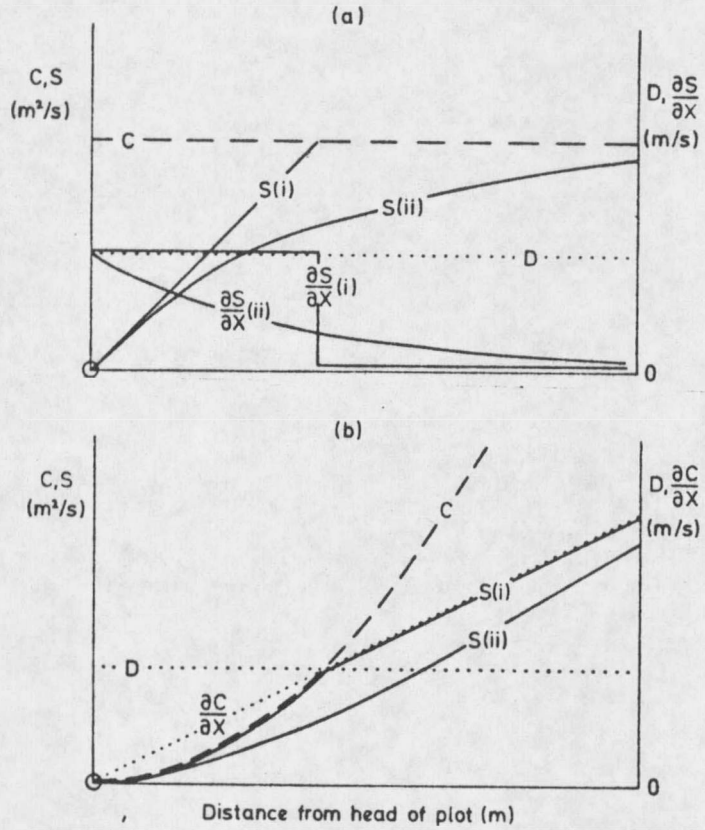


Figure 21. Transport/detachment interaction models. (a) Initially clean flow of constant (C) and detachment (D) capacities, flowing down a plot and eroding soil as it flows. (b) Rainfall on a plot with increasing flow and transport capacity, but with constant detachment capacity. Actual sediment transported (S) predicted by two models:

(i) Transport/detachment comparison (Meyer and Wischmeier, Wischmeier, 1969)

(ii) Transport deficit model (Foster and Meyer, 1972)

The purpose of these equations was to provide a planning tool for soil and water conservation technicians, but they were not designed to meet the present need for a detailed mathematical model to simulate soil erosion as a dynamic process based on hydromechanical theory. Few equations have been applied to surface-mined areas due to a shortage of available data.

To fully define this mathematical simulation model, some basic conditions must be assumed:

a. the state and regime of the region of flow

b. the basic equations of flow within this region

c. the boundary and initial conditions around the boundaries of this flow region

d. the kinematic-wave theory, must be valid, which describes the water surface profiles increase along the limiting characteristic curve (Fig. 18) and remain constant after this curve reached the point in question

e. the erosion system is a steady-state system and satisfies continuity equation of flow

f. a mathematical solution to this model

Therefore, a five-step process is involved including:

1. an examination of the physical processes of erosive agents
2. replace this physical process by an equivalent mathematical equation
3. solution of the mathematical equation with the accepted techniques of mathematics
4. superimpose boundary conditions upon the general solution of this model to make a simplified mathematical equation
5. interpret the mathematical results in terms of the physical process

Based on these assumptions and simulation processes the state of overland flow is laminar uniform steady. Its conceptual explanation is given by Figures 22 and 23. In addition, we also assume that short-term erosion, inter-rill-erosion, and rill erosion are the major erosion types in this approach. Thus, the basic equation of overland flow is developed on the basis of the equation for sediment transport continuity (Foster and Meyer, 1975) which states that the net rate of fluid mass flow into any elemental control volume within a porous media must equal the time rate of change of fluid mass storage within the element (Kirkby, 1978). Neglecting dispersion and assuming uniform steady state, the continuity equation is:

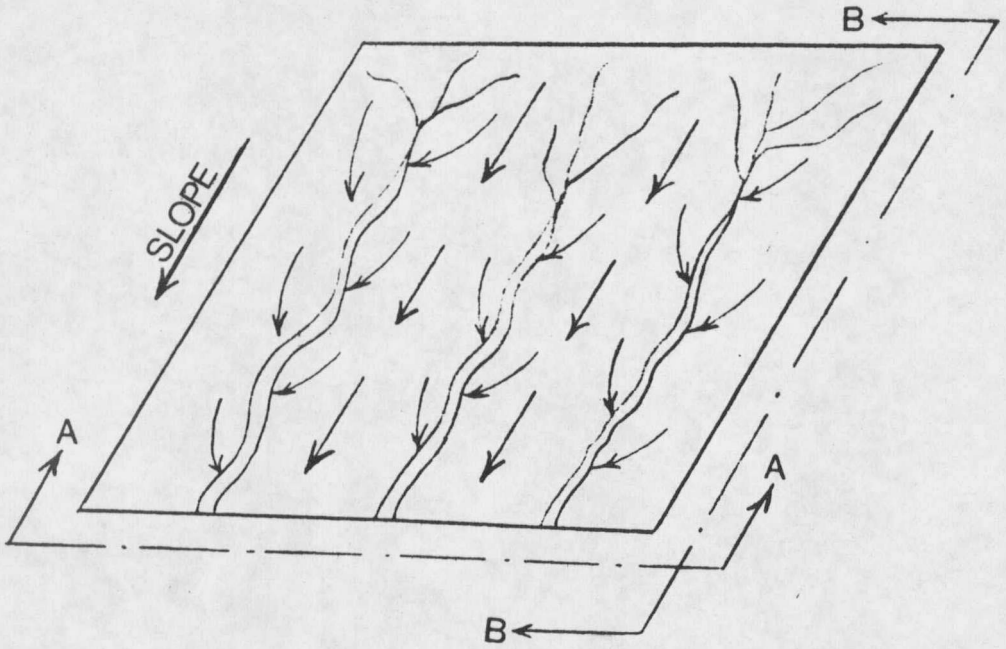


Figure 22. Rill and interrill erosion on sloping surface.

$$\rho_b \left(\frac{\partial y_b}{\partial t}\right) = \frac{\partial G}{\partial x} = D_R + D_i \qquad (31)$$

where ρ_b = the mass density of deposited sediment

y_b = the elevation of deposited materials

t = time

G = sediment load (mass/unit time/unit width)

x = distance downslope

D_R = detachment rate of rill erosion

D_i = delivery rate of particles detached by interrill erosion to rill flow (mass/unit time/unit width)

Equation 31 is the mathematical description of the conceptual model of Foster and Meyer (1975), which is shown in Figure 24.

Another equation used in the model is the first order equation proposed by Foster and Meyer (1972)

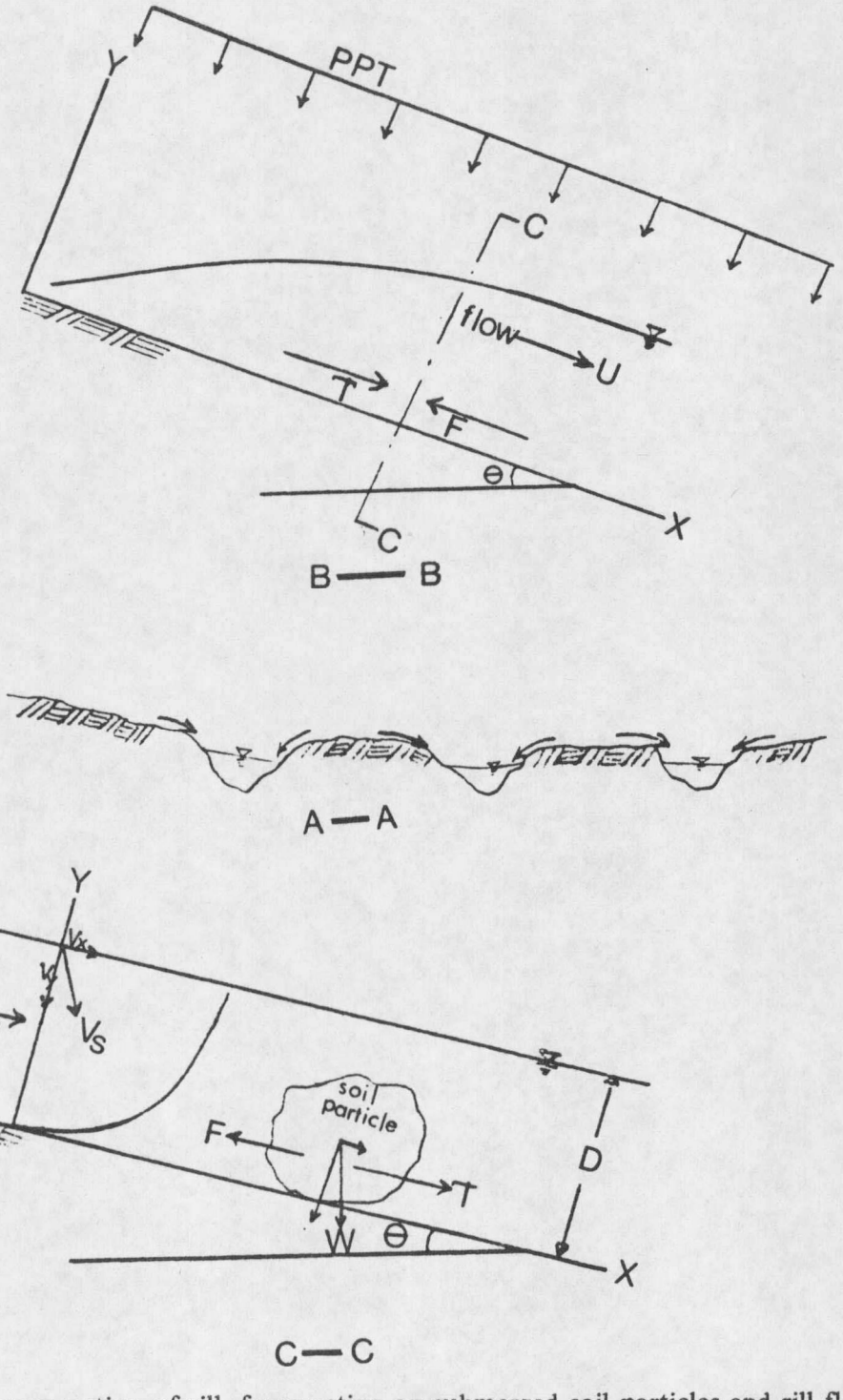


Figure 23. The cross-section of rill, force acting on submerged soil particles and rill flow conditions assumed for theoretical analysis.

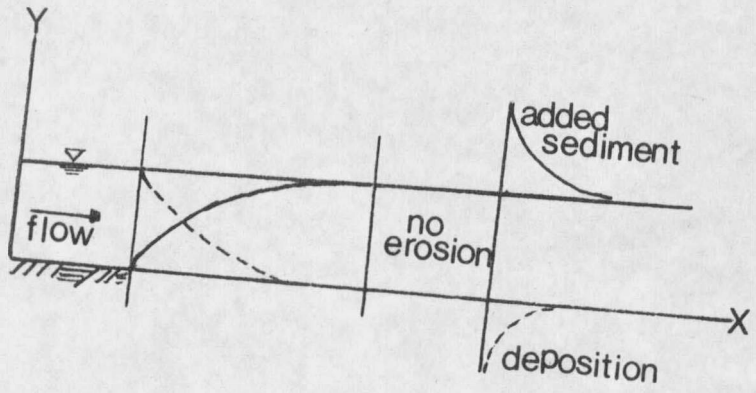


Figure 24. Flow detachment-sediment load interaction (Foster & Meyer).

$$D_R = \alpha (T_c - G) \tag{32}$$

where α is kinetic coefficient (1/unit width) and T_c is transport capacity (mass/unit time/unit width). By arranging:

$$\frac{D_R}{\alpha T_c} + \frac{G}{T_c} = 1 \tag{33}$$

According to the definition of G, we know that it is impossible to be negative, i.e., $G \geqslant 0$; when G=0, then $D_R = \alpha T_c = D_{max} = D_c$. Hence, equation 33 can also be rewritten:

$$\frac{D_R}{D_c} + \frac{G}{T_c} = 1 \tag{34}$$

that is:

$$\frac{\text{detachment rate by flow}}{\text{detachment capacity by flow}} + \frac{\text{sediment load in flow}}{\text{transport capacity of flow}} \cong 1$$

Based on the assumption of steady uniform flow in this study, Chezy's formula can be used for calculating the mean velocity of flow. The Chezy's formula is:

$$V = C \sqrt{RS} \tag{35}$$

where V is mean velocity (fps), R is hydraulic radius, S is slope and C is Chezy's constant, a factor of flow resistance.

Since surface runoff (overland flow) in surface-mined areas is relatively wide and that the flow, in general, is uniform and steady. The discharge per unit width of channel (overland flow) may be represented by Chezy's formula:

$$q = C\ S^{1/2}\ y^{3/2} \tag{36}$$

where q is the discharge per unit width, C and S was the same as equation (35) and y is the flow depth. By following the Darcy-Weisbach formula, for uniform and nearly uniform flow, the friction factor (f) can be expressed:

$$f = \frac{8\ gRS}{V^2} \tag{37}$$

where g is the accleration due to gravity, R, V, S are hydraulic radius, velocity and slope gradient, respectively.

When water flows on the surface or in a channel, a force is developed that acts in the direction of flow on the channel bed or ground surface. This force, which is simply the pull of water on a wetted area, is known as the tractive force. This is illustrated in Figure 23. In a uniform form the tractive force is apparently equal to the gravity force acting on the body of water parallel to the channel bottom or ground surface and equal to γ ALS, where γ is the unit weight of water, A is the wetted area, L is the length of channel or surface ground and S is slope. Thus, the average value of the tractive force per unit wetted area or the so-called unit tractive force (τ):

$$\tau = \gamma ALS/pL = \gamma RS \tag{38}$$

and

$$A/p = R$$

where p is the wetted perimeter. In the very wide channel, the hydraulic radius (R) is equal to the depth of flow (y). Equation 38 can be rewritten:

$$\tau = \gamma yS \tag{39}$$

Solving equations (36) (37) (39) for y, the flow depth (y) can be expressed:

$$y = C' \left(\frac{f}{8gs}\right)^{1/3} q^{2/3} \tag{40}$$

Then substitute y for equation 39:

$$\tau = C'' S^{2/3} q^{2/3} \tag{41}$$

and

$$C'' = \gamma \left(\frac{f}{8g}\right)^{1/3} \tag{42}$$

For the simplification of analysis, we can set:

$$D_c = C_1 \tau^{3/2} \tag{43}$$

$$T_c = C_2 \tau^{3/2} \tag{44}$$

where C_1 and C_2 = constant

D_c = the amount of soil being detached by runoff.

T_c = the amount of soil being transported by runoff.

We also assume that the rainfall intensity is fixed and the duration of rainfall is long enough to create a balanced condition between input rainfall amount and the quantity of output surface runoff. Hence, the amount of surface runoff is:

$$q = q_0 X_0 \tag{45}$$

and

$$X_0 = \frac{X}{L} \tag{46}$$

where q = the runoff discharge per unit width

X = partial slope length between any two point

L = total slope length

q_0 = the runoff discharge per unit width at the toe of the slope

To rewrite D_c and T_c as a non-dimension variable:

$$\frac{D_c}{D_b} = \frac{C_1 S_c q X_o}{C_1 S_b q \cdot 1} = \frac{S_c}{S_b} X_o = S_* X_o \quad (47)$$

$$\frac{T_c}{T_b} = \frac{C_2 S_c q X_o}{C_2 S_b q \cdot 1} = \frac{S_c}{S_b} X_o = S_* X_o \quad (48)$$

where D_b = the amount of soil being detached by runoff at the toe of the slope

T_b = the amount of soil being transported by runoff at the toe of the slope

By substitution equations 47 and 48 into equation (34):

$$\frac{D_R}{D_b} + \frac{G}{T_b} = S_* X_o \quad (49)$$

By taking the partial derivative of equation 49 with respect to X_o:

$$\frac{\partial}{\partial X_o}\left(\frac{D_R}{D_b}\right) + \phi \frac{D_R}{D_b} = \frac{\partial}{\partial X_o}(u) - \psi \quad (50)$$

and

$$\phi = \frac{L D_b}{T_b} \quad (51)$$

$$\psi = \frac{L D_i}{T_b} \quad (52)$$

$$u = S_* X_o \quad (53)$$

By integration of equation 50:

$$\frac{D_R}{D_b} = e^{-\phi X_o}\left[\int \left(\frac{\partial u}{\partial X_o} - \psi\right) e^{\phi X_o} \partial X_o + C\right] \quad (54)$$

By replacement of D_R/D_b in equation 49:

$$\frac{G}{T_b} = u - e^{-\phi X_o}\left[\int \left(\frac{\partial u}{\partial X_o} - \psi\right) e^{\phi X_o} \partial X_o + C\right] \quad (55)$$

C is an integration constant which depends on the boundary conditions that we superimposed. When $S_c = S_b$, then S_* is equal to one and $\partial u/\partial X_0$ is also equal to one. Hence, equation 55 can be rewritten:

$$G = T_b \left[X_0 - \frac{1}{\phi} (1 - \psi)(1 - e^{-\phi X_0})\right] \tag{56}$$

This is the equation that we can use for predicting soil loss on surface-mined areas. When the partial slope length, which we suppose to measure, is equal to the total slope length, then the X_0 is equal to unity. Equation 56 can be simplified in this study.

$$G = T_b \left[1 - \frac{1}{\phi} (1 - \psi)(1 - e^{-\phi})\right] \tag{57}$$

Hence the G/T_b ratio is only a function of two constants, ϕ and ψ, which are the key constants used for modification and verification of this mathematical model.

Model Modification

To obtain as much accuracy as possible from this model, we must become as familiar as possible with the derivation of these factors and how they are determined in practice. Unfortunately, in most mined areas sufficient data does not exist to test this type of model. Also, it is generally too expensive to apply a complicated mathematical model repeatedly to predict the sediment yield from storms. On the other hand, a weakness of any model and even a theoretical system, such as the model described previously, is that it is not the real system but a mimic of it. It is no better than the degree to which it actually responds as the true system. For significantly different watersheds or mined areas we cannot expect the data to fit the same equation. Hence, a modification of this model is not only necessary but also important. However, if the mathematical model is calibrate for each storm, accurate data can be generated from this modified model to fit a real system. From this model rapid soil loss estimates can be made.

Most of the parameters of this dynamic simulation system are based on measurable factors which can be directly or indirectly obtained by means of laboratory experimentation. After all parameter values have been obtained, the model should be thoroughly tested and modified. These tests and modifications should be designed to answer such questions as: how sensitive is this model to both variable and parameter values, and how accurate is the expected estimation? In addition to testing the model, it must be validated and checked with data that have been collected in the field or in the laboratory. This will not only provide a check on the sensitivity analysis but will also help to evaluate the accuracy and stability of the simulated system. Hence, if the system is conceptually sound, there should be very little difference between its response and that of the real system. A key assumption that we made is that the soil loss by measurement (G_m) should be equal to that by estimation (G_e). It can be explained in terms of mathematical expression:

$$MF = \frac{G_e}{G_m} = 1 \tag{58}$$

The ratio of G_e and G_m can be defined as the Modification Factor (MF) of this model. The soil loss (G_m) can be obtained by using a rainfall simulator that can apply a range of rainfall intensities to a soil erosion plot with adjustable slope. Because the plot length is relatively short, a small simulator can be used to obtain different soil losses in the laboratory. It can also be used to evaluate losses under 3 X 3 X 4 X 5 treatment combinations (Intensity X Runoff X Slope X Soil Texture). Thus, in one experimental cycle it may be possible to obtain the information needed to study a given soil texture. Because the model is conceptually sound, data collected for short time periods from several different soil types, slopes, rainfall intensities and runoff patterns covering the extremes of possible field condition should provide the information needed to modify the model and to analyze many field conditions.

Values of ϕ and ψ were calculated by numerical analysis techniques and were used to calculate value of G (i.e., G_e) for the erosion plot under different treatment combinations. The distribution of modification factor (MF) which is the ratio of G_e and G_m, with respect to ϕ and ψ as given by equation 57 is graphically explained in Figures 29 through 34. From equation 57, the value of ϕ cannot be zero. Hence, the value of ϕ, ψ and MF should be identified at a reasonably limited range. This can be shown in Table 11.

Table 11. Limited Range of ϕ, ψ and MF for Different Soil Texture and Runoff Rate.

Soil texture	Runoff (cm^3/sec)	ϕ	MF	ψ
Sandy loam	0	$0 < \phi \leq 1$	$1 \leq MF < 0$	$0 \leq \psi \leq 4.78$
Sandy loam	21	"	"	$0 \leq \psi \leq 10.02$
Sandy loam	42	"	"	$0 \leq \psi \leq 12.08$
Sandy clay loam	0	"	"	$0 \leq \psi \leq 2.00$
Sandy clay loam	21	"	"	$0 \leq \psi < 5.52$
Sandy clay loam	42	"	"	$0 \leq \psi \leq 6.53$

CHAPTER V

RESULTS AND DISCUSSION

Soil erosion by rainfall and runoff is a complex process that has been simulated by empirical equations (Meyer and Wischmeier, 1969). The proposed mathematical model of the erosion-sedimentation process considers the relative contributions of four individual subprocesses and describes soil movement along a slope. However, each of these subprocesses is a function of complex interrelations between parameters. Tables 12 through 51 and Figures 25 through 34 illustrate typical results of this experimental application of the model. These accompanying tables and graphs show how various physical parameters affect the results obtained by using this simulation system. They illustrate the individual and collective effects of detachment and transport of soil by rainfall and runoff, based on the assumed relationship.

Rainfall Simulation

Chow and Harbaugh (1965) indicated that tubing tips of the selected rainfall simulator produced drops of 3.20 mm diameter. This was confirmed by collecting and weighing a known number of drops and then calculating the average drop size (3.30 mm diameter) which is shown in Table 12. Figure 25 shows the relationship between rainfall intensity and floatmeter reading. This was determined by measuring the amount of artificial rainfall in 16 containers over a known time interval and at a fixed floatmeter reading (Tables 13 and 14). During the calibration, the intensity of rainfall was found to vary at different points over the plot area (Table 14). At rainfall intensity of 64.01 mm (2.52 inches) per hour, the factor of water pressure inside the rainfall chamber for all the tubes becomes

Table 12. Raindrop Size Calculation.

No. of Can	No. of Trial	Tare (g)	Can + Water (g)	Water (g)	No. of Drops	Dia. of Drop (mm)
261	1	8.626	11.203	2.577	150	3.200
152	2	8.505	10.343	1.838	100	3.274
240	3	8.605	10.379	1.774	150	3.236
286	4	8.646	11.606	2.960	150	3.353
161	5	8.525	10.869	2.344	150	3.102
273	6	8.636	12.354	3.718	200	3.287
251	7	8.635	10.505	1.870	100	3.293
106	8	8.647	11.556	2.909	150	3.333
278	9	8.697	11.717	3.020	150	3.375
6	10	8.657	10.424	1.767	100	3.232
231	11	8.435	10.334	1.899	100	3.310
279	12	8.737	12.586	3.849	200	3.325
100	13	8.616	12.253	3.637	200	3.263
191	14	8.717	11.455	2.738	150	3.267
310	15	8.726	11.657	2.931	150	3.342
264	16	8.404	12.192	3.788	200	3.307
236	17	8.666	10.404	1.738	100	3.214
181	18	8.657	12.808	4.151	200	3.410
137	19	8.596	12.454	3.858	200	3.327
261	20	8.465	11.313	2.848	150	3.310
242	21	8.768	10.697	1.929	100	3.327
142	22	8.656	11.344	2.688	150	3.247
146	23	8.546	12.737	4.191	200	3.421
110	24	8.738	12.809	4.071	200	3.388
147	25	8.647	10.666	2.019	100	3.378

μ(Dia. of raindrop) $\approx$ 3.301 mm $\approx$ 3.30 mm.
σ(Dia. of raindrop) $\approx$ 0.07 mm.

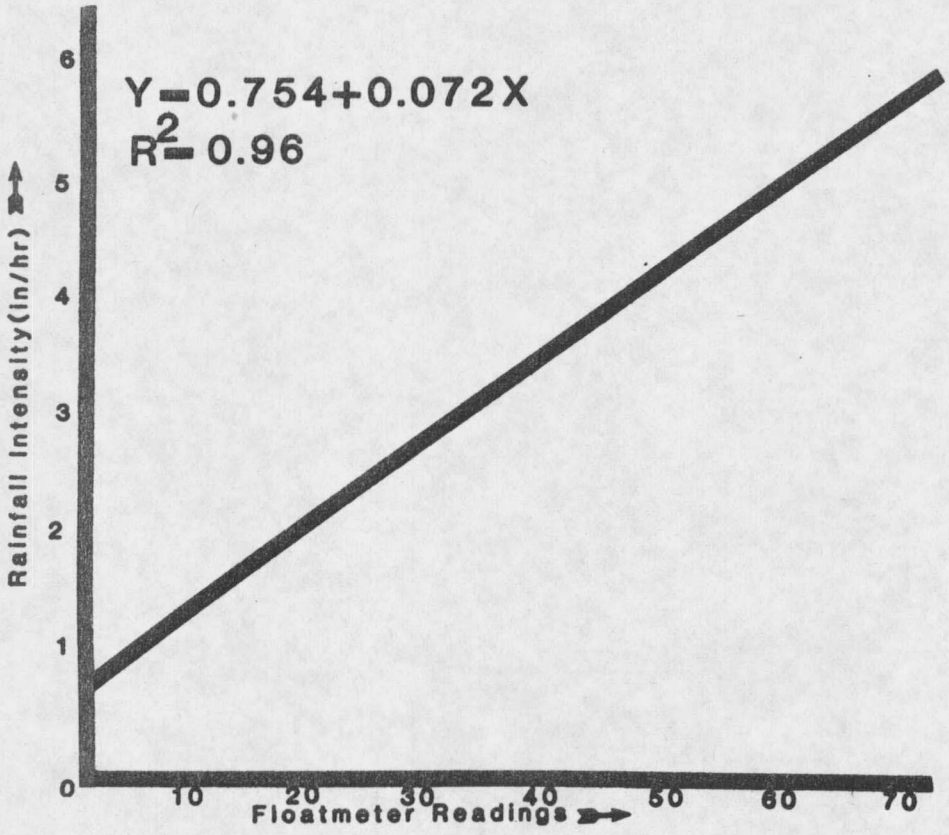


Figure 25. Linear relationship between rainfall intensity and floatmeter reading.

Table 13. Floatmeter Reading vs. Variation of Rainfall Intensity Over the Plot Area.

	μ		σ_1		$\bar{\mu}$		σ_2	
R_d	(ml)	(inch)	(ml)	(inch)	(ml)	(inch)	(ml)	(inch)
10	150.75	1.97	58.66	0.76				
10	159.56	2.08	59.30	0.77				
10	141.88	1.85	51.59	0.67	150.73	1.96	7.35	0.095
20	163.56	2.13	58.38	0.76				
20	158.75	2.07	60.04	0.78				
20	164.68	2.14	60.38	0.79	162.33	2.11	2.57	0.033
30	195.63	2.55	57.36	0.75				
30	193.43	2.52	56.06	0.73				
30	190.93	2.49	56.93	0.74	193.33	2.52	2.05	0.057
40	248.13	3.23	49.65	0.65				
40	266.25	3.47	47.81	0.62				
40	259.69	3.38	50.08	0.65	258.44	3.36	3.34	0.043
50	318.75	4.15	47.71	0.62				
50	329.38	4.29	48.54	0.63				
50	331.33	4.31	49.24	0.64	327.50	4.26	5.53	0.072
60	399.38	5.20	53.32	0.69				
60	298.44	5.17	54.71	0.71				
60	389.06	5.06	57.67	0.75	395.63	5.15	4.66	0.06
70	480.31	6.25	69.92	0.31				
70	454.75	5.92	65.84	0.86				
70	463.75	6.04	55.66	0.72	466.27	6.07	10.58	0.138

R_d = Floatmeter reading.
μ = Mean of each trial.
σ_1 = Standard deviation within each trial.
$\bar{\mu}$ = General mean rainfall intensity (3 trial).
σ_2 = Standard deviation among each trial.

Table 14. Rainfall Intensity Calibration Data* (see Fig. 8, referred to the # of container).

		Amount of Measured Simulated Rainfall (ml/can)																	
R_d	Time (min)	11* (ml)	12 (ml)	13 (ml)	14 (ml)	21 (ml)	22 (ml)	23 (ml)	24 (ml)	31 (ml)	32 (ml)	33 (ml)	34 (ml)	41 (ml)	42 (ml)	43 (ml)	44 (ml)	μ (ml)	σ (ml)
10	10 min	220	235	225	185	200	205	200	130	135	145	145	95	85	80	65	60	151	59
10	"	225	250	225	195	225	215	200	130	160	150	150	98	100	90	70	70	160	59
10	"	200	225	200	165	190	190	180	120	140	135	140	90	85	85	65	60	142	52
μ		215	237	217	182	205	203	193	127	145	143	145	94	90	85	67	63	151	57
20	"	230	255	230	185	210	215	200	135	180	162	170	110	110	90	70	65	164	59
20	"	225	250	230	180	210	220	205	130	165	150	160	100	100	85	70	60	159	60
20	"	250	255	220	180	220	230	200	140	175	150	165	110	110	100	70	60	165	60
μ		235	253	227	182	213	222	202	135	173	154	165	107	107	92	70	62	162	63
30	"	280	290	250	210	250	250	220	170	200	180	195	130	160	140	105	100	196	57
30	"	280	285	245	210	240	240	220	170	200	175	200	140	160	130	100	100	193	56
30	"	270	280	240	215	240	245	230	160	200	170	200	130	150	125	100	100	191	57
μ		277	285	245	212	243	245	223	167	200	175	198	133	157	132	102	100	193	57
40	"	300	320	290	280	300	300	300	240	270	260	280	200	240	200	190	170	288	65
40	"	320	320	310	290	310	300	300	230	290	260	300	200	250	210	190	180	266	48
40	"	310	320	300	290	310	300	290	220	290	250	290	200	240	200	180	165	260	50
μ		310	320	300	287	307	300	297	230	283	257	290	200	243	203	287	173	261	49
50	"	380	380	400	360	320	380	350	300	310	295	300	260	270	265	260	270	318	48
50	"	380	390	400	380	340	380	380	320	320	320	290	260	300	260	260	290	329	49
50	"	400	400	400	400	330	380	380	310	320	320	300	260	300	270	280	300	331	49
μ		387	390	400	380	330	380	370	310	317	312	297	260	290	265	267	287	327	43
60	"	440	440	450	430	380	480	450	400	450	390	400	280	380	330	320	370	399	53
60	"	490	440	450	400	410	470	440	380	440	365	390	280	380	380	310	350	398	55
60	"	490	440	450	420	380	460	430	395	440	360	360	270	360	340	300	330	389	58
μ		457	440	450	417	397	473	443	392	445	375	390	283	377	350	317	353	396	53
70	"	540	600	590	500	480	550	490	440	500	450	490	330	445	480	360	440	680	70
70	"	535	530	520	430	516	555	468	390	500	412	464	350	440	445	336	385	455	66
70	"	530	530	540	460	500	540	480	420	480	440	480	340	440	440	400	400	464	56
μ		535	553	550	463	499	548	479	417	493	434	478	340	442	455	365	408	466	65

critical. The variation between trials, beyond this critical point begins to increase (Table 13). For this reason, the minimum intensity for this simulator is suggested to be 6.4 cm/hr (2.5 in/hr) at a minimum height of 2.33 m. The maximum intensity that the unit can deliver depends on the difference in elevation between the tops of the drop forms and the base of the bubbler tube. The maximum intensity of 21.6 cm/hr (8.5 in/hr) was investigated by increasing elevation difference up to 20 cm (8 inches) (Munn, 1971). The relationship between simulated rainfall intensity and floatmeter reading was analyzed by using statistical techniques including linear regression analysis, analysis of covariance and test of homogeneity of adjusted means (Tables 15 through 17). The purpose of this statistical analysis was to determine whether differences existed among four linear regressions which were shown in Table 15. These linear regressions had similar slopes ($\beta_1 = \beta_2 = \beta_3 = \beta_4 \neq 0$) and Y-axis intercepts. For this reason, the fourth regression in Table 15 was chosen to explain the relationship between floatmeter reading and simulated rainfall intensity (Fig. 25).

The kinetic energy produced by this simulator for a 30 minute event with a 2.33 meter fall height, a drop size of 3.30 mm diameter, and a 5.8 meter per second velocity, is 3.17×10^{-4} Joules per drop and 207.5 ton-m/ha-cm (699.7 ft-tons/acre-in) per volume which is equivalent to a natural intensity (I) of 0.56 cm/hr (0.22 in/hr) (Table 18) by using the relationship presented in Wischmeier et al. (1958):

$$KE = 916 + 331 \log_{10} I \qquad (58)$$

In general, the rainfall simulator yields a lower energy, mainly because simulated raindrops have not reached their terminal velocity. In this study, this simulator produced approximately 87% of the terminal velocity produced by a natural rainstorm with a 2.54 cm/hr (1 in/hr) intensity. Table 18 shows that the KE per volume of rainfall for this simulator is greater than that of any of the hand portable units which were reviewed and compares very favorably to the larger nozzle operated units. The KE variation due to slope is determined

Table 15. Linear Regression Analysis of Intensity vs. Floatmeter Reading.

No.	Regression	r^2	F	H_0
1	$\hat{Y}_X = 0.0736X + 0.694$	0.95	96.01**	β_1 @ = 0
2	$\hat{Y}_X = 0.0696X + 0.653$	0.96	115.98**	$\beta_2 = 0$
3	$\hat{Y}_X = 0.0723X + 0.720$	0.97	168.74**	$\beta_3 = 0$
4	$\hat{Y}_X = 0.0720X + 0.754$	0.96	131.41**	$\beta_4 = 0$

**Significant difference at $\alpha = 0.01$.
@ $\mu_{y,x} = \alpha + \beta X$ is to be estimated by $\hat{Y}_X = a + bX$.

Table 16. Analysis of Covariance for Test of Homogeneity of Regression Coefficients.

SV	SS	DF	MS	F	H_0
Regression due to $\bar{b}$	57.83	1	57.83	4900.85**	$\bar{\beta} = 0$
Variation among b's	0.05	3	0.017	0.144	$\beta_1 = \beta_2 = \beta_3 = \beta_4$
Pooled residual	2.35	20	0.118		
Total	60.23	24			

**Significant difference at $\alpha = 0.01$.

Table 17. Test of Homogeneity of Adjusted Means with Equal Regression Coefficients.

SV	SS	DF	MS	F	H_0
Variation among $\hat{Y}_X$	0.84	3	0.28	2.38	$\mu_1 = \mu_2 = \mu_3 = \mu_4$
Pooled residual	2.35	20	0.12		
Total	3.19	23			

Table[a] 18. KE vs. Drop Diameter and Velocity for Selected Rainfall Simulators.

Simulator	$D_{(mm)}$	Fall Height (m)	V(m/sec)	KE/drop[b] (10^{-4} J)	KE/vol.[c] ft-tons/acre-in	Equivalent[d] Natural I (in/hr)
Meeuwig	3.0	0.38	2.5	0.365	118.8	0.004
Adams et al.	5.56	1.00	4.29	6.85	359.7	0.019
McQueen	5.61	1.50	5.17	10.20	507.8	0.058
Type-F	Nozzle	pressure	—	—	571.9	0.091
Tahoe Basin; Ca*	3.30	2.33-2.67	5.8-6.2	3.17∿3.62	699.7∿799.8	0.22∿0.45
Rainulator	Nozzle	pressure	—	—	786.4	0.40

[a] Data from Meyer, 1965.
[b] KE/drop = $(2.618 \times 10^{-7})\ D^3\ V^2$ Joules.
[c] KE/vol. = $20.8 \times V^2$ ft-tons/acre-in.
[d] From Wischmeier and Smith (1958)
KE (ft-tons/acre-in) = $916 + 331 \log_{10} I$.
I = Natural Storm Intensity (in/hr).
*Selected rainfall simulator in this study.

by the difference in drop fall distance between the top and bottom of the plot. This causes drop fall velocities to increase, with a resultant increase in KE from the top to the base of the plot. Total KE variation due to slope is only 3.5% from the top to the base of the slope (Tables 19 and 20), because the rate at which drop fall velocity increases lessens as the height of fall becomes greater. Also, the uniform drop size and lower energy produced by the simulator make it impossible to simulate the relationship between energy, intensity, terminal velocity, drop size and fall height that exist in natural storms. There are other factors, such as momentum, spatial distribution of momentum, velocity and energy that further complicate the simulated problem.

Particle Size Distribution

An improved method of representing the different particle sizes in a soil is the logarithmic chart shown in Figures 26 through 28. The entire range in particle sizes, plotted on a logarithmic scale, forms the horizontal divisions, while the percentage by weight of the soil particles that are finer than a given size forms the vertical divisions. In Figures 26, 27, and 28, curve A represents the eroded sediment from the sandy loam, sandy clay loam and mixed soil respectively. Curve B represents the particle size curves of those soils before erosion. The gaps between these two curves can be explained in terms of relative soil erodibility of different particle sizes. The gaps increase with an increase in soil erodibility. For this reason, the gaps shown in Figure 26 are larger than that of Figure 27. Hence, the soil erodibility of the sandy loam is larger than that of sandy clay loam. Also, notice that the finest particle sizes and the coarsest particle sizes are much more resistant to soil erosion. This can be confirmed because the smallest difference between curves occurs at the coarse and fine particle size ranges (Figs. 26, 27, and 28). Fine particles are more cohesive than coarse ones and resist soil erosion. Coarse particles are not readily transported by runoff. The intersection points on Figures 26 through 28 represents the critical particle size in

Table 19. Variation in Plot Dimensions vs. Percent Slope.

(%)	(°)	Cos θ	L (cm)	Area (cm^2)	% of Area Variation	Variation in drop fall (in)
1	0°34'	≅1.0	61.0	3721	0	0
20	11°19'	0.9806	62.2	3869	2.0	±2.4
40	21°48'	0.9285	65.7	4316	7.7	±4.8
60	30°58'	0.8575	71.1	5055	16.6	±7.2

Table[a] 20. KE Variation Due to Slope Changes.

				H(cm)		KE/drop (10^{-4} J)	
S (%)	Sin θ	L (cm)	ΔH (cm)	max	min	max	min
1	0	60.96	0	233	267	3.17	3.62
20	0.1961	60.96	11.95	221.1	225.1	2.95	3.50
40	0.3714	60.96	22.64	210.4	244.4	2.85	3.17
60	0.5145	60.96	31.36	201.6	235.6	2.74	3.06

[a] Assumptions:
1) Raindrop should be sphere and rigid,
2) Air friction is small enough to be neglected,
3) Vertical rainfall due to still air condition,
4) No energy loss during simulation process,
5) At room temperature.

[b] % of KE variation:

$2.33 < H < 2.67$ (m)

$5.80 < V < 6.20$ (m/sec)

$3.17 < KE_1 < 3.62$ (10^{-4} J) (by changing fall height)

$2.74 < KE_2 < 3.17$ (10^{-4} J) (at H_{min}, by changing slope)

$3.06 < KE_2 < 3.62$ (10^{-4} J) (at H_{max}, by changing slope)

$3.17 < KE_4 < 3.06$ (10^{-4} J) vs. $KE_{ave} = 3.12 \times 10^{-4}$ J

$\cong \pm 0.11 \times 10^{-4}$ J

$\cong$ 3.5% of variation

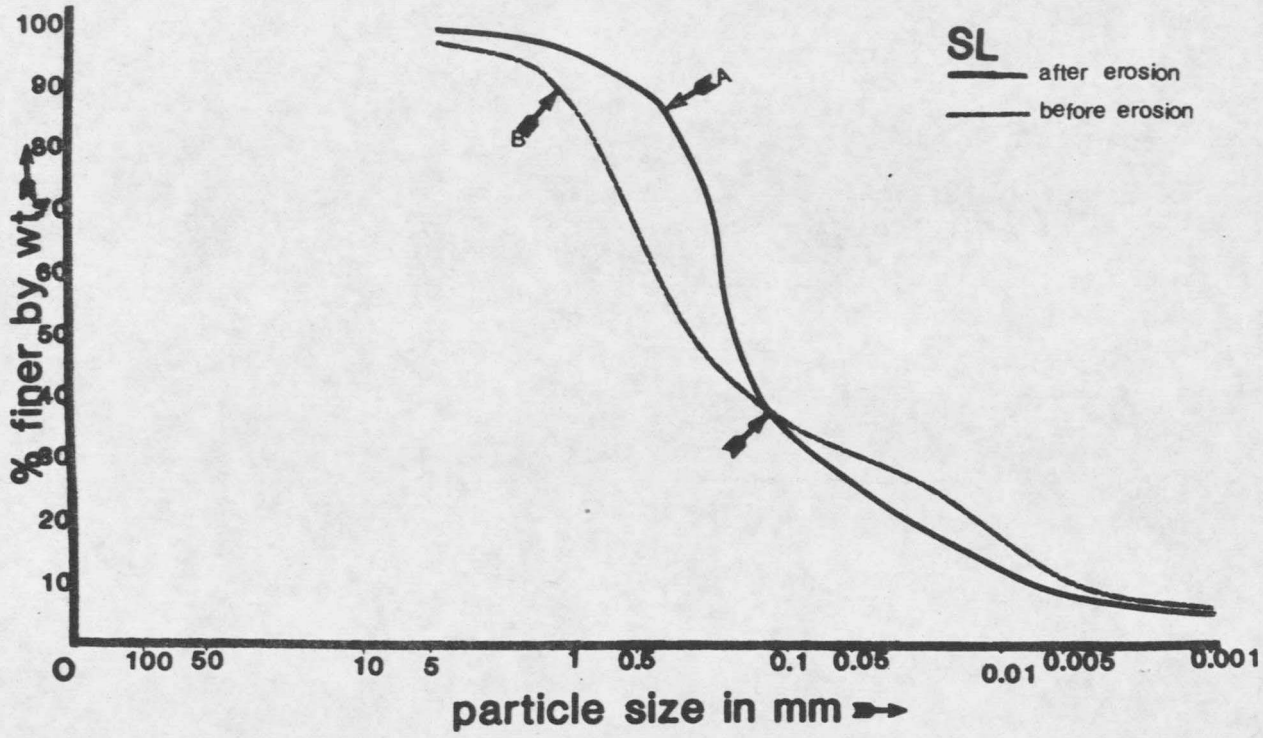


Figure 26. Particle size curves for sandy loam after erosion and before erosion.

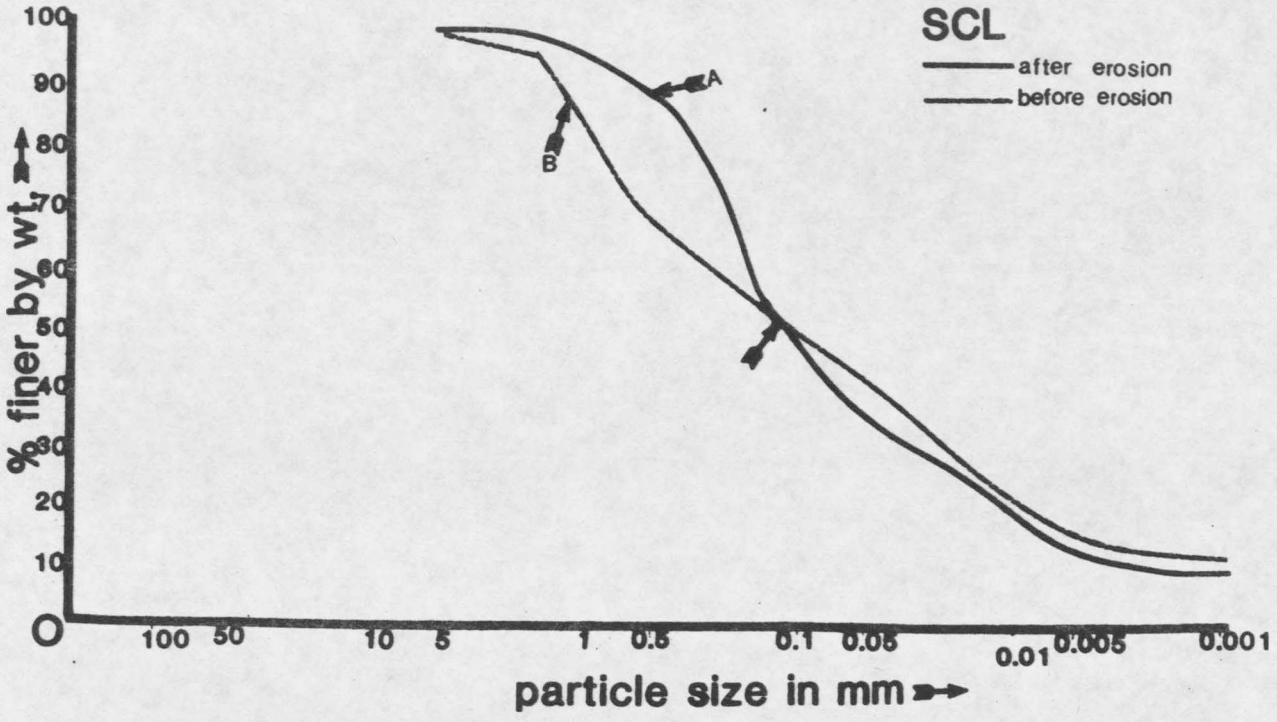


Figure 27. Particle size curves for sandy clay loam after erosion and before erosion.

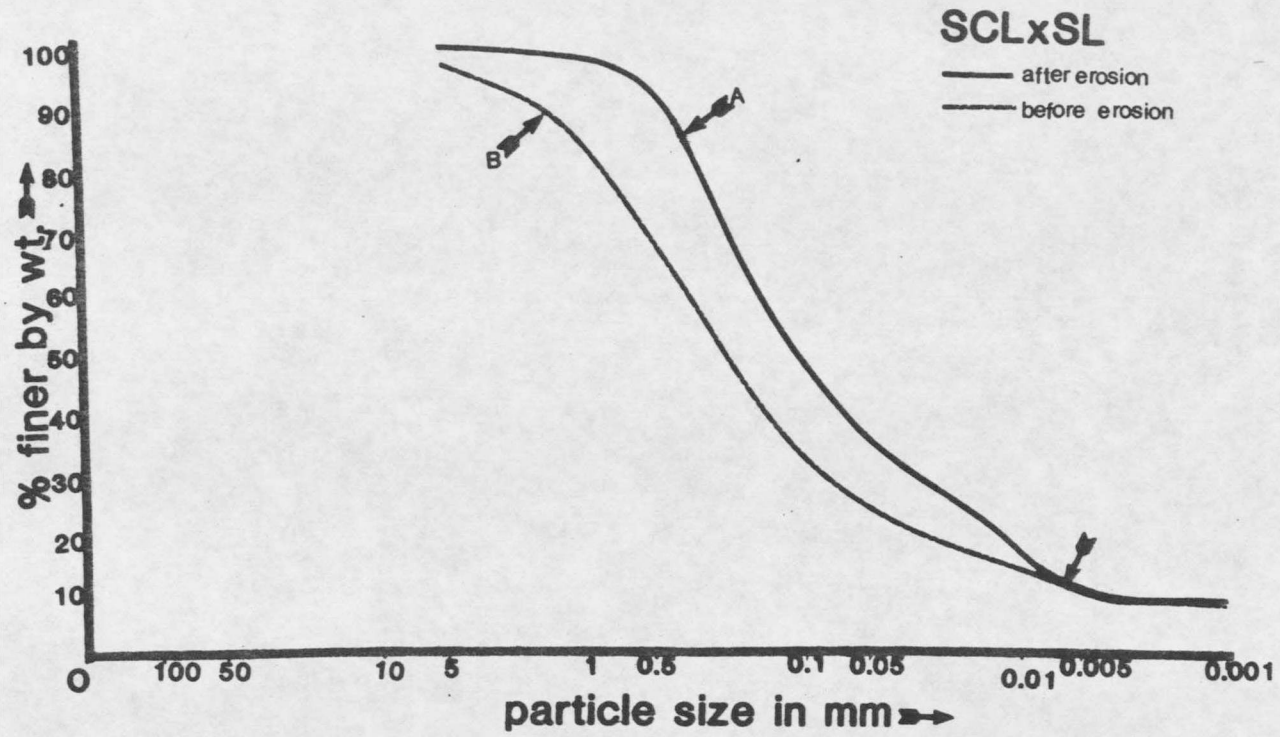


Figure 28. Particle size curves for mixed soils (SL mixed with SCL) after erosion and before erosion.

terms of erodibility. In the study, the critical sizes are 0.05 mm, 0.18 mm and 6.5 μm for sandy loam, sandy clay loam and mixed soil respectively. The three soils have steep particle size curves in the sand range that gradually become long, flat curves in the fine range. This may indicate that the soils were formed by mechanical weathering and later altered by chemical weathering (Sowers, 1979). Hence, those soils can be termed weathered-uniform soils.

Sediment Yields Estimation

A hydromechanical erosion model would provide a comprehensive expression of the underlying physical and mechanical processes involved in erosion and sedimentation. With it, data needed for a thorough study of the effects of important interactions among soil texture, rainfall intensity, runoff and topographic variables (Table 21) could be evaluated rapidly. Statistical techniques, such as factorial analysis of variance, individual degree of freedom, multiple comparisons among treatment means and Duncan's multiple range test (MRT) would be helpful to analyze these data collected from the completely randomized experiments (CRD). The MSUSTAT program, an interactive statistical analysis package, was used to analyze the data (Lund, 1979). Throughout this study, α=0.05 and/or α=0.01 probability level of significance were selected to evaluate whether or not an individual independent variable would be significant in the experiment. In order to evaluate whether an independent variable, such as slope, intensity, soil, and runoff, is significantly related to a dependent variable, sediment yield, in the completely randomized experiments, one must consider the total number of independent variables and the interactions among these independent variables. Significant variables were compared to previous research results as a means of verification.

Table 21. Average Sediment Yield for Each Soil Under 36 Treatment Combinations.

R (cm^3/sec)	I (in/hr)	Slope (%)	Soil loss: Average Sediment Yield (g/plot) SL	SCL	SL/SCL	SCL/SL	SL x SCL
0	1.5	0	0.09†	0.07	0.10	0.06	0.08
		20	3.13	3.14	3.48	2.91	3.03
		40	8.36	7.17	8.98	6.55	7.32
		60	29.79	13.13	30.03	12.44	24.94
	2.0	0	0.12	0.10	0.15	0.08	0.09
		20	4.18	3.66	4.89	3.48	3.93
		40	12.84	8.36	14.19	7.88	12.23
		60	36.08	16.46	39.15	15.06	32.44
	2.5	0	0.18	0.14	0.22	0.12	0.15
		20	6.42	4.61	6.56	4.32	5.93
		40	15.79	10.60	16.61	9.62	12.74
		60	45.77	19.59	47.57	18.27	39.98
21	1.5	0	0.33	0.25	0.47	0.19	0.32
		20	13.46	9.40	14.93	8.68	12.58
		40	39.60	24.10	40.69	22.89	39.23
		60	125.50	48.70	129.38	45.80	121.00
	2.0	0	0.42	0.37	0.58	0.28	0.39
		20	16.48	12.54	17.84	11.21	16.16
		40	54.40	37.80	56.59	35.31	53.17
		60	151.80	86.80	156.31	77.40	144.20
	2.5	0	0.47	0.42	0.63	0.33	0.45
		20	18.63	14.70	19.54	14.31	16.97
		40	70.50	40.20	73.78	35.74	67.02
		60	184.94	106.60	194.29	102.94	171.93
42	1.5	0	0.50	0.39	0.67	0.36	0.47
		20	15.77	11.18	16.22	10.35	15.04
		40	55.62	36.39	56.74	36.15	54.26
		60	189.32	74.89	197.01	72.13	178.39
	2.0	0	0.68	0.53	0.82	0.48	0.57
		20	20.03	14.58	21.06	13.72	18.68
		40	88.44	45.72	90.04	42.40	84.25
		60	220.48	102.78	232.66	91.10	204.86
	2.5	0	0.84	0.71	1.03	0.62	0.81
		20	25.13	16.86	25.73	15.22	22.24
		40	103.44	48.81	112.75	44.33	98.18
		60	259.24	238.84	273.44	114.84	241.98

†Each number is the mean of three replicate trials.

Tables 22 and 23 show the analysis of variance (ANOV) between the independent variables, soil texture, and soil losses. The comparisons among soil textures using the multiple range test indicated that soil losses from two soil textures (SL and SCL) were significantly different. The following soil comparisons were not significantly different: sandy loam ↔ M1 type soil, sandy clay loam ↔ M2 type soil, M1 type soil ↔ M3 type soil (Tables 24 and 25). There were no significant difference between layered soils (M1 and M2) and natural soils (sandy loam and sandy clay loam) as shown in Table 22. The results of factorial ANOV for each soil are shown in Tables 26, 30, 34, 38 and 42. All independent variables and interactions among them had significant differences at the 1% probability level. Therefore, previous erosion research results can be confirmed by this study. To determine if the three factors were different with respect to soil losses based on each soil texture, the multiple comparisons among each factorial groups were used (Tables 27 through 45). The results of this test showed that all three factors, slope, runoff, and intensity, were significantly different at either α=0.05 or α=0.01 with respect to soil loss for each soil texture base. Tables 26 through 45 also strongly indicate that plots with steeper slopes and higher rainfall intensity and runoff rates were more sensitive to erosion by raindrop and runoff. In each soil type, as the slope, intensity, and runoff increased, the sediment yield also increased significantly.

Tables 46 through 51 give the results of flow regimes when runoff occurs. In general, a Froude number (F_r) of more than 1 can be described as supercritical flow which is more erosive than subcritical flow. A Reynolds number (R_e) less than 500 denotes laminar flow which is less erosive than turbulent flow. Field studies by Morgan (1979) indicate that most of runoff is laminar with an R_e between 1 and 50 and F_r are between 0.01 and 0.1. All of these research results were confirmed by the study shown in Tables 46 through 51. In this study most runoff flow regimes were subcritical-laminar ($R_e = 3 \sim 70$, $F_r = 0.02 \sim 0.41 \times 10^{-2}$).

Equation 55 is a non-linear hyperbolic partial differential equation. Even though it can be simplified by superimposing boundary conditions, a considerable number of numerical schemes are still required for its solution (Burden et al., 1981). The solution of this equation can best be explained graphically as they are shown on Figures 29 through 34 which show the distribution of solutions with respect to two unknown constants ψ and ϕ referred to in the previous discussion. Table 52 and Figures 35 through 40 show that the differences in soil loss of actual measurement and model prediction are not highly significant. Figures 35 through 40 indicate that the effects of erosive factors (slope, soil texture, rainfall intensity, runoff) on simulated soil loss are non-linear, because sediment yields are not only dependent upon individual erosive factors but also upon the interaction of these factors. Therefore, a hyperbolic equation would be expected to describe the mechanical processes of erosion. The application of this model, which has been drawn graphically, will be discussed in more detail in the following section.

Table 22. ANOV of Comparisons Among Soil Texture.

SV	SS	DF	MS	F
TRT	151.34	4	37.835	33.54**
SL vs. SCL	83.85	1	83.85	74.34**
M1[a] vs. M2[b]	62.86	1	62.86	55.73**
SL & SCL vs. M1 & M2	2.51	1	2.51	2.23
Residual	2.12	1	2.12	
ERR	11.28	10	1.128	
TOT	162.62	14		

**Significant difference at $\alpha = 0.01$.
[a] M1:SL/SCL layered soil
[b] M2:SCL/SL layered soil

Table 23. ANOV of Comparisons Among Soil Texture.

SV	SS	DF	MS	F
TRT	151.34	4	37.835	33.54**
SL vs. M1[a]	3.01	1	3.01	2.67
SCL vs. M2[b]	0.26	1	0.26	0.23
SCL vs. M3[c]	26.71	1	27.61	23.68**
Residual	121.36	1	121.36	
ERR	11.28	10	1.128	
TOT	162.62	14		

**Significant difference at $\alpha = 0.01$.
[a] M1:SL/SCL layered soil
[b] M2:SCL/SL layered soil
[c] M3:SL mixed with SCL

Table 24. Duncan's Multiple Range Test

g	Varieties	Difference	SSR[a]	Conclusion
5	SL ↔ M2	7.89	2.09	*
4	SL ↔ SCL	7.48	2.02	*
3	SL ↔ M3	3.26	2.01	*
2	SL ↔ M1	1.42	1.92	NS
4	M1 ↔ M2	6.47	2.02	*
3	M1 ↔ SCL	6.06	2.01	*
2	M1 ↔ M3	1.84	1.92	NS
3	M3 ↔ M2	4.63	2.01	*
2	M3 ↔ SCL	4.22	1.92	*
2	SCL ↔ M2	0.41	1.92	NS

[a]SSR = significant student range.
* = significant difference at $\alpha = 0.05$.
NS = non-significant difference.
SL = sandy loam; SCL = sandy clay loam.
M1 = SL/SCL layered soil; M2 = SCL/SL layered soil; M3 = SL mixed with SCL.

Table 25. Results of Duncan's Multiple Range Test.

Varieties	M2	SCL	M3	M1	SL
Means	———		———		

Table 26. ANOV of Factorial Experiment for Sandy Loam.

SV	DF	SS	MS	F
TRT	35			
Runoff (R)	2	85240	42620	63430**
Intensity (I)	2	7804	3902	5308**
R X I	4	2003	500.7	745.3**
Slope (S)	3	311500	103800	154500**
R X S	6	97240	16200	24120**
I X S	6	6735	1123	1671**
R X I X S	12	1827	152.3	226.6**
ERR	72	48.37	0.6719	

**Significant difference at $\alpha = 0.01$.

Slope Base:

Table 27. Multiple Slope Comparisons of Sandy Loam.

Varieties	Mean Difference	t
1% ↔ 20%	13.29	59.55**
1% ↔ 40%	49.48	221.80**
1% ↔ 60%	137.70	617.20**
20% ↔ 40%	36.20	162.2 **
20% ↔ 60%	124.40	557.7 **
40% ↔ 60%	88.21	395.4 **

**Significant difference at $\alpha = 0.01$.

Intensity Base:

Table 28. Multiple Intensity Comparisons of Sandy Loam.

Varieties (in/hr)	Mean Difference	t
1.5 ↔ 2.0	10.37	53.69**
1.5 ↔ 2.5	20.82	107.80**
2.0 ↔ 2.5	10.45	54.09**

**Significant difference at $\alpha = 0.01$.

Runoff Base:

Table 29. Multiple Runoff Rate Comparisons of Sandy Loam.

Varieties (cm^3/sec)	Mean Difference	t
0 ↔ 21	42.82	221.6 **
0 ↔ 41	68.06	352.3 **
21 ↔ 42	25.25	130.7 **

**Significant difference at $\alpha = 0.01$.

Table 30. ANOV of Factorial Experiment for Sandy Clay Loam.

SV	DF	SS	MS	F
TRT	35			
Runoff (R)	2	21050	10525	15460**
Intensity (I)	2	3387	1694	2488**
R × I	4	1114	278.4	409.1**
Slope (S)	3	68920	22970	33760**
R × S	6	21230	3539	5201**
I × S	6	4310	718.3	1055**
R × I × S	12	1629	135.7	199.4**
ERR	72	49	0.6806	

**Significant difference at $\alpha = 0.01$.

Slope Base:

Table 31. Multiple Slope Comparisons of Sandy Clay Loam.

Varieties	Mean Difference	t
1% ↔ 20%	9.736	43.36**
1% ↔ 40%	28.45	126.70**
1% ↔ 60%	66.08	294.30**
20% ↔ 40%	18.72	83.36**
20% ↔ 60%	56.34	250.90**
40% ↔ 60%	37.63	167.6 **

**Significant difference at $\alpha = 0.01$.

Intensity Base:

Table 32. Multiple Intensity Comparisons of Sandy Clay Loam.

Varieties (in/hr)	Mean Difference	t
1.5 ↔ 2.0	8.40	43.20**
1.5 ↔ 2.5	13.59	69.90**
2.0 ↔ 2.5	5.19	26.70**

**Significant difference at $\alpha = 0.01$.

Runoff Base:

Table 33. Multiple Runoff Rate Comparisons of Sandy Clay Loam.

Varieties (cm^3 /sec)	Mean Difference	t
0 ↔ 21	24.57	126.4 **
0 ↔ 42	32.89	169.1 **
21 ↔ 42	8.31	42.76**

**Significant difference at $\alpha = 0.01$.

Table 34. ANOV of Factorial Experiment for M1 (SL/SCL) Soil.

SV	DF	SS	MS	F
TRT	35			
Runoff (R)	2	93570	46785	69640**
Intensity (I)	2	9381	4691	6982**
R X I	4	2549	637.2	948.4**
Slope (S)	3	340400	113400	168800**
R X S	6	107500	17930	26690**
I X S	6	8213	1369	2037**
R X I X S	12	2262	189.3	281.8**
ERR	72	48.37	0.6719	

**Significant difference at $\alpha = 0.01$.

Slope Base:

Table 35. Multiple Slope Comparisons of M1 Soil.

Varieties	Mean Difference	t
1% ↔ 20%	13.95	62.53**
1% ↔ 40%	51.74	231.90**
1% ↔ 60%	144.00	645.30**
20% ↔ 40%	37.79	169.40**
20% ↔ 60%	130.00	582.80**
40% ↔ 60%	92.22	413.40**

**Significant difference at $\alpha = 0.01$.

Intensity Base:

Table 36. Multiple Intensity Comparisons of M1 Soil.

Varieties (in/hr)	Mean Difference	t
1.5 ↔ 2.0	11.30	58.49**
1.5 ↔ 2.5	22.83	118.20**
2.0 ↔ 2.5	11.53	59.67**

**Significant difference at $\alpha = 0.01$.

Runoff Base:

Table 37. Multiple Runoff Rate Comparisons of M1 Soil.

Varieties (cm^3/sec)	Mean Difference	t
0 ↔ 21	44.43	230.0 **
0 ↔ 42	71.39	369.5 **
21 ↔ 42	26.97	139.6 **

**Significant difference at $\alpha = 0.01$.

Table 38. ANOV of Factorial Experiment for M2 (SL/SCL) Soil.

SV	DF	SS	MS	F
TRT	35			
Runoff (R)	2	13760	88835	25080**
Intensity (I)	2	2527	1263.5	3567**
R × I	4	872.0	218.0	615.5**
Slope (S)	3	58360	19450	54920**
R × S	6	17610	2936	8278**
I × S	6	3456	576.0	1626**
R × I × S	12	1387	115.6	326.5**
ERR	72	25.50	0.3452	

**Significant difference at $\alpha = 0.01$.

Slope Base:

Table 39. Multiple Slope Comparisons of M2 Soil.

Varieties	Mean Difference	t
1% ↔ 20%	9.059	55.93**
1% ↔ 40%	26.46	163.40**
1% ↔ 60%	60.83	375.50**
20% ↔ 40%	17.40	107.40**
20% ↔ 60%	51.77	319.60**
40% ↔ 60%	34.37	212.20**

**Significant difference at $\alpha = 0.01$.

Intensity Base:

Table 40. Multiple Intensity Comparisons of M2 Soil.

Varieties (in/hr)	Mean Difference	t
1.5 ↔ 2.0	6.656	47.45**
1.5 ↔ 2.5	11.820	84.24**
2.0 ↔ 2.5	5.161	36.79**

**Significant difference at $\alpha = 0.01$.

Runoff Base:

Table 41. Multiple Runoff Rate Comparisons of M2 Soil.

Varieties (cm^3/sec)	Mean Difference	t
0 ↔ 21	22.86	163.0 **
0 ↔ 42	30.09	214.5 **
21 ↔ 42	7.228	51.53**

**Significant difference at $\alpha = 0.01$.

Table 42. ANOV of Factorial Experiment for M3 (SL mixed with SCL) Soil.

SV	DF	SS	MS	F
TRT	35			
Runoff (R)	2	77840	38920	6824**
Intensity (I)	2	6581	3290	576.9**
R × I	4	1708	427.0	74.87**
Slope (S)	3	269700	89900	15760**
R × S	6	87790	14630	2566**
I × S	6	5150	858.4	150.5**
R × I × S	12	1485	123.7	21.69**
ERR	72	410.6	5.703	

**Significant difference at $\alpha = 0.01$.

Slope Base:

Table 43. Multiple Slope Comparisons of M3 Soil.

Varieties	Mean Difference	t
1% ↔ 20%	13.22	20.34**
1% ↔ 40%	47.22	76.65**
1% ↔ 60%	128.50	197.70**
20% ↔ 40%	34.00	52.32**
20% ↔ 60%	115.30	177.30**
40% ↔ 60%	81.26	125.00**

**Significant difference at $\alpha = 0.01$.

Intensity Base:

Table 44. Multiple Intensity Comparisons of M3 Soil.

Varieties (in/hr)	Mean Difference	t
1.5 ↔ 2.0	9.520	16.91**
1.5 ↔ 2.5	19.120	33.97**
2.0 ↔ 2.5	9.601	17.06**

**Significant difference at $\alpha = 0.01$.

Runoff Base:

Table 45. Multiple Runoff Rate Comparisons of M3 Soil.

Varieties (cm^3/sec)	Mean Difference	t
0 ↔ 21	42.37	75.27**
0 ↔ 42	64.74	115.0 **
21 ↔ 42	22.37	39.74**

**Significant difference at $\alpha = 0.01$.

Table 46. Runoff Over Sandy Loam Surface With R = 0 cm^3 /sec.

I (in/hr)	S (%)	Q (in^3 /sec)	V (10^{-4} ft/sec)	R_e	F_r (10^{-4})	T_b (lb/ft^2)	Flow-Regime
1.5	1	0.10	2.89	2.68	1.61	4.7×10^{-5}	Subcritical-Laminar
"	20	0.26	8.21	6.96	4.78	1.52×10^{-3}	"
"	40	0.31	11.95	8.30	6.56	3.31×10^{-3}	"
"	60	0.45	17.36	12.06	11.16	5.98×10^{-3}	"
2.0	1	0.16	3.97	4.28	2.05	5.95×10^{-5}	"
"	20	0.35	9.35	9.37	5.00	1.76×10^{-3}	"
"	40	0.37	12.77	9.91	7.08	3.61×10^{-3}	"
"	60	0.49	18.90	13.13	11.34	6.24×10^{-3}	"
2.5	1	0.18	4.17	4.81	2.08	6.32×10^{-5}	"
"	20	0.41	10.17	10.98	5.25	1.90×10^{-3}	"
"	40	0.43	12.44	11.52	7.65	3.90×10^{-3}	"
"	60	0.59	20.49	15.81	12.50	6.85×10^{-3}	"

Table 47. Runoff Over Sandy Clay Loam Surface With R = 0 cm^3 /sec.

I (in/hr)	S (%)	Q (in^3 /sec)	V (10^{-4} ft/sec)	R_e	F_r (10^{-4})	T_b (lb/ft^2)	Flow-Regime
1.5	1	0.12	2.97	3.22	1.53	5.15×10^{-5}	Subcritical-Laminar
"	20	0.31	9.00	8.30	5.01	1.66×10^{-3}	"
"	40	0.35	12.15	9.37	7.41	3.52×10^{-3}	"
"	60	0.45	19.53	12.06	13.33	5.98×10^{-3}	"
2.0	1	0.20	4.34	5.35	2.10	6.65×10^{-5}	"
"	20	0.35	9.35	9.37	5.00	1.76×10^{-3}	"
"	40	0.39	12.31	10.44	7.16	3.71×10^{-3}	"
"	60	0.55	19.09	14.74	11.64	6.62×10^{-3}	"
2.5	1	0.24	4.90	6.43	2.29	7.28×10^{-5}	"
"	20	0.43	10.66	11.52	5.50	1.95×10^{-3}	"
"	40	0.49	14.17	13.13	7.89	4.16×10^{-3}	"
"	60	0.61	21.18	16.35	12.91	6.97×10^{-3}	"

Table 48. Runoff Over Sandy Loam Surface With R = 21 cm^3/sec.

I (in/hr)	S (%)	Q (in^3/sec)	V (10^{-4} ft/sec)	R_e	F_r (10^{-4})	T_b (lb/ft^2)	Flow-Regime
1.5	1	0.77	15.11	20.70	7.07	1.30×10^{-4}	Subcritical-Laminar
"	20	1.50	34.72	40.31	17.29	3.64×10^{-3}	"
"	40	1.67	44.60	44.69	23.86	7.69×10^{-3}	"
"	60	1.79	62.15	47.94	37.91	11.92×10^{-3}	"
2.0	1	0.81	15.63	21.80	7.11	1.34×10^{-4}	"
"	20	1.79	38.85	47.94	18.76	3.97×10^{-3}	"
"	40	1.91	47.37	51.22	24.44	8.20×10^{-3}	"
"	60	2.07	65.34	55.57	38.03	12.82×10^{-3}	"
2.5	1	0.87	16.78	23.43	7.63	1.38×10^{-4}	"
"	20	1.93	39.42	51.76	18.45	4.13×10^{-3}	"
"	40	2.03	50.35	54.48	25.98	8.48×10^{-3}	"
"	60	2.16	68.18	57.76	39.68	13.13×10^{-3}	"

Table 49. Runoff Over Sandy Clay Loam Surface With R = 21 cm^3/sec.

I (in/hr)	S (%)	Q (in^3/sec)	V (10^{-4} ft/sec)	R_e	F_r (10^{-4})	T_b (lb/ft^2)	Flow-Regime
1.5	1	0.81	15.62	21.70	7.11	1.34×10^{-4}	Subcritical-Laminar
"	20	1.67	36.24	44.74	17.50	3.85×10^{-3}	"
"	40	1.95	45.14	52.24	23.29	8.32×10^{-3}	"
"	60	2.03	64.08	54.39	37.94	12.72×10^{-3}	"
2.0	1	0.85	16.40	22.76	7.46	1.37×10^{-4}	"
"	20	1.83	39.71	49.04	19.18	4.02×10^{-3}	"
"	40	1.99	47.65	53.31	24.59	8.40×10^{-3}	"
"	60	2.34	67.71	62.69	39.40	13.67×10^{-3}	"
2.5	1	0.89	17.17	23.85	7.81	1.40×10^{-4}	"
"	20	1.99	40.64	53.31	19.22	4.20×10^{-3}	"
"	40	2.16	50.00	57.87	25.80	8.75×10^{-3}	"
"	60	2.44	70.60	65.37	41.09	13.95×10^{-3}	"

Table 50. Runoff Over Sandy Loam Surface With R = 42 cm^3 /sec.

I (in/hr)	S (%)	Q (in^3/sec)	V (10^{-4} ft/sec)	R_e	F_r (10^{-4})	T_b (lb/ft^2)	Flow-Regime
1.5	1	1.38	28.19	37.06	13.19	1.74×10^{-4}	Subcritical-Laminar
"	20	1.91	41.45	51.22	20.02	4.10×10^{-3}	"
"	40	1.95	48.36	52.31	24.95	8.29×10^{-3}	"
"	60	2.46	85.71	65.89	35.15	4.00×10^{-3}	"
2.0	1	2.09	38.19	56.09	16.92	2.15×10^{-4}	"
"	20	2.43	46.88	65.24	21.33	4.63×10^{-3}	"
"	40	2.61	53.31	69.93	24.96	9.60×10^{-3}	"
"	60	2.95	68.29	78.93	36.01	15.33×10^{-3}	"
2.5	1	2.41	41.84	64.57	17.61	2.31×10^{-4}	"
"	20	2.63	53.62	70.44	25.14	4.81×10^{-3}	"
"	40	2.79	60.55	76.69	29.25	9.92×10^{-3}	"
"	60	2.97	73.67	79.59	38.01	15.35×10^{-3}	"

Table 51. Runoff Over Sandy Clay Loam Surface With R = 42 cm^3 /sec.

I (in/hr)	S (%)	Q (in^3/sec)	V (10^{-4} ft/sec)	R_e	F_r (10^{-4})	T_b (lb/ft^2)	Flow-Regime
1.5	1	1.32	25.46	35.42	11.58	1.71×10^{-4}	Subcritical-Laminar
"	20	2.07	42.48	55.57	19.78	4.27×10^{-3}	"
"	40	2.32	53.70	62.11	26.74	9.07×10^{-3}	"
"	60	2.40	64.10	64.30	34.29	13.84×10^{-3}	"
2.0	1	1.65	30.15	44.12	13.35	1.91×10^{-4}	"
"	20	2.16	44.12	57.76	20.65	4.38×10^{-3}	"
"	40	2.44	52.95	65.39	25.57	9.30×10^{-3}	"
"	60	2.48	66.24	66.44	35.44	14.06×10^{-3}	"
2.5	1	1.87	32.47	50.09	14.03	2.04×10^{-4}	"
"	20	2.24	45.75	59.94	21.41	4.45×10^{-3}	"
"	40	2.52	54.69	65.72	26.42	9.44×10^{-3}	"
"	60	2.60	69.44	69.67	37.15	14.41×10^{-3}	"

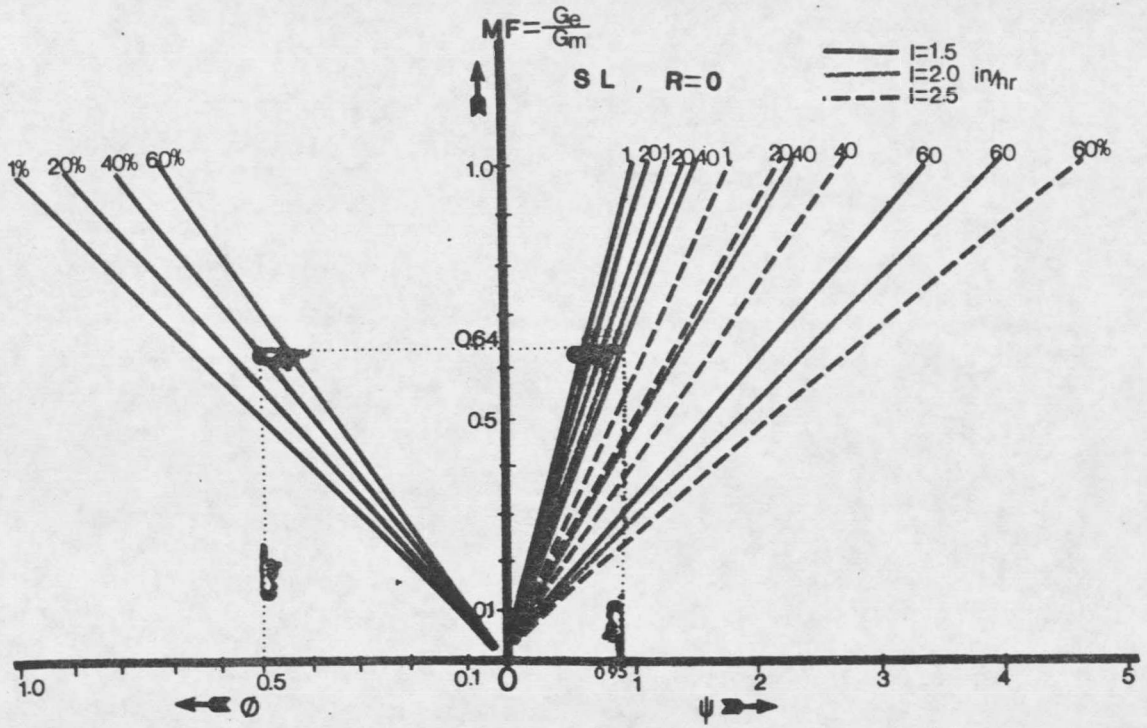


Figure 29. MF distribution with respect to ψ and ϕ for sandy loam with R = 0 cm^3 /sec.

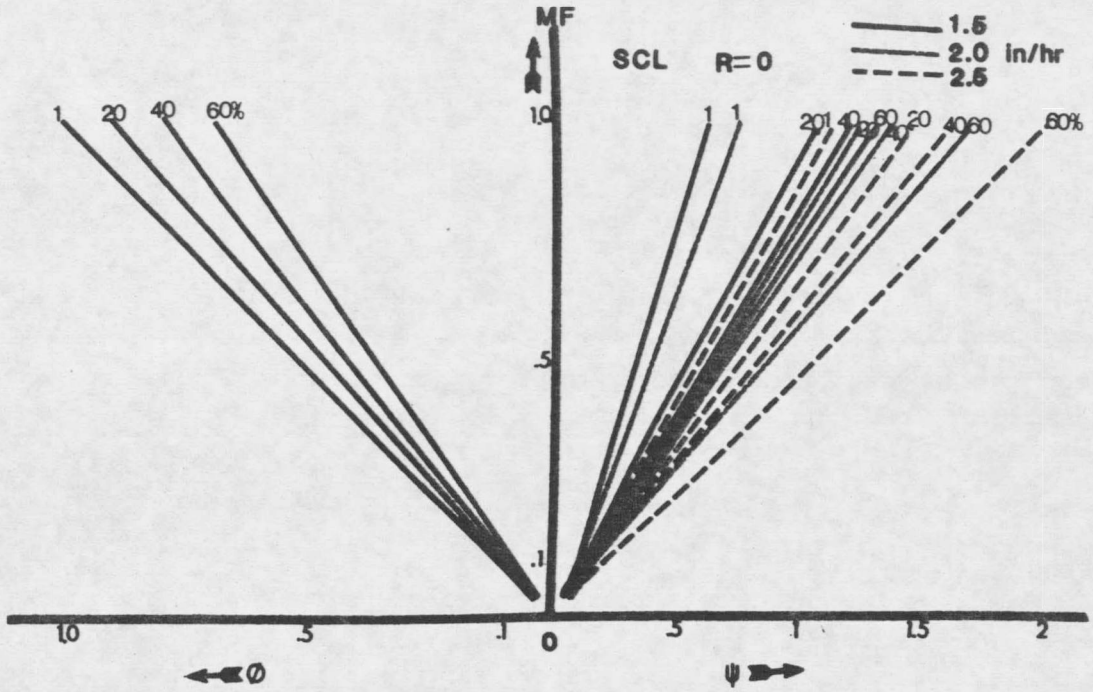


Figure 30. MF distribution with respect to ϕ and ψ for sandy clay loam with R = 0 cm^3/sec.

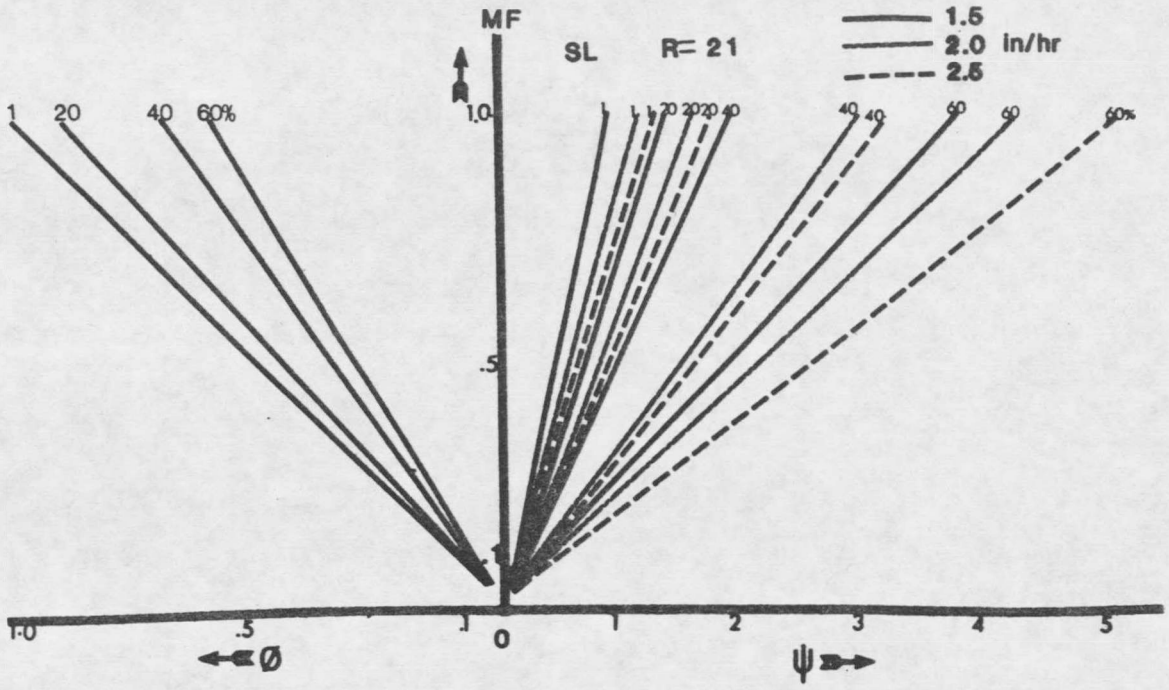


Figure 31. MF distribution with respect to ϕ and ψ for sandy loam with R = 21 cm^3/sec.

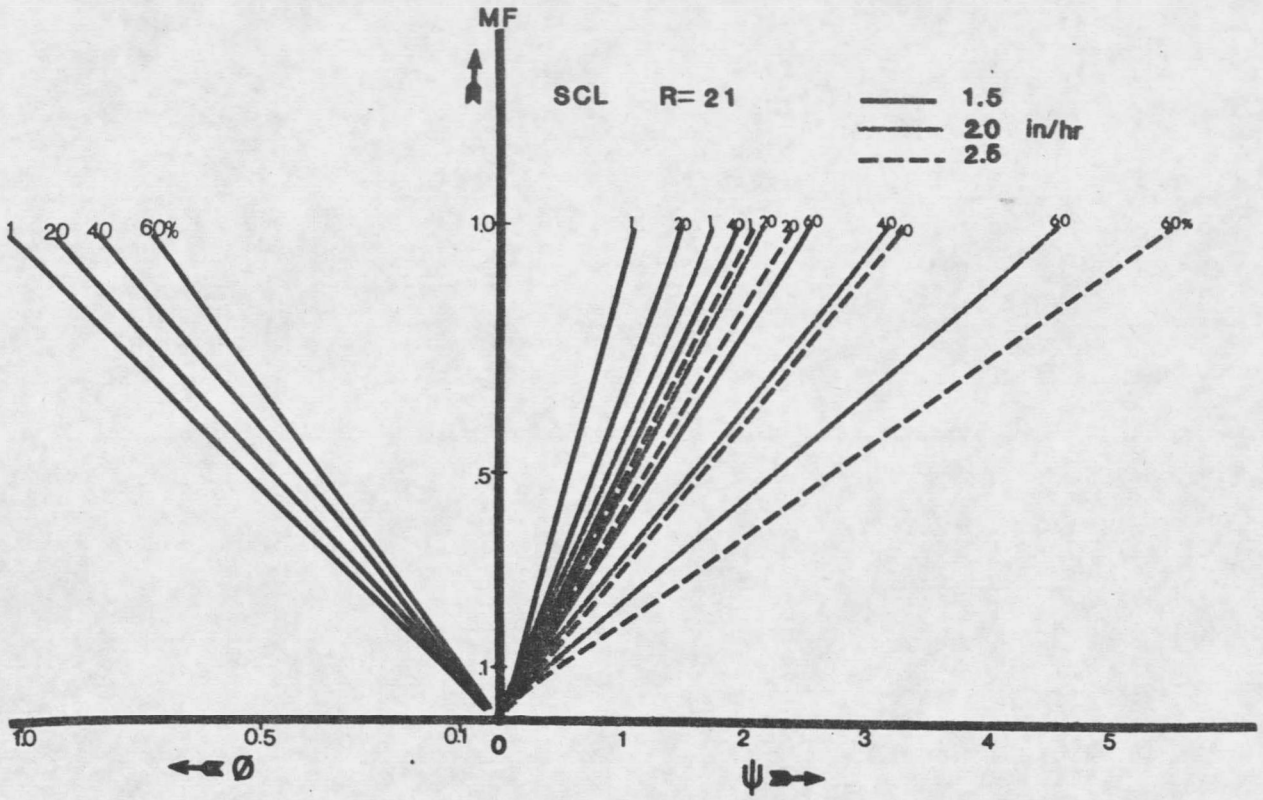


Figure 32. MF distribution with respect to ϕ and ψ for sandy clay loam with R = 21 cm^3 /sec.

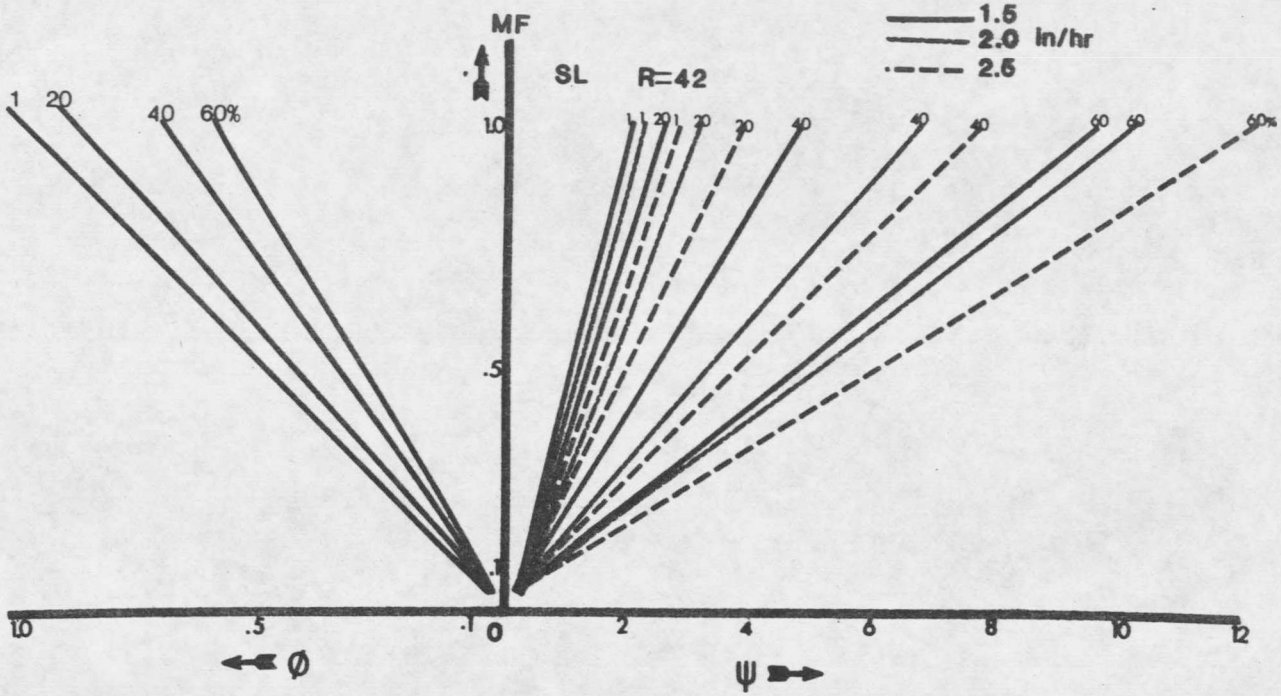


Figure 33. MF distribution with respect to ϕ and ψ for sandy loam with R = 42 cm^3 /sec.

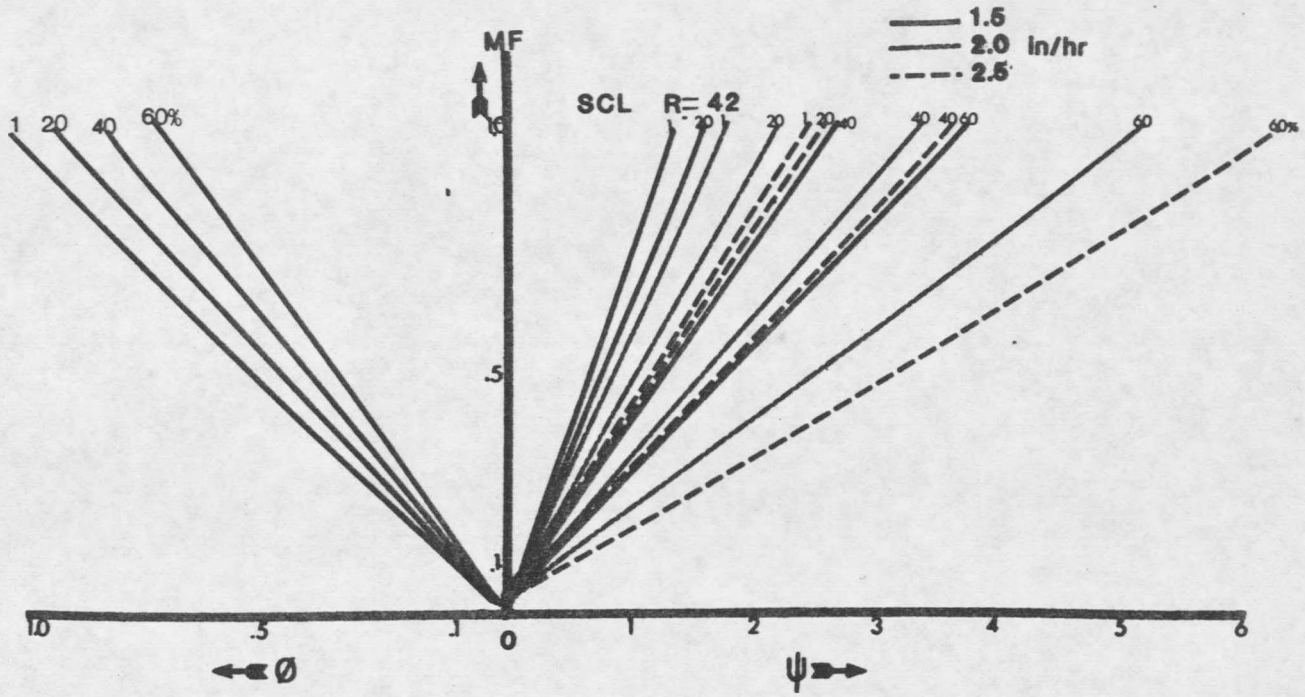


Figure 34. MF distribution with respect to ϕ and ψ for sandy clay loam with R = 42 cm^3 /sec.

Table 52. Sediment Yield Difference Between Actual Measurement and Model Prediction.

R (cm^3/sec)	I (in/hr)	Slope (%)	Soil Loss / Soil Texture	Average Sediment Yield (g/plot)	
				SL (measured)	SL (predicted)
0	1.5	0		0.09	0.10
		20		3.13	3.57
		40		8.36	9.02
		60		29.79	33.46
	2.0	0		0.12	0.16
		20		4.18	5.26
		40		10.84	13.86
		60		36.08	34.29
	2.5	0		0.18	0.26
		20		6.42	8.09
		40		15.79	16.71
		60		45.77	43.74
21	1.5	0		0.33	0.40
		20		13.46	13.90
		40		39.60	43.78
		60		125.50	132.68
	2.0	0		0.42	0.49
		20		16.48	19.29
		40		54.40	60.45
		60		151.80	164.76
	2.5	0		0.47	0.54
		20		18.63	21.34
		40		70.50	76.86
		60		184.94	191.32
42	1.5	0		0.50	0.63
		20		15.77	18.85
		40		55.62	60.35
		60		189.32	180.28
	2.0	0		0.68	0.84
		20		20.03	23.70
		40		88.44	94.64
		60		220.48	228.66
	2.5	0		0.84	1.04
		20		25.13	29.61
		40		103.44	111.55
		60		259.24	271.19

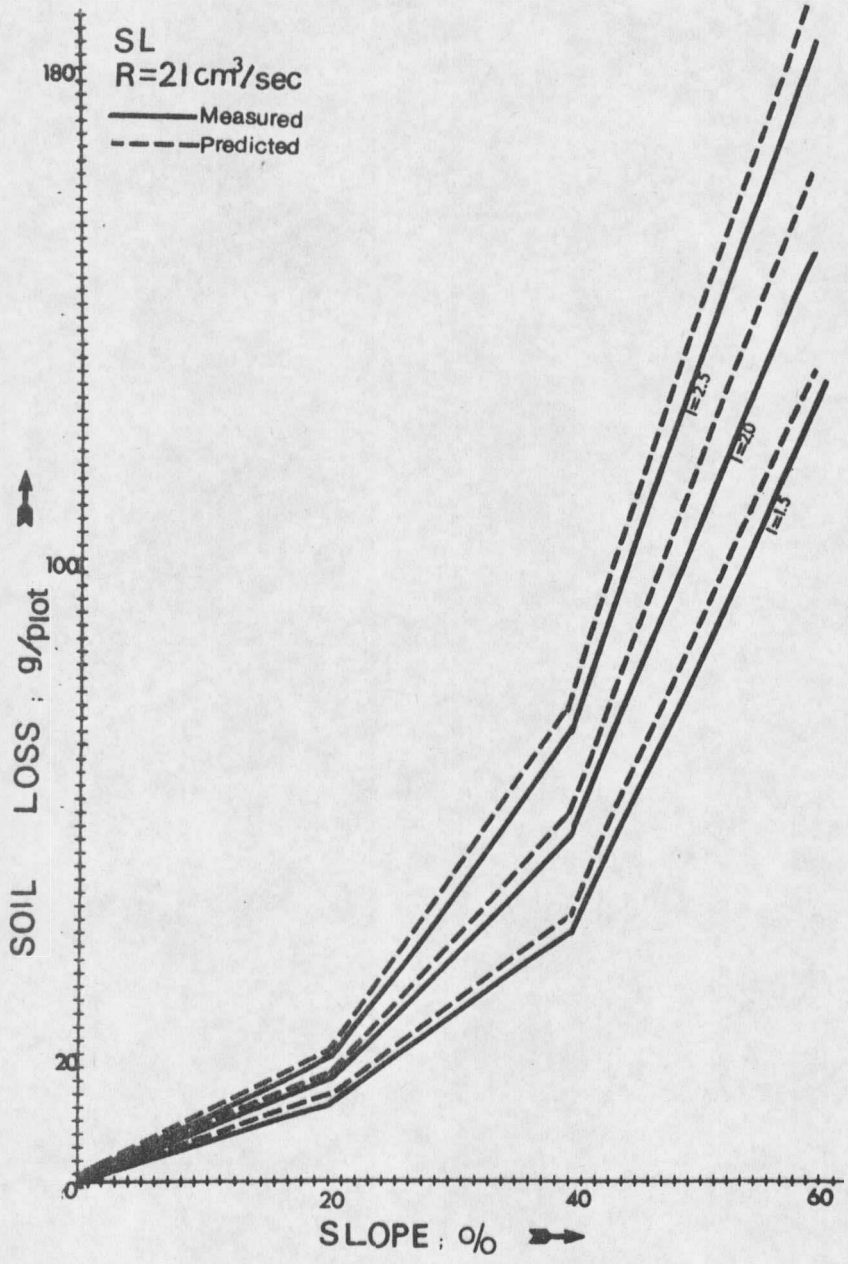


Figure 35. Slope-dependent soil loss for different intensities (SL).

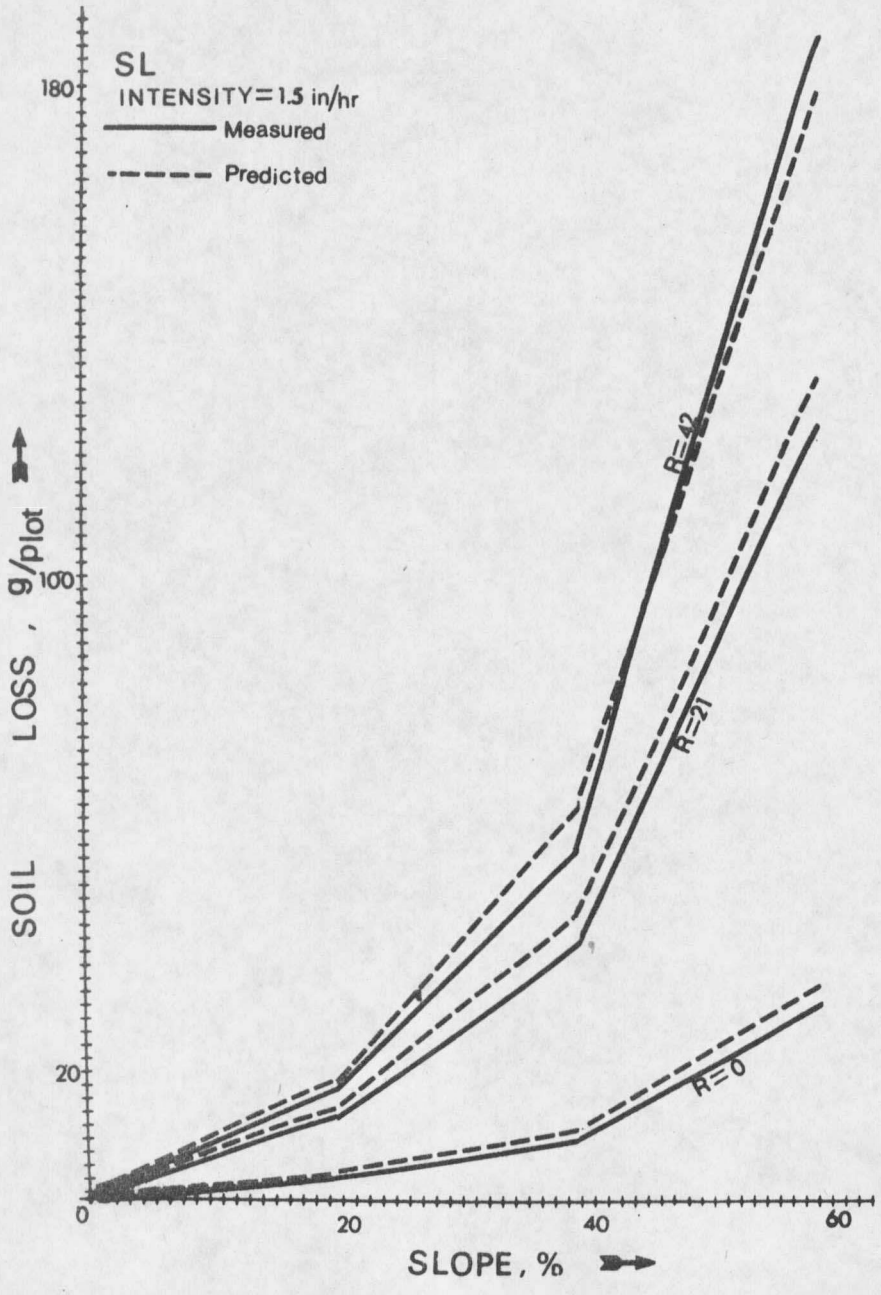


Figure 36. Slope-dependent soil loss for different runoff rates (SL).

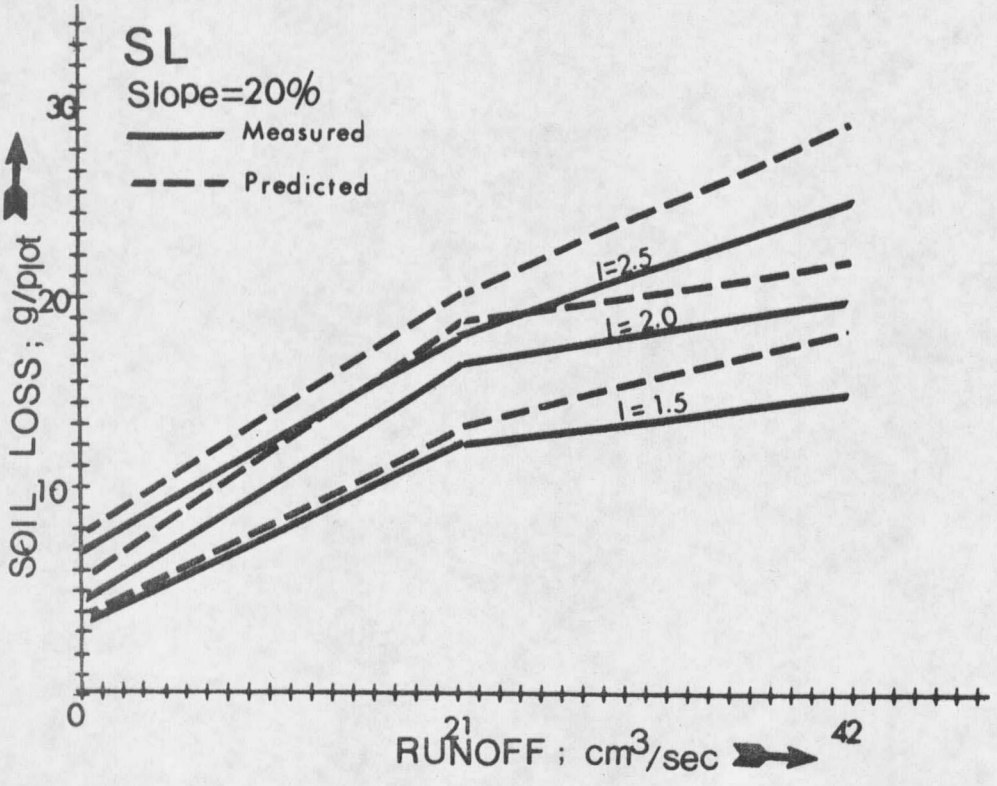


Figure 37. Runoff-dependent soil loss for different intensities (SL).

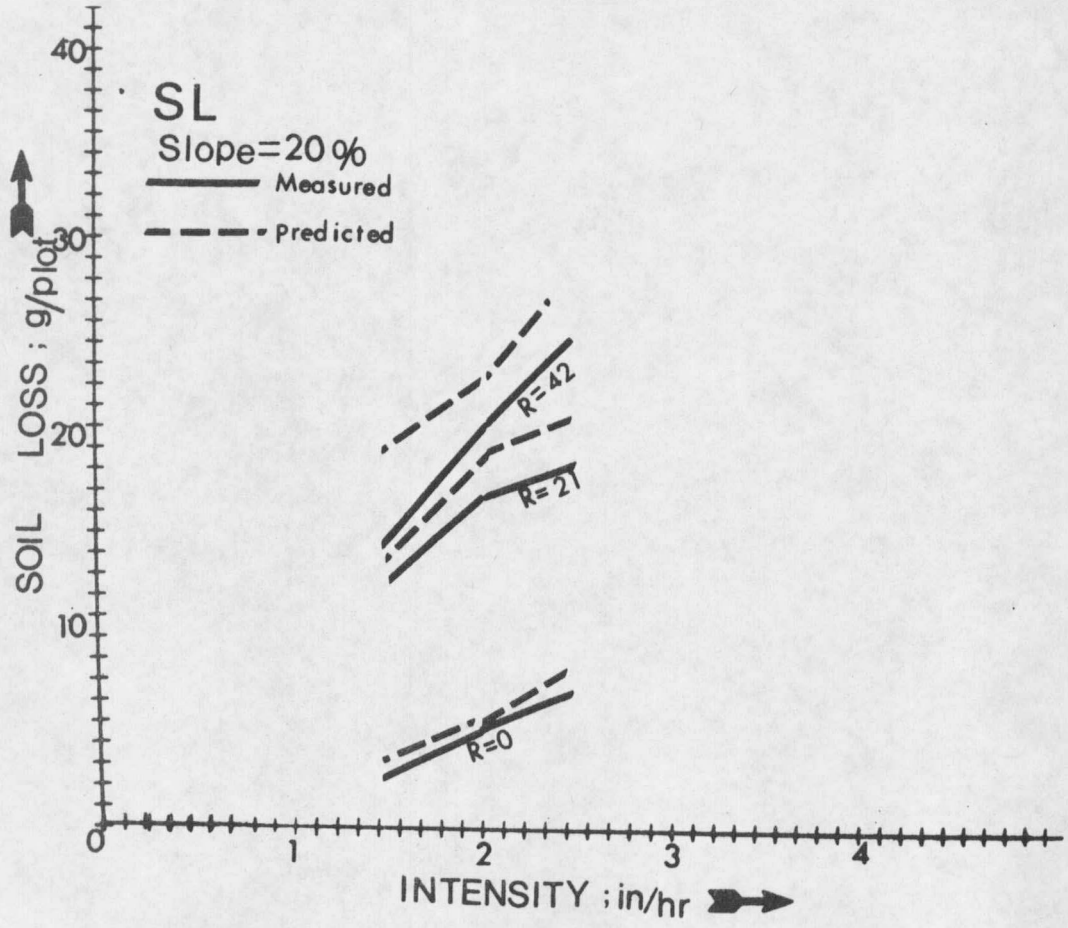


Figure 38. Intensity-dependent soil loss for different runoff rates (SL).

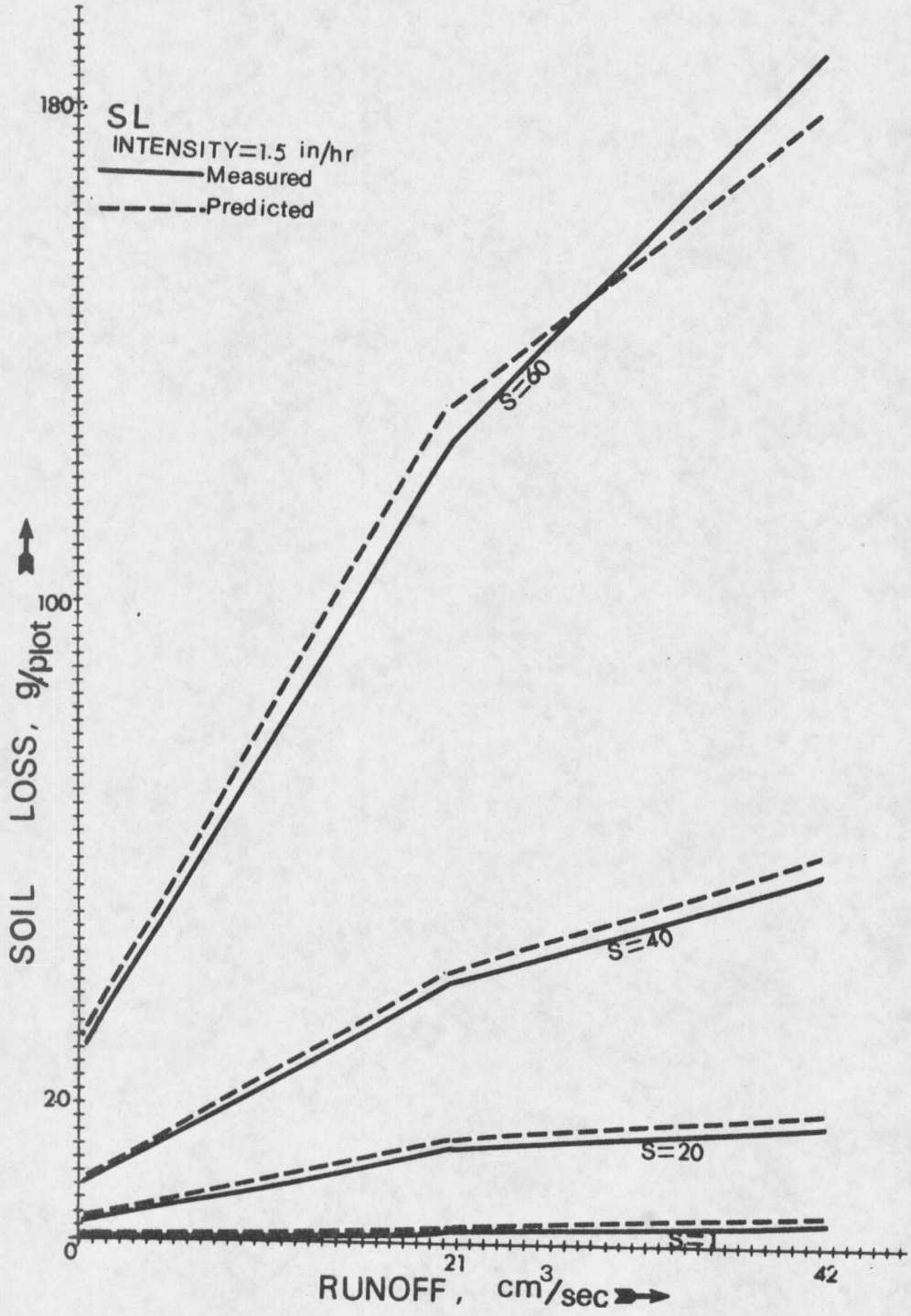


Figure 39. Runoff-dependent soil loss for different slopes (SL).

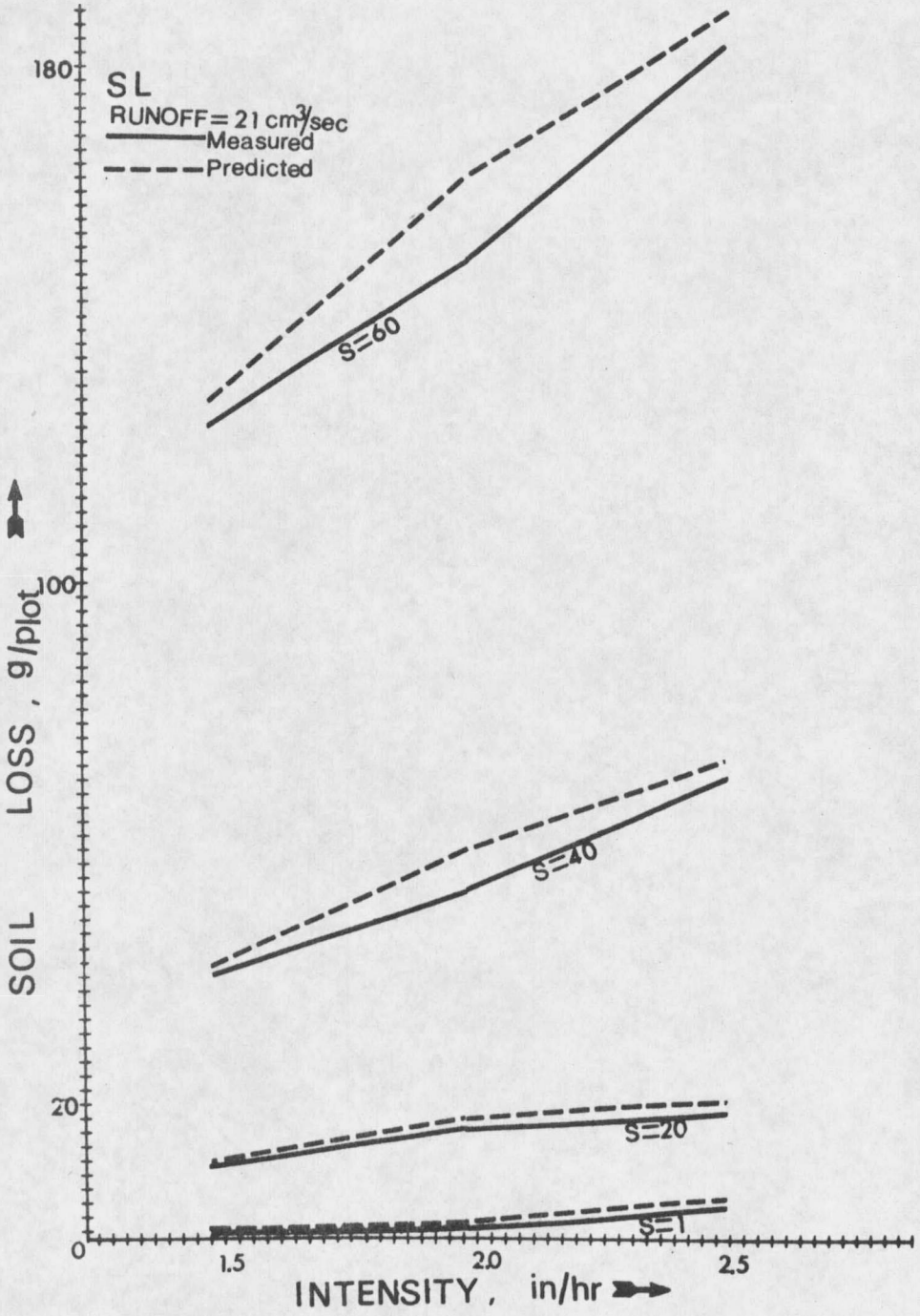


Figure 40. Intensity-dependent soil loss for different slopes (SL).

CHAPTER VI

EROSION MODEL APPLICATION AND DISCUSSION

The hydromechanical erosion model, primarily conceptual at present, needs to be applied to field conditions. Application of the model described above may be clarified by an example.

EXAMPLE:

Assume water erosion occurred at a Colstrip mined-area which is located in south-eastern Montana, a storm intensity = 3.8 cm/hr (1.5 in/hr) for 30 minutes, S (slope) = 40%, and soil texture of sandy loam. No inflow will be added from upslope (R = 0). (a) What soil loss could be expected for this area before reclamation if you use the model described in this study. (b) What soil loss would be predicted by the USLE? (Crop factor C, and practice factor P = 1.) Assume other factors are the same, the organic matter content of this sandy loam is 1.93%, L (slope length) is 61 m (200 ft) and transporting capacity T_b is 16.20×10^{-3} kg/m^2 (3.31×10^{-3} lb/ft^2).

Solution:

(a) 1) Assume $\phi = 0.5$ (ϕ ranges from 0 to 1 in this model)

2) From Figure 29, read MF = 0.64 and $\psi = 0.95$ for the given conditions. (Follow dashed line).

3) From given assumption, $T_b \cong 3.31 \times 10^{-3}$ lb/ft^2.

4) Substitution in equation 57.

$$G_e = T_b[1 - \frac{1}{\phi}(1 - \psi)(1 - e^{-\phi})]$$

$$= 3.31 \times 10^{-3}[1 - \frac{1}{0.5}(1 - 0.95)(1 - e^{-0.5})]$$

$$= 3.18 \times 10^{-3} \text{ lb/ft}^2$$

$$\cong 155.18 \text{ kg/ha}$$

5) Since MF = 0.64 = G_e/G_m = 155.18/G_m

G_m = 155.18/0.64 = 242.47 kg/ha

b) 1) Since crop factor (C) and conservation practice factor (P) for bare ground are equal to one, the CP factor is equal to 1 (CP = 1).

2) K factor:

From nomograph of USLE, read

K = 0.23, when organic matter content is 1.93%

3) R factor:

R factor can be estimated by

$R = \Sigma EI_{30}$; I_{30} = maximum 30-min intensity (in/hr)

$E = 916 + \log I$; I = natural intensity (in/hr)

$R_{(natural)} = (9.74)(0.75) = 7.31$; I = 1.5 in/hr

$R_{(simulate)} = (6.98)(0.11) = 0.77$; I = 0.22 in/hr

4) LS factor:

LS factor can be calculated by

$LS = (\lambda/72.6)^m (65.41 \sin^2\theta + 4.56 \sin\theta + 0.065)$

where λ = slope length (ft)

θ = angle of slope (degree)

m = 0.5 for slope > 5%

$LS_{(field)} = (200/72.6)^{0.5} (65.41 \sin^2 21.8° + 4.56 \sin 21.8° + 0.065)$

$= 17.89$ (for 200 ft field)

$LS_{(plot)} = (2/72.6)^{0.5} (65.41 \sin^2 21.8° + 4.56 \sin 21.8° + 0.065)$

$= 1.83$ (for 2 ft plot)

5) Substitute in USLE

$A = RKLSCP$

$= (7.31)(0.23)(17.89)(1)$

$= 30.08$ tons/acre

$\cong 67424$ kg/ha

6) Comparison between USLE and Model:

It would be necessary to adjust both LS factor and R factor to field condition when the comparison was made between USLE and Model.

Hence:

$R_{(natural)}/R_{(simulate)} = \alpha$; α = coefficient for R adjustment

$LS_{(field)}/LS_{(plot)} = \beta$; β = coefficient for LS adjustment

So:

$\alpha = 7.31/0.77 = 9.49$

$\beta = 17.89/1.83 = 9.78$

7) Adjust soil loss estimated by model to field condition:

Table 53. Soil Losses Comparison Between USLE and Model.

No.	Varieties	Soil Loss (kg/ha)	α	β	Adjusted Soil Loss (kg/ha)	Ratio
1	USLE prediction	67424	1	1	67424	3.23
2	Model estimation	242	9.49	9.78	22504	1.08*
3	Laboratory measurement	225	9.49	9.78	20888	1.00

*Accuracy % = (1 - 1.08 - 1.00/1.00) × 100% = 92%.

Using these data, the soil loss estimated by the model can approximately reach accuracy of 92% which is described by the given example. However, the predicted sediment yields derived from the USLE were poorly correlated with actual loss (Ferrell, 1982; Table 52). Several reasons are suggested to explain the disparity between predicted and actual losses:

1) The USLE might overpredict soil loss because the "LS" factor for this equation is not truly representative for a micro plot whose length is only 61 cm (2 feet).
2) Even though R factor has been adjusted, the differences in intensities and patterns of rainfall (R factor) in the two models are not likely to agree in all respects.
3) Because the topsoil in the constructed micro plot is compacted, the soil particles are not readily detached and transported by the runoff. This results in a smaller soil loss than was predicted by the model.
4) The USLE is a semi-empirical equation based on statistical analysis. Soil loss predicted by this equation could result in error due to the complicated interactions between mechanical forces governing soil loss rates.
5) The truly transport-limited overland flow did not occur on this micro plot, because there was not enough flow depth developed during the simulated processes in the laboratory. Therefore the disparity between predicted and actual losses was expected.
6) Runoff rate is an important factor influencing sediment yield. For any given set of conditions, a doubling of the runoff rate will more than double the sediment yield. Laboratory constraints (slope length and soil profile depth) prevented a comprehensive evaluation of the effects of the runoff rate.

CHAPTER VII

CONCLUSIONS AND RECOMMENDATIONS

Because of the importance of predicting sediment yields and changes in yields due to land use conversions, such as mining operations, and because of the prohibitive costs of using complicated mathematical models, a need arises for the development of a simple, effective model for estimating sediment yield with sufficient accuracy for engineering and reclamation of surface-mined areas. The method presented here provides a basis for soil loss and total sediment yield prediction. It is also possible to extend or modify the coefficients, ψ and ϕ, used here for a given surface-mined areas or watershed through the use of data collected from field or laboratory.

In summary, the factors controlling the soil erosion system are the magnitude of the eroding agents, the erodibility of the soil, the slope of the land, the surface roughness and the climatic conditions. In order to understand when, where, what and how much erosion is possible, the major factors that influence erosion must be examined in detail and the interrelationship between them should be identified. A lack of field experimental information from surface-mined areas must be overcome. As more data are made available, the model presented here can be modified and updated to make it more generally applicable to all types of mined areas and watersheds. As a result, the following conclusions and recommendations can be made:

1) The proposed soil erosion model must be verified and studied through actual field testing in the future.

2) Studies by other investigators (Sherard et al., 1973) indicate that the chemical properties of eroding water can affect erosion rate especially in soils that are subject to dis-

persion by high sodium levels. Hence, it is suggested that distilled water be used to more closely simulate the chemical properties of natural rain.

3) The main advantage of using a rainfall simulator is close monitoring and control of the energy, intensity and quantity of rainfall. The apparatus is easily portable and can be operated by one person. Economic water consumption is another advantage of this simulator.

4) Further research should make it possible to develop a yearly average prediction of erosion from this model because the total annual yield is also important for planning.

5) Future studies should consider the time required for soil and water to move downslope and the manner in which some of the soil properties that affect detachment and transport change with respect to time.

6) Other important items that should be taken into account in future studies include:

   a) Land topography and microtopography as they affect storage, overland flow, and depression.

   b) Vegetation and crop residues as they affect the erosive potential of rainfall and runoff.

   c) Other natural or man-made actions such as regrading, tillage systems and soil manipulation, as they influence soil detachment and transportation.

   d) Freezing and thawing actions as they affect soil erodibility.

   e) Seepage and other sub-surface flow phenomena as they affect soil erosion.

   f) Surface water depth as it affects rainfall detachment and runoff transportation.

   g) Surface roughness and rill geometry as they influence the hydraulic characteristics of erosion.

   h) Additional interrelationships among the subprocesses.

REFERENCES CITED

REFERENCES CITED

Al-Durrah, M. M. and J. M. Bradford. 1982. Parameters for describing soil detachment due to single waterdrop impact. J. Soil Sci. Soc. Am. Vol. (46):836-840.

Al-Durrah, M. M. and J. M. Bradford. 1981. New methods of studying soil detachment due to waterdrop impact. J. Soil Sci. Soc. Am. Vol. (45):949-953.

Anderson, C. E. and Briggs. 1979. Planning erosion control for coal mining and reclamation. J. Soil and Water Cons. 34(5):234-236.

ASAE. 1977. Soil erosion and sedimentation. St. Joseph, Michigan. ASAE:31-43, 69-90, 137-146.

Averitt, P. 1975. Coal resources of the United States, Jan. 1974. Bull. 1412. U.S. Geol. Surv., Reston, Va.

Barnett, A. P. and A. E. Dooley. 1972. Erosion potential of natural rainfall and simulated rainfall compared. Trans. Am. Soc. Agric. Engr. 19:1112-1114.

Bennett, H. H. and W. R. Chapline. 1928. Soil erosion a national menace. USDA Cir. 33.

Burden, R. L., J. D. Faires, and A. C. Reynolds. 1981. Numerical Analysis, 2nd edition, pub. Prindle, Weber & Schmidt, Boston, Massachusetts.

Carson, M. A., and Kirkby, M. J. 1972. "Hillslope form and process." Cambridge University Press.

Chow, V. T. 1959. Open channel hydraulics. McGraw-Hill, N.Y., pp. 7-8, 13, 43, 168-173.

Chow, V. T. and T. E. Harbaugh. 1965. Simulation of rainfall and soils for laboratory research. Trans. Am. Soc. Agric. Engr. 8:73-74.

Chow, V. T. and T. E. Harbaugh. 1965. Raindrop production for laboratory watershed experimentation. J. Geophys. Res. 70:6111-6119.

Clyde, C. G., C. E. Israelson, P. E. Packer, E. E. Farmer, J. E. Fletcher, E. K. Israelsen, F. W. Haws, N. V. Rao, and J. Hansen. 1976. Erosion control during highway construction. Rep. Nat. Coop. Highway Res. Bd. proj. 16-3, Vols. 1, 2, 3, Nat. Acad. Sci. Trans. Res. Bd., Washington, D.C.

Coenenberg, J. 1982. Practical considerations in establishing diverse plant community on mine soils. Symposium on surface coal mining and reclamation in the northern great plains. Billings, MT, pp. B-6-1.

CSCHE (Chinese Society of Civil & Hydraulic Engineering). 1975. Handbook of Engineering. Chap. 2: Applied hydraulics, CSCHE: 2-4.

Curtis, W. R. 1901. Strip-mining, erosion and sedimentation. Trans. Am. Soc. Agric. Engr. Vol. (16):434-436.

Dangler, E. W. and S. A. El-Swaify. 1976. Erosion of selected Hawaii soils by simulated rainfall. J. Soil Sci. Soc. Am. Vol. (40):769-776.

D'Souza, V. P. C. and R. P. C. Morgan. 1976. A laboratory study of the effect slope steepness and curvature on soil erosion. J. Agric. Engr. Res. 21:21-31.

Eaglesen, P. S. 1970. Dynamic hydrology. McGraw-Hill, Inc., N.Y., Chap. 15:325-368.

Ekern, P. C. 1951. Raindrop impact as the force initiating soil erosion. Proceedings, Soil Sci. Soc. Am. 15:7-10.

Ellison, L. D. 1947. Soil erosion studies. Agric. Exp. 28:145-146, 187-301, 245-248, 287-300, 349-351.

Emmett, W. W. 1970. The hydraulics of overland flow on hillslopes. U.S. Gel. Surv. prof. paper 662-A.

Ferrell, M. 1982. "Overburden Erosion Analysis," M.S. thesis, The University of Wyoming, Laramie, Wyoming.

Floyd, C. N. 1981. A mobile rainfall simulator for small plot field experiments. J. Agric. Engr. Res. 26:307-314.

Foster, G. R. and L. D. Meyer. 1975. A closed form soil erosion equation for upland areas. In H. W. Shan (ed.), Sedimentation symposium to honor Professor H. A. Einstein, pp. 121-129.

Grierson, I. T. and J. M. Oades. 1977. A rainfall simulator for field studies of runoff and soil erosion. J. Agric. Engr. Res. 22:37-44.

Hayes, E. T. 1979. Energy resources available to the U.S. 1985 to 2000. Sci. 203(4377): 233-239.

Highfill, R. E. and L. W. Kimberlin. 1977. Current soil erosion and sediment control technology for rural and urban lands. ASAE pub. 4-77:14.

Hill, R. D. 1971. Reclamation and revegetation of strip mined lands for pollution and erosion control. Trans. Am. Soc. Agric. Engr. 16:268-272.

Hjulstorm, F. 1935. Studies of the morphological activity of rivers as illustrated by river Fyries. Uppsala. Geological Institute, Bull. 25:221-527.

Hudson, N. W. 1965. The influence of rainfall on the mechanics of soil erosion. MSc. Thesis, U. of Cape Town.

Hudson, N. W. 1981. Soil conservation. Cornell University Press, Ithaca, N.Y. 2nd ed., pp. 48-61.

Iwagaki, Y. 1955. Fundamental studies on the runoff analysis by characteristics disaster prevent. Res. Inst. Bull. 10. Kyoto University, Dec. 1955.

Kirkby, M. J. 1978. Hillslope hydrology. John Wiley & Sons, N.Y. Chap. 6:183-214.

Kirkby, M. J. and R. P. C. Morgan. 1980. Soil erosion. John Wiley & Sons, N.Y. Chap. 6: 183-215.

Kohuke, H. and A. R. Bertrand. 1959. Soil conservation. McGraw-Hill, N.Y.

Laws, J. D. 1940. Recent studies in raindrops and erosion. J. Agric. Engr. 11:431-433.

Laws, J. O. 1941. Measurements of the fall velocity of waterdrops and raindrops. Trans. Am. Geophys. Union 22:709-721.

Laws, J. O. and D. A. Parsons. 1943. The relation of raindrop size to intensity. Trans. Am. Geophys. Union 24:452-459.

Li, J. C. R. 1966. Statistical influence. Edwards Brothers, Inc., Ann Arbor, Michigan. Chap. 19:393-436.

Lighthill, M. H. and G. B. Whitham. 1955. One kinematic waves. I. Flood movement in long rivers. Proc. Roy. Soc. Ser. Am. 229:281-316.

Lund, R. E. 1979. A user's guide to MSUSTAT, an interactive statistical package, pub. Dept. of Mathematical Sciences, MSU, Bozeman.

Meeuwig, R. O. 1971. Infiltration and water repellency in granitic soils. USDA Forest Service Res. paper INT-111.

Meyer, L. D. 1958. An investigation of methods of simulating rainfall on standard runoff plots and a study of the raindrop size, velocity, and kinetic energy of selected spray nozzles. USDA. ARS. Spec. Rpt. 81.

Meyer, L. D. 1965. Simulation of rainfall for soil erosion research. Trans. Am. Soc. Agric. Engr. 12(6):63-65.

Meyer, L. D. and E. J. Monke. 1965. Mechanics of soil erosion by rainfall and overland flow. Trans. Am. Soc. Agric. Engr. 12(6):572-580.

Meyer, L. D. and W. H. Wischmeier. 1969. Mathematical simulation of the process of soil erosion by water. Trans. Am. Soc. Agric. Engr. 16(6):754-758.

Meyer, L. D., G. R. Foster, and M. J. M. Romkens. 1975. Source of soil eroded by water from upland slopes. In present and perspective technology for predicting sediment yields and sources. Proc. sediment yield workshop. USDA. Sedimentation Laboratory, Oxford, Mississippi. Nov. 28-30, 1972, USDA. ARS-5-40, pp. 177-189.

Mihara, Y. 1952. Effect of raindrops and grass on soil erosion. In Proc. 6th Intern. Grassland Congr., pp. 987-990.

Morgan, R. P. C. 1979. Soil erosion. Topics in applied geology. National College of Agric. Engr. Silsoe, Bedfordshire, pub. Longman, N.Y., p. 41.

Munn, J. R. 1971. Development and use of portable rainfall simulator to determine the erosion characteristics of several soils in the Lake Tahoe Basin, MS Thesis, pp. 8-29.

Munshower, F. F. and E. J. Depuit. 1976. The effects of stack emissions on the range resource in the vicinity of Colstrip, MT. Montana Agric. Expt. Sta. Res. Rept. 98:112.

Mutchler, C. K. and L. F. Hermsmeier. 1965. A review of rainfall simulator. Trans. Am. Soc. Agric. Engr. 12(6):67-68.

Mutchler, C. K. 1967. Parameters for describing raindrop splash. J. Soil and Water Cons. 22:91-94.

Palmer, R. S. 1964. The influence of a thin water layer on waterdrop impact forces. Int. Assoc. Sci. Hydro. pub. 65:141-148.

Palmer, R. S. 1965. Waterdrop impact forces. Trans. Am. Soc. Agric. Engr. 12(6):63-70, 72.

Pearce, A. J. 1976. Magnitude and frequency of erosion by Hortonian overland flow. J. Geology 84:65-80.

Persse, F. H., D. W. Lockard, and A. E. Lindquest. 1977. Coal surface mining reclamation costs in the Western U.S. Bur. Mines, Washington, D.C.

Power, J. F., R. E. Ries, and F. M. Sandoval. 1978. Reclamation of coal-mined land in the north great plains. J. Soil and Water Cons. 33(2):69-74.

Rubey, W. W. 1952. Geology and mineral resources of the Hardin and Brussels. Quadrangles, Illinois, U.S. Geol. Surv. prof. paper 218.

SCSA. 1976. Soil erosion; prediction and control. The proceedings of a national conference on soil erosion, May 24-26, 1976, Purdue University, West Lafayette, Indiana, pp. 3-84.

Schafer, W. M., G. A. Nielsen, D. J. Dollhopf, and K. Temple. 1979. Soil genesis, hydrological properties, root characteristics and microbial activity of 1 to 50 year old stripmine soils. USDA. EPA-600/7-79-100, pp. 22-30, 43-73.

Schaller, F. W. and P. Sutton. 1978. Reclamation of drastically disturbed lands. pub. ASA, CSSA and SSSA, Chap. 2:11-23.

Schwab, G. O., R. K. Frevert, T. W. Edminster, and K. K. Barnes. 1981. Soil and water conservation engineering, pub. John Wiley & Sons, N.Y. 3rd edition, Chap. 5:92-121.

Sherard, J. L., R. S. Decker, and N. L. Ryker. 1973. Hydraulic fracturing in low dams of dispersive clay. Proc. specialty conference on performance of earth and earth supported structures, ASCE 1(1):653-689.

Smith, D. D. and W. H. Wischmeier. 1962. Rainfall erosion. Advances in Agron. 14:107-148.

Sowers, G. F. 1979. Introductory soil mechanics and foundations: Geotechnical engineering. 4th ed. Macmillan Publishing Co., Inc., pp. 1-45.

Stall, J. B. 1966. Man's role in affecting the sedimentation of streams and reservoirs. Proc. of the 2nd annual American water resources conference. American Water Resource Association, U. of Chicago, pp. 79-85.

Sweeney, L. R. 1979. Surface mining reclamation in Appalachia. Impact of the 1977 surface mining control and reclamation act. J. Soil and Water Cons. 34(5):179-203.

USDA. 1978. Predicting rainfall erosion losses. Prepared by Science and Education Administration, Agricultural Handbook #537, pp. 1-47.

EPA. 1976. Erosion and sediment control. Surface mining in the eastern U.S. Vol. (1). Planning, EPA-625/3-76-006, Washington, D.C., pp. 3-12.

Vanoni, V. A. 1977. Sedimentation engineering. ASCE, Headquarters of Society, N.Y. Chap. III:437.

Ward, A. D. and C. T. Haan. 1980. Evaluation of stripmine sediment detention basins in Kentucky. Trans. Am. Soc. Agric. Engr. 27:854-858.

Wischmeier, W. H., D. D. Smith, and R. E. Uhland. 1958. Evaluation of factors in soil-loss equation. J. Agric. Engr. 39:39, 8, 458-462, 474.

Wischmeier, W. H. 1960. Cropping management factor evaluation for a USLE. Proc. Soil Sci. Soc. Am. 24:322-326.

Wischmeier, W. H. and D. D. Smith. 1960. A universal soil loss equation to guide conservation farm planning. Trans. 7th Int. Cong. of Soil Sci. 1:418-425.

Wischmeier, W. H. 1962. Rainfall erosion potential. J. Agric. Engr. 43(4):212-215, 225.

Wischmeier, W. H. and D. D. Smith. 1965. Predicting rainfall erosion losses from cropland east of the Rocky Mountains. USDA. ARS. Agric. Handbook 282.

Woolhiser, D. A. and P. Todoravic. 1971. A stochastic model of sediment yield for ephemeral streams. Proc. USDA Int. Assoc. for statistics in the physical sci. symposium on statistical hydrology. USDA, Washington, D.C., pub. #1275.

Young, R. A. and J. L. Wierama. 1973. The role of rainfall impact on soil detachment and transport. Water Res. Res. 9:1629-1636.

Zanchi, C. and D. Torri. 1981. Evaluation of rainfall in central Italy. In M. De Boodt and D. Gabriels (ed.), Assessment of erosion. Wiley, Chichester.

Zingg, A. W. 1940. Degree and length of land slope as it affects soil loss in runoff. Agric. Engr. 21(2):59-64.

MONTANA STATE UNIVERSITY LIBRARIES
3 1762 10011639 9

D 378
T 782
cop.2